Advancement Towards a Biorefinery Platform using the Cyanobacterium *Synechococcus* sp. strain PCC 7002

By

Travis C. Korosh

A dissertation submitted in partial fulfillment of
the requirements for the degree of

Doctor of Philosophy
(Environmental Chemistry and Technology Program)

at the
UNIVERSITY OF WISCONSIN-MADISON
2018

Date of final oral examination: 1/10/2018

The dissertation is approved by the following members of the Final Oral Committee:

Katherine McMahon, Professor, Civil and Environmental Engineering
Daniel R. Noguera, Professor, Civil and Environmental Engineering
Brian F. Pfleger, Associate Professor, Chemical and Biological Engineering
Christina K. Remucal, Assistant Professor, Civil and Environmental Engineering
Thatcher Root, Professor, Chemical and Biological Engineering

TABLE OF CONTENTS

ACKNOWLEDGEMENTS

"Earth is a terrific planet!! But it needs all the help it can get!! Including mine!!"
- Superman in Superman's Pal Jimmy Olsen #148

I would like to thank my advisors, Drs. Kathrine McMahon and Brian F. Pfleger for supporting me throughout my graduate career. They were able to convince an idealistic kid from the New York to leave the big city for a welcoming and warm environment in the Midwest. I appreciate all their understanding through all the good times and the bad, and molding me into the scientist I am today.

The members of the Pfleger lab were instrumental in providing advice and entertainment. I will never forget all the great barbeques, fantasy drafts, and general ruckus in the lab. Drs. Markley, Copeland, and Cameron were a great help when I was just starting out in the lab. I'd like to acknowledge members of the Bone Slums (Matt, Ryan, Chris Jones, Dylan, and Taylor) for keeping the office weird, and being a sounding board for all my bad ideas. I'd like to thank Mark, Jackie, Gina, Chris Mehrer, Nestor, and Austin for staying good sports even though I would make terrible jokes and drawings on the whiteboard. I'd like to thank all the members of the McMahon lab for providing me an alternative to gene-jocking and the windowless prison of Engineering Hall, and for the wider insight into microbial ecology and bioinformatics. Must of this research wouldn't be possible without the pipetting of my undergrads. Matt, Rich, and Derek thank you.

I would also like to thank my sludge brothers Ben, Chris, Pancho, Matt and Zach for lively and passionate discussions on the terribleness of the Oilers, the greatest kung-fu movies of all time, participating in the hot sauce challenge, and good times at the terrace. Eric, Claudia, and Jason were great outlets when I need a break from the lab and need to interact with normal members of society.

My family has been a bedrock of support since I've left New York. My parents lend an ear whenever I need to complain about something. My younger brothers, Brandon and Zachary, are a pleasure to annoy when I come home to visit. Uncle Wayne, Aunt Dotty, and Uncle Ken kept me going through my studies, even though I've been in school forever.

And last, but not least, I would like to thank my girlfriend Abby for sticking with me even though I am a curmudgeonly old man who would rather watch the Great British Baking show and read comic books all day than go outside. She has been understanding when I need to work late and provides morale when things don't go as planned.

Advancement Towards a Biorefinery Platform using the Cyanobacterium *Synechococcu*s sp. strain PCC 7002

Travis C. Korosh

Ph.D., University of Wisconsin-Madison

Under the supervision of Professors Kathrine McMahon and Brian F. Pfleger

ABSTRACT

Cyanobacteria are prokaryotic oxygen photoautotrophs that have high areal productivity and can thrive in diverse ecosystems. These features have made them attractive biological catalysts for the sustainable production of specialty and commodity chemicals. This thesis examines the use of the exceptionally tolerant cyanobacterium, *Synechococcu*s sp. strain PCC 7002, for the ability to use a municipal wastewater stream as a nutrient source under several conditions. We explore the capacity of *Synechococcu*s sp. strain PCC 7002 for the production for proof of concept molecules, L-lactate and L-lysine. We discuss metabolic engineering design principles that enable high productivities and carbon partitioning, with an emphasis on leveraging the coordination between carbon and nitrogen metabolism.

LIST OF TABLES

Table Page

LIST OF FIGURES

Figure Page

CHAPTER 1 MOTIVATION AND GOALS FOR RESEARCH

1.1. Introduction

Due to the uncertainty brought about by climate change, nations are developing the framework for the renewable production of energy and goods. These renewable technologies must have low specific greenhouse gas emissions and an inexhaustible supply to successfully mitigate the rise in global temperatures. While the current share of renewable energy in the total energy market is small, adoption has been steadily increasing throughout the last decade, due in part to changes in governmental policy and the decreasing production costs of many of these technologies (Moomow et al., 2011). These renewable sources of energy include wind, solar, hydropower, geothermal, and biomass, each with its own technoeconomic and environmental advantages and disadvantages (Ellabban et al., 2014). Geographic availability, production variability, and storage capacity are key factors that will govern the successful integration of renewable resources into the larger energy portfolio (Sims et al., 2011).

Analogous to petroleum fuels, biomass can also act as a feedstock for the conversion to various products, such as commodity or specialty chemicals. The high-energy density, storability, and ability to generate power and heat on demand are thought to make biofuel energy a major part of the future renewable energy resources. These inherent properties are especially valuable in the transportation sector, where it is projected to serve between 5-14% of global transport by 2035, representing 2.7-5.6% of global electricity generation (Chum et al., 2011). Other drivers for biofuel development include the existing global infrastructure for similar products, allowing for cost effective integration into the supply chain (Chum et al., 2011).

In the United States, conventional biofuels are produced from commercial crops such as corn and soybean to produce ethanol and biodiesel, respectively. Researchers have found that over the entire life cycle of these first generation biofuels, the sustainability and environmental impacts are still relatively high (Williams and Inman, 2009). Other developing technologies in the biofuel market are the use of lignocellulosic biomass, which may be produced from waste residues (Creutzig et al., 2015). However, the variability in sources of lignocellulosic biomass and technologies for biomass processing increases the uncertainty of the effect of scale up and real world performance (Sathaye et al., 2011). These sources of biofuels have pressing concerns with increased fertilizer use and the potential for eutrophication, loss of biodiversity, fresh water depletion, and the use of arable land (Chum et al., 2011). Thus, strategies to produce biomass with a minimal environmental footprint is an active and attractive area of research (Ort et al., 2015).

Due to their small areal footprint, high areal productivity, and ability to use non-potable water, cyanobacteria and microalgae are attractive feedstocks for the production of next generation biofuels (Moreno-Garcia et al., 2017). Cyanobacteria are the most abundant photosynthetic organisms on Earth and are responsible for large fraction of the photosynthetic production of oxygen and the conversion of inorganic compounds e.g. (CO_2, NH_4, PO_4) into the organic biomass that is the source of carbon and energy in many ecosystems (Scanlan et al., 2009). Cyanobacteria, like higher plants, utilize multisubunit membrane-protein complexes during oxygenic photosynthesis to convert light into the chemical energy used generate biomass and biofuels. Cyanobacteria may also be genetically modified to convert CO_2 into specific compounds of interest, thereby circumventing the inefficiencies of biomass processing into sugars which are fed to producer organisms. Microalgae and cyanobacteria are estimated to have

CO_2 fixation efficiency of 10–50 times higher than terrestrial plants (Li et al., 2008), making them attractive options for CO_2 mitigation. A variety of compounds, including alcohols, sugars, and organic acids, have been produced with genetically engineered cyanobacterial hosts (Angermayr et al., 2015). Furthermore, cyanobacteria have been demonstrated to use domestic and municipal wastewater as nutrient sources, simultaneously producing biomass, while also remediating these streams of excess nutrients (Aciién et al., 2016; Bohutskyi et al., 2015; Dalrymple et al., 2013; Martins et al., 2011; Rawat et al., 2011; Ruiz-Martinez et al., 2012; Wang et al., 2016). This has spurred academic interest for use of these organisms in a biorefinery process, outlined in **Fig. 1-1**.

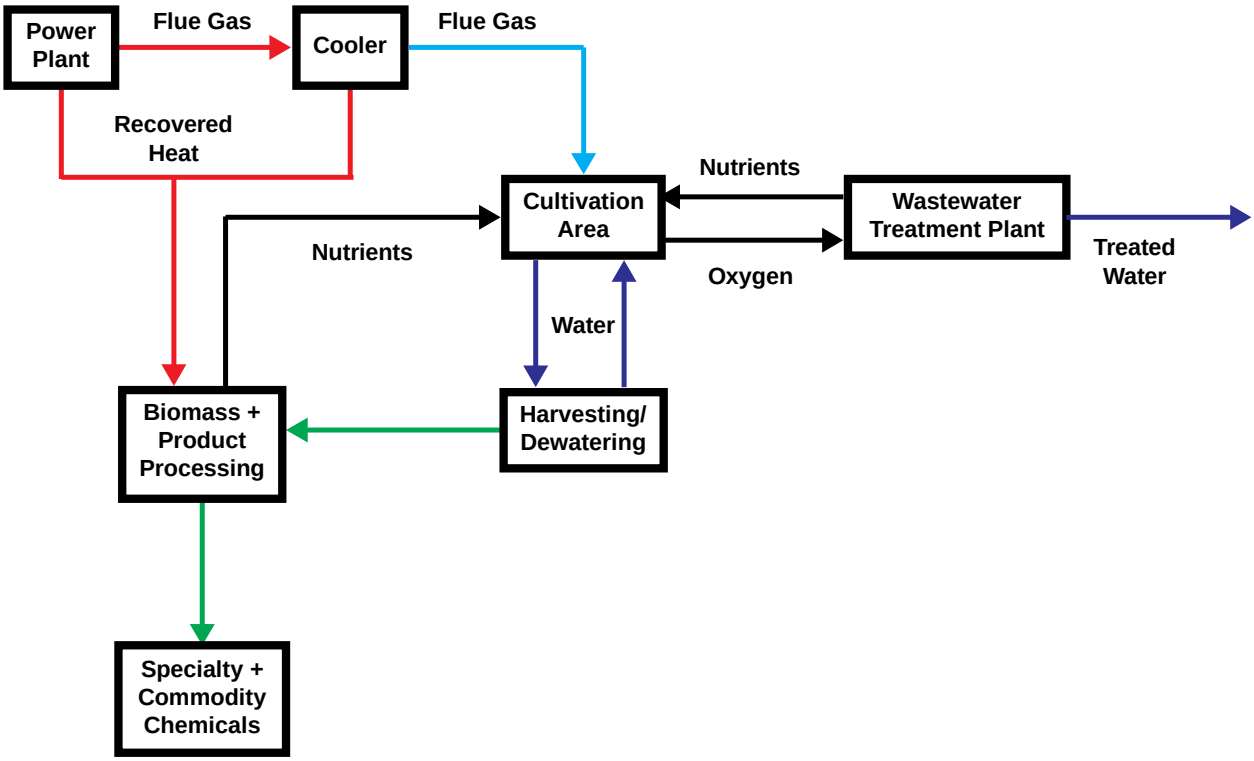

Figure 1-1. Schematic of a Cyanobacterial Biorefinery.
Flue gas CO_2 will be used to provide inorganic carbon to a photosynthetic cultivation area which is coupled with wastewater treatment for the exchange of nutrients and oxygen. Generated biomass and products will be processed, and nutrients and water are recycled back to the cultivation area.

Much of the basic research on cyanobacteria has been performed with the strains *Synechococcus elongatus* PCC 7942, *Synechococcus* sp. PCC 7002, and *Synechocystis* sp. PCC

6803 (hereafter PCC 7942, PCC 7002, PC C6803, respectively), due to their fully sequenced genomes and established tools for genetic manipulation. Accordingly, these hosts have proven useful for fundamental studies on oxygenic photosynthesis (Jensen and Leister, 2014; Orf et al., 2016). The cyanobacterium used in this research, PCC 7002, has a number of advantages over other cyanobacteria model strains due to its high light and temperature tolerance, fast growth rate, and ability to adapt to a wide range of salinities (Ruffing, 2014).

My original contribution to the field is the successful utilization of a municipal wastewater stream as a nutrient source, and the production of several chemical classes under standard and non-standard media conditions using PCC 7002 as microbial host. First, the thesis elaborates on the importance of environmental conditions and the physiological adaptations necessary to utilize municipal wastewater as a source of nutrients. Second, this work describes the metabolic engineering strategies to engineer high productivities of L-lactate and L-lysine in a photoautotrophic host.

1.2. Project Overview

Chapter 2 provides a literature review for the concepts necessary for the actualization of a cyanobacteria biorefinery and is divided into two sections. The first half delves into the potential and challenges for wastewater based microalgal production. The latter half goes into detail on the unique aspects of cyanobacteria physiology and relevant metabolism, with an emphasis on the complexities of photosynthetic electron flow and coordination of nitrogen and carbon metabolism.

Chapter 3 investigates the utility of a municipal wastewater stream as a nutrient source. We found diffuse forms of dissolved organic carbon with increasing concentrations of this gravity

belt filtrate stream. We observed dose-dependent toxicity at high cultivation temperatures and interference with photosynthetic electron transfer under all cultivation conditions. Potential mechanisms for the tolerance observed at low temperatures are discussed.

Chapter 4 explores metabolic engineering design principles for a cyanobacterial host using the organic acid, L-lactate. We found that enzymatic cofactor preference played a large role in enhancing productivity. Overexpression of a glycolytic transcriptional regulator significantly increased carbon partitioning to L-lactate. Conditionally downregulating an enzyme involved in the synchronization of carbon and nitrogen metabolism resulted in the highest L-lactate volumetric productivity for a cyanobacterium strain to date.

Chapter 5 examines the applicability of using a cyanobacterial host to produce the essential amino acid, L-lysine. Simultaneous expression of a feedback inhibition resistant aspartate kinase and lysine transporter were necessary for high productivities, but this was also met with a decreased chlorophyll content and reduced growth rates. Productivities were enhanced by utilizing reduced nitrogen sources in defined and undefined media formulations.

Chapter 6 provides a summary of the work discussed in this thesis and makes recommendations for future research directions.

1.3. Literature Cited

Aciién, F.G., Gómez-Serrano, C., Morales-Amaral, M.M., Fernández-Sevilla, J.M., Molina-Grima, E., 2016. Wastewater treatment using microalgae: how realistic a contribution might it be to significant urban wastewater treatment? Appl. Microbiol. Biotechnol. 100, 9013–9022. doi:10.1007/s00253-016-7835-7

Angermayr, S.A., Gorchs Rovira, A., Hellingwerf, K.J., 2015. Metabolic engineering of cyanobacteria for the synthesis of commodity products. Trends Biotechnol. 33, 352–361. doi:10.1016/j.tibtech.2015.03.009

Bohutskyi, P., Liu, K., Nasr, L.K., Byers, N., Rosenberg, J.N., Oyler, G. a., Betenbaugh, M.J., Bouwer, E.J., 2015. Bioprospecting of microalgae for integrated biomass production and

phytoremediation of unsterilized wastewater and anaerobic digestion centrate. Appl. Microbiol. Biotechnol. doi:10.1007/s00253-015-6603-4

Chum, H., Faaij, A., Moreira, J., Berndes, G., Dhamija, P., Dong, H., Gabrielle, B., Eng, A.G., Lucht, W., Mapako, M., Cerutti, O.M., McIntyre, T., Minowa, T., Pingoud, K., 2011. Bioenergy, in: Edenhofer, O., Pichs-Madruga, R., Sokona, Y., Seyboth, K., Matschoss, P., Kadner, S., Zwickel, T., Eickemeier, P., Hansen, G., Schlömer, S., von Stechow, C. (Eds.), IPCC Special Report on Renewable Energy Sources and Climate Change Mitigation. Cambridge University Press, Cambridge, United Kingdom and New York, NY, USA.

Creutzig, F., Ravindranath, N.H., Berndes, G., Bolwig, S., Bright, R., Cherubini, F., Chum, H., Corbera, E., Delucchi, M., Faaij, A., Fargione, J., Haberl, H., Heath, G., Lucon, O., Plevin, R., Popp, A., Robledo-Abad, C., Rose, S., Smith, P., Stromman, A., Suh, S., Masera, O., 2015. Bioenergy and climate change mitigation: An assessment. GCB Bioenergy 7, 916–944. doi:10.1111/gcbb.12205

Dalrymple, O.K., Halfhide, T., Udom, I., Gilles, B., Wolan, J., Zhang, Q., Ergas, S., 2013. Wastewater use in algae production for generation of renewable resources: a review and preliminary results. Aquat. Biosyst. 9, 2. doi:10.1186/2046-9063-9-2

Ellabban, O., Abu-Rub, H., Blaabjerg, F., 2014. Renewable energy resources: Current status, future prospects and their enabling technology. Renew. Sustain. Energy Rev. 39, 748–764. doi:10.1016/j.rser.2014.07.113

Jensen, P.E., Leister, D., 2014. Cyanobacteria as an Experimental Platform for Modifying Bacterial and Plant Photosynthesis. Front. Bioeng. Biotechnol. 2, 1–4. doi:10.3389/fbioe.2014.00007

Li, Y., Horsman, M., Wu, N., Lan, C.Q., Dubois-Calero, N., 2008. Biofuels from microalgae. Biotechnol. Prog. 24, 815–20. doi:10.1021/bp070371k

Martins, J., Peixe, L., Vasconcelos, V.M., 2011. Unraveling cyanobacteria ecology in wastewater treatment plants (WWTP). Microb. Ecol. 62, 241–56. doi:10.1007/s00248-011-9806-y

Moomow, W., Yamba, F., Kamimoto, M., Maurice, L., Nyboer, J., Urama, K., Weir, T., 2011. Renewable Energy and Climate Change, in: Edenhofer, O., Pichs-Madruga, R., Sokona, Y., Seyboth, K., Matschoss, P., Kadner, S., Zwickel, T., Eickemeier, P., Hansen, G., Schlömer, S., von Stechow, C. (Eds.), IPCC Special Report on Renewable Energy Sources and Climate Change Mitigation. Cambridge University Press, United Kingdom and New York, NY, USA.

Moreno-Garcia, L., Adjallé, K., Barnabé, S., Raghavan, G.S. V, 2017. Microalgae biomass production for a biorefinery system: Recent advances and the way towards sustainability. Renew. Sustain. Energy Rev. 76, 493–506. doi:10.1016/j.rser.2017.03.024

Orf, I., Timm, S., Bauwe, H., Fernie, A.R., Hagemann, M., Kopka, J., Nikoloski, Z., 2016. Can cyanobacteria serve as a model of plant photorespiration? - a comparative meta-analysis of metabolite profiles. J. Exp. Bot. 67, erw068. doi:10.1093/jxb/erw068

Ort, D.R., Merchant, S.S., Alric, J., Barkan, A., Blankenship, R.E., Bock, R., Croce, R., Hanson, M.R., Hibberd, J.M., Long, S.P., Moore, T.A., Moroney, J., Niyogi, K.K., Parry, M.A.J.,

Peralta-Yahya, P.P., Prince, R.C., Redding, K.E., Spalding, M.H., van Wijk, K.J., Vermaas, W.F.J., von Caemmerer, S., Weber, A.P.M., Yeates, T.O., Yuan, J.S., Zhu, X.G., 2015. Redesigning photosynthesis to sustainably meet global food and bioenergy demand. Proc. Natl. Acad. Sci. 112, 1–8. doi:10.1073/pnas.1424031112

Rawat, I., Ranjith Kumar, R., Mutanda, T., Bux, F., 2011. Dual role of microalgae: Phycoremediation of domestic wastewater and biomass production for sustainable biofuels production. Appl. Energy 88, 3411–3424.

Ruffing, A.M., 2014. Improved Free Fatty Acid Production in Cyanobacteria with Synechococcus sp. PCC 7002 as Host. Front. Bioeng. Biotechnol. 2, 17. doi:10.3389/fbioe.2014.00017

Ruiz-Martinez, A., Martin Garcia, N., Romero, I., Seco, A., Ferrer, J., 2012. Microalgae cultivation in wastewater: Nutrient removal from anaerobic membrane bioreactor effluent. Bioresour. Technol. 126, 247–253.

Sathaye, J., Lucon, O., Rahman, A., Christensen, J., Denton, F., Fujino, J., Heath, G., Mirza, M., Rudnick, H., Schlaepfer, A., Shmakin, A., 2011. Renewable Energy in the Context of Sustainable Development, in: Edenhofer, O., Pichs-Madruga, R., Sokona, Y., Seyboth, K., Matschoss, P., Kadner, S., Zwickel, T., Eickemeier, P., Hansen, G., Schlömer, S., von Stechow, C. (Eds.), IPCC Special Report on Renewable Energy Sources and Climate Change Mitigation. Cambridge University Press, Cambridge, United Kingdom and New York, NY, USA.

Scanlan, D.J., Ostrowski, M., Mazard, S., Dufresne, A., Garczarek, L., Hess, W.R., Post, A.F., Hagemann, M., Paulsen, I., Partensky, F., 2009. Ecological genomics of marine picocyanobacteria. Microbiol. Mol. Biol. Rev. 73, 249–99. doi:10.1128/MMBR.00035-08

Sims, R., Mercado, P., Krewitt, W., Bhuyan, G., Flynn, D., Holttinen, H., Jannuzzi, G., Khennas, S., Liu, Y., Nilsson, L.J., Ogden, J., Ogimoto, K., O'Malley, M., Outhred, H., Ulleberg, Ø., Hulle, F. van, 2011. Integration of Renewable Energy into Present and Future Energy Systems, in: Edenhofer, O., Pichs-Madruga, R., Sokona, Y., Seyboth, K., Matschoss, P., Kadner, S., Zwickel, T., Eickemeier, P., Hansen, G., Schlömer, S., von Stechow, C. (Eds.), IPCC Special Report on Renewable Energy Sources and Climate Change Mitigation. Cambridge University Press, Cambridge, United Kingdom and New York, NY, USA.

Wang, Y., Ho, S.H., Cheng, C.L., Guo, W.Q., Nagarajan, D., Ren, N.Q., Lee, D.J., Chang, J.S., 2016. Perspectives on the feasibility of using microalgae for industrial wastewater treatment. Bioresour. Technol. 222, 485–497. doi:10.1016/j.biortech.2016.09.106

Williams, P., Inman, D., 2009. Environmental and Sustainability Factors Associated With Next-Generation Biofuels in the U . S .: What Do We Really Know ? Environ. Sci. Technol. 43, 4763–4775. doi:10.1021/es900250d

CHAPTER 2 REVIEW OF THE LITERATURE

2.1 Opportunities and Challenges for Wastewater Integration into a Cyanobacteria Biorefinery

Microalgal production of biofuels is regarded as a potential strategy to mitigate greenhouse gas emissions due to microalgae's ability to be cultivated in non-arable lands with high areal productivity (Bozell and Petersen, 2010; Fairley, 2011). Early studies have compared the life cycle analysis (LCA) and energy return on investment (EROI) of microalgal biofuels to first generation biofuels sources such as corn, switchgrass, and canola (Colin M. Beal et al., 2012; Clarens et al., 2010). Using quantitative metrics such as land use, water use, greenhouse gas emissions, energy consumption, and eutrophication potential, researchers have found that microalgae biomass performs worse on all metrics except for land use and eutrophication potential when grown in raceway ponds with application of traditional nitrogen and phosphorus-rich fertilizer. This is most likely due to the inherent energy usage embedded within fertilizer production (Razon, 2014). However, integration with forms of partially treated wastewater, in particular source separated urine, shift these LCA criteria to be significantly more favorable than other sources of biomass (Clarens et al., 2010). By using this dual-purpose system, the need for energy intensive secondary treatment processes for wastewater are lessened, resulting in a mutually beneficial EROI for wastewater treatment and microalgal biomass production (Colin M Beal et al., 2012). Several studies have successfully cultivated microalgae in raceway ponds (Olguín et al., 1997), photobioreactors (Ruiz-Martinez et al., 2012), and chemostats (Dickinson et al., 2015), having very high nutrient removal rates in wastewater-derived media.

Due the high nutrient demand for biomass, the anaerobic digestate stream of wastewater is typically used for microalgal cultivation (Dickinson et al., 2015). The dominant nitrogen source in this wastewater stream will be in the form of NH_4^+, which is also inhibitory towards many photosynthetic organisms at high concentrations (Collos and Harrison, 2014). This stream also typically contains high levels of dissolved organic matter (DOM) and redox-active metals (Metcalf et al., 1972), and is typically diluted to prevent growth retardation (Wang et al., 2010). Various studies have demonstrated DOM toxicity to photosynthetic organisms (Laue et al., 2014; Neilen et al., 2017; Pflugmacher et al., 2006, 1999), although the molecular mechanism behind this toxicity remain unclear. Photochemically, DOM is also an ecologically important chromophore and can contribute to reactive oxygen species (ROS) formation (Mostafa and Rosario-Ortiz, 2013) and trace metal bioavailability (Rose, 2012) in natural systems. Previous studies have revealed that wastewater DOM exhibits high quantum yields of (O_2-) and ($OH^{\cdot}$) under simulated sunlight conditions, which may be due to a combination of soluble microbial products, natural organic matter, and trace pollutants (D. Zhang et al., 2014).

Despite its potential for a nutrient feedstock, if all the wastewater processed in the United States were used to produce microalgal biofuels at current efficiencies, it would result in less than 1% of the United States' annual energy consumption (Peccia et al., 2013). Nutrient (Y. Zhang et al., 2014) and water (Farooq et al., 2015) recycling are likely to be critical factors for reducing the economic and environmental impacts of algal biofuels, and LCA have demonstrated this (Orfield et al., 2014). Due to its maturity and high nitrogen recycling potential, anaerobic digestion is thought to be a better option for nutrient recycling than hydrothermal gasification in the near-term (Y. Zhang et al., 2014). Furthermore, studies examining the onsite use of residual water from the hydrothermal gasification of algal biomass found significant acute toxicity that

affected the biomass generation (Patzelt et al., 2015a) and photosystem activity (Patzelt et al., 2015b) of tested species. This residue had a high phenolic index and required activated carbon treatment to obtain growth comparable to a control medium (Patzelt et al., 2015a), which would potentially increase operating costs. Additional research should be performed on how these toxic compounds are formed and how these compounds interfere with photosynthetic metabolism.

2.2 Physiology of Cyanobacteria and Oxygenic Photoautotrophic Metabolism

2.2.1 Photon Absorption and Electron Flow

Cyanobacteria are prokaryotes that use absorbed light as a source of energy for growth (White et al., 2012). To perform this task, cyanobacteria possess specialized internal thylakoid membrane system where a variety of electron transport processes undergo in parallel (Mullineaux, 2014). Linear photosynthetic electron transport in cyanobacteria (summarized in **Fig. 2-1)** employ light harvesting antennae (phycobilisomes) to aid in the absorption of photons in the visible spectrum, then direct the energy via resonance energy transfer to a pigment-protein reaction complex in photosystem II (PSII) (Lea-Smith et al., 2016). H_2O is used as an electron donor in PSII, donating 2 electrons to the mobile electron carrier plastiquinone (PQ) while 2 protons and 1/2 O_2 are released into the thylakoid lumen (Nagarajan and Pakrasi, 2001). The reduced PQ diffuses through the thylakoid membrane to react with the cytochrome b_6f complex, where an electron is then transferred to either plastocyanin (PC) or cytochrome c6 (cyt c6), depending on the environmental conditions (Nomura and Bryant, 1999). Those soluble electron carriers then reduce photosystem I (PSI), which acts as a light-driven oxidoreductase, creating reduced ferredoxin (Fd_{red}), which then reduces the terminal electron acceptor $NADP^+$ (Rochaix,

2011). The other electron is then used to regenerate PQ in a series of redox reactions (Lea-Smith et al., 2016). The protons generated from the splitting of H_2O form a chemiosmotic ΔpH to drive ATP synthase, producing a ratio of 1.5 ATP/NADPH in optimal conditions (Kramer and Evans, 2011). This ATP and NADPH is then used to perform various metabolic functions throughout the cell.

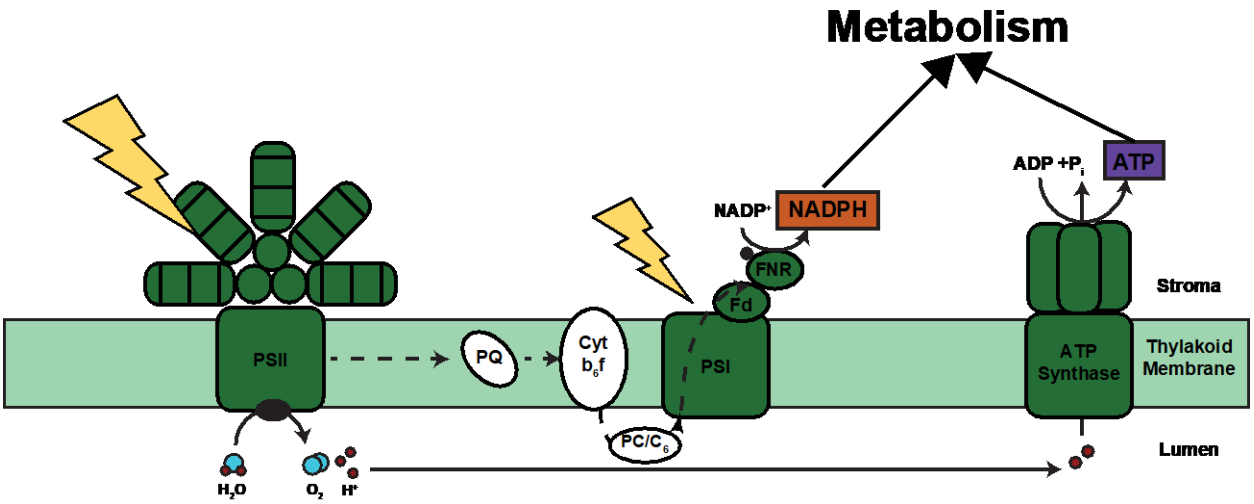

Figure 2-1. Linear Electron Transport is the Major Source of NADPH and ATP in Cyanobacteria.
Linear electron transport is used to generate reducing equivalents and chemical energy in oxygenic photoautotrophs.

The absorption of light is inherently damaging due to the photosensitive Mn_4CaO_5 cluster at the reaction center of PSII (Zavafer et al., 2015) in a process known as photoinhibition (Keren and Krieger-Liszkay, 2011). The D1 protein of PSII is the primary target of this photoinhibitory damage and is constantly degraded and resynthesized to maintain photosynthetic activity (Mulo et al., 2012). Multiple environmental stresses, such as osmotic, temperature, pH, and light stress (Nishiyama and Murata, 2014) may act to synergistically to enhance the rate of photoinhibition (Athanasiou et al., 2010), causing ROS generation and rapid loss of photosynthetic activity (Keren and Krieger-Liszkay, 2011). ROS production aggravates the loss of repair mechanisms necessary for de-novo D1 protein synthesis by oxidation of specific cysteine residues in the

ribosomal elongation factor, EF-Tu (Yutthanasirikul et al., 2016), leading to decreased rates of both CO_2 fixation and NADPH oxidation. (This phenomenon is summarized in **Fig. 2-2**). As $NADP^+$ is a major acceptor of electrons in PSI, loss of free $NADP^+$ accelerates the generation of ROS through transient reactions of O_2 with reduced ferredoxin, and leads to cell death (Voss et al., 2013).

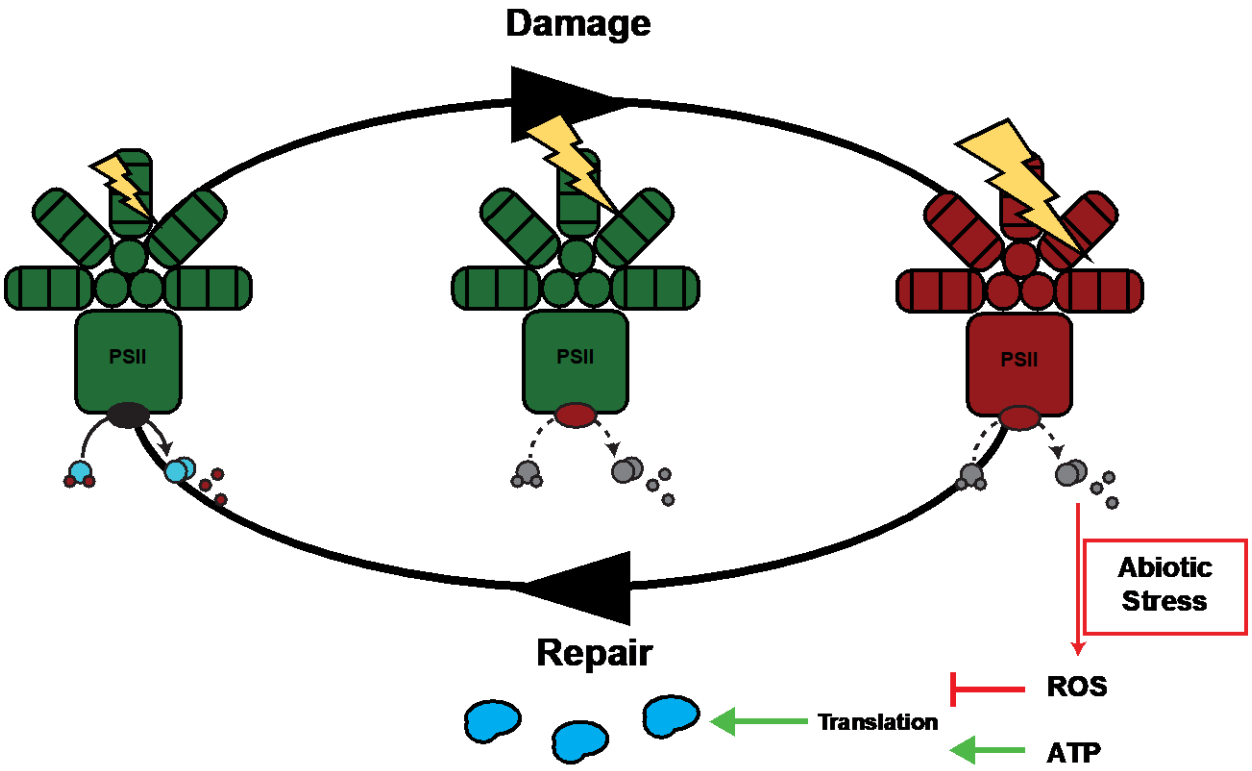

Figure 2-2. Tolerance to Photoinhibition is the Balance Between the Rate of Damage and Repair.
Absorption of light leads to the destruction of the D1 protein in the reaction center of PSII. This protein in constantly turned over to maintain PSII activity. Abiotic stress inhibits de-novo protein translation and D1 turn over through ROS production.

Regulated primarily by the reversible redox state of thiol groups (Buchanan and Balmer, 2005), photosynthetic organisms have developed several mechanisms to deal with light stress. These include modulating the stoichiometry of photosystem complexes (Chow et al., 1990), dissipating excess energy as heat (Nishiyama and Murata, 2014), quenching accumulated ROS (Latifi et al., 2009), as well as respiratory and alternative electron transport (AET) processes

(Nishiyama and Murata, 2014), which all occur in proximity to linear electron flow on the cytoplasmic and thylakoid membranes (summarized in **Fig. 2-3)**. Electron transport processes in cyanobacteria utilize several mobile membrane-bound electron shuttling complexes (Nagarajan and Pakrasi, 2001), and proper thylakoid membrane synthesis and fluidity is necessary to ensure optimal electron flow in changing environments (Yamamoto, 2016). Of particular note is the need for PQ to effectively diffuse through the thylakoid and cytoplasmic membranes to ensure proper interactions with its photosynthetic or respiratory redox partners (Klementiev et al., 2017; Williams, 1998). This in turns governs the redox state of PQ, which regulates large segments of photosynthetic metabolism (Hihara et al., 2003). As part of the homeoviscous adaptation (Wada and Murata, 1998), cyanobacteria upregulate membrane-bound desaturases to increase the unsaturated content of both the cytoplasmic and thylakoid membranes under conditions of high light (Ludwig and Bryant, 2011) or low temperature (Ludwig and Bryant, 2012a). Replacement of all polyunsaturated fatty acids by a monounsaturated fatty acid rendered mutant strains of PCC 6803 more susceptible to photoinhibition at low temperatures (Tasaka et al., 1996).

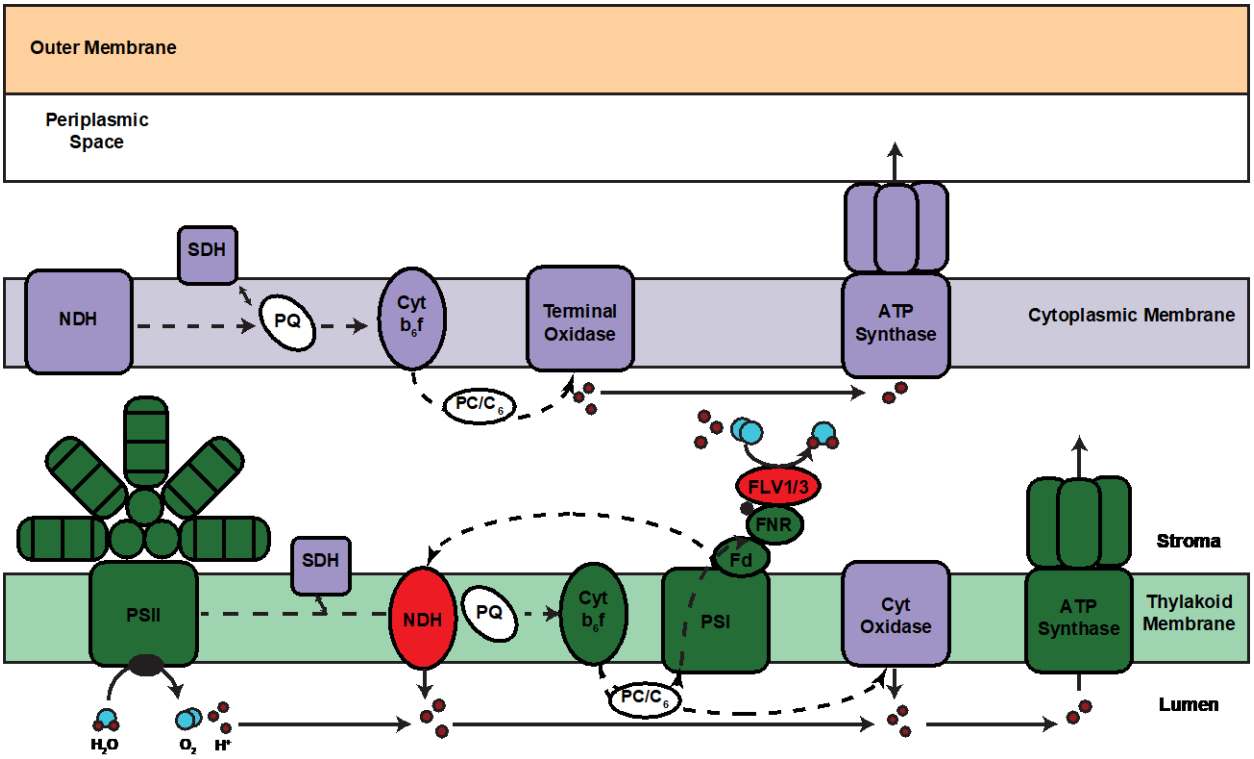

Figure 2-3. Multiple Adjacent Electron Transport Processes Co-Occur in Cyanobacteria. Photosynthetic (green), respiratory (blue), and alternative (red) electron processes co-occur on the thylakoid and cytoplasmic membranes. Mobile electron shuttles (white) allow for proper electron (dashed lines) and proton flow (solid lines) in dynamic environments.

Respiratory and AET processes balance the generation and consumption of both ATP and NADPH to control the ATP/NADPH ratio on several timescales depending on light availability (Foyer et al., 2012; Voss et al., 2013).Electrons generated from reactions with respiratory substrates (NADPH, Succinate) and corresponding dehydrogenases are shuttled to a number of terminal oxidases to generate a ΔpH across the thylakoid membrane for ATP synthesis under conditions of low or no light (Liu et al., 2012). Under conditions of rapid fluctuations in light intensity or CO_2, electrons from NADPH are transferred to flavodiiron proteins to reduce O_2 to H_2O via the Mehler pathway to dissipate excessive reductive pressure (Allahverdiyeva et al., 2013; Bersanini et al., 2014; Zhang et al., 2009). Under high-light, cyclic electron flow is also used to generate a ΔpH across the thylakoid membrane via NADPH dehydrogenases through electron transfer from PQ back to PSI using FD_{red} or NADPH as a reductant, generating ATP

with no net change in NADPH levels (Leister and Shikanai, 2013). This also aids in dissipating excess light energy as heat in a process known as non-photochemical quenching (Takahashi et al., 2009). AET processes have already proved invaluable in studies examining the effects of production of compounds, such as alkanes (Berla et al., 2015) and alcohols (Baroukh et al., 2015) in photosynthetic organisms.

2.2.2 Carbon Fixation and Flux During Autotrophic Conditions

In cyanobacteria, the rate of CO_2 fixation is governed by the slow catalytic rate and low affinity of the enzyme ribulose-bisphosphate carboxylase/oxygenase (RuBisCO) in the Calvin-Benson-Bassham cycle (Parry et al., 2012). Three forms of RuBisCO have been found in nature and all catalyze the Mg^{2+} dependent carboxylation or oxygenation of ribulose 1,5-bisphosphate after activation or carbamylation of a specific lysine residue (Tabita et al., 2008). Form 1 RuBisCO is found in plants, eurkaryotic algae, and cyanobacteria, and is comprised of eight 52 kDa subunits and eight 15 kDa subunits (Mueller-Cajar et al., 2014). Carboxylation of ribulose 1,5-bisphosphate yields an unstable an C6 intermediate that is spontaneously hydrolyzed into two molecules of 3-phosphoglycerate, which are subsequently reduced to glyceraldehyde-3-phosphate. From this step, a number of sugar rearrangement reactions ensue to ultimately regenerate ribulose 1,5-bisphosphate for the Calvin-Benson-Bassham cycle to continue, consuming 9 ATP and 6 NADPH for every molecule of glyceraldehyde-3-phosphate produced (Berg, 2011).

In ambient concentrations of CO_2, cyanobacteria undergo an adaptive response known as the CO_2 concentrating mechanism (CCM) to increase the intracellular concentration of HCO_3^- and shift towards the carboxylation reaction of RuBisCO (Price et al., 2008). This response

includes upregulation of inorganic carbon transporters and the creation of the carboxysome, a semipermeable protein micro-compartment that creates a local environment rich in CO_2 (Price, 2011). A number of the genes involved in CCM are regulated by CcmR, a LysR-type transcriptional regulator (Woodger et al., 2007). α-ketoglutarate (AKG) and $NADP^+$ have been identified as co-repressors of CcmR, enhancing binding to putative promoter regions for genes involved in high-affinity inorganic carbon uptake (Daley et al., 2012). These inorganic carbon transporters include a suite of active HCO_3^-- transporters: (i) the BCT1 complex which is ATP dependent and has high-affinity, (ii) SbtA, an inducible, high-affinity Na^+/HCO_3^- symporter, and (iii) BicA, a high-flux, low-affinity Na^+/HCO_3^- symporter. Also, capable of inorganic carbon uptake are specialized respiratory NADPH dehydrogenase complexes that passively diffuse CO_2 into to the cell (Ogawa and Mi, 2007). This includes the low-affinity NDH-1_4 system which is constitutively expressed, and the high-affinity NDH-1_3 system which is induced under carbon limitation (Price, 2011). The BicA protein in PCC 7002 has a relatively high flux rate compared to other strains and is inducible under ambient concentrations of CO_2 (Price et al., 2004).

It is important to note that the Calvin-Benson-Bassham cycle shares a number of common enzymes with glycolysis and the oxidative pentose phosphate pathways (Chen et al., 2016), and metabolite labelling experiments show high flux through these pathways under photoautotrophic conditions (Hendry et al., 2017; Young et al., 2011). These three pathways are also relatively flexible in adjusting their fluxes under a number of environmental conditions (Wan et al., 2017). It has been suggested that future metabolic engineering efforts in cyanobacteria should focus on products that utilize their metabolic intermediates, rather than the rather inflexible TCA-cycle (Angermayr et al., 2015; Wan et al., 2017). This discussion is further elaborated in the comparison between production rates and fitness of engineered strains of PCC

7002 during the synthesis of two chemicals, L-Lactate and L-Lysine, as discussed in **Chapters 4** and **5**, respectively.

2.2.3 Coordination of Nitrogen and Carbon Metabolism

To maintain metabolic homeostasis in dynamic environments, cells coordinate anabolic and catabolic processes via signal transduction pathways (Chubukov et al., 2014). The coordination of nitrogen and carbon metabolism is of note in cyanobacteria due to their roles as prominent reductant sinks, and is heavily regulated on several transcriptional and post-translational levels (de Marsac et al., 2001; Wright et al., 2014). Once actively transported into the cell, all forms of nitrogen are eventually converted into NH_4^+ through a series of enzymatic reduction reactions utilizing Fd_{red} (Flores and Herrero, 2004). The major route of incorporation of nitrogen in cyanobacteria is through the sequential action of glutamine synthetase (GS) and glutamate synthase (GOGAT) in the GS-GOGAT cycle (Muro-Pastor and Florencio, 2003) (Summarized in **Fig. 2-4**). First, GS catalyzes an ATP dependent amidation reaction with glutamate to yield glutamine. Using Fd_{red}, GOGAT then produces two molecules of glutamate from the transfer of the amide group to AKG. AKG, a metabolic intermediate of the TCA cycle, is intertwined in both nitrogen and carbon assimilation as the carbon skeleton necessary for nitrogen assimilation (Huergo and Dixon, 2015).

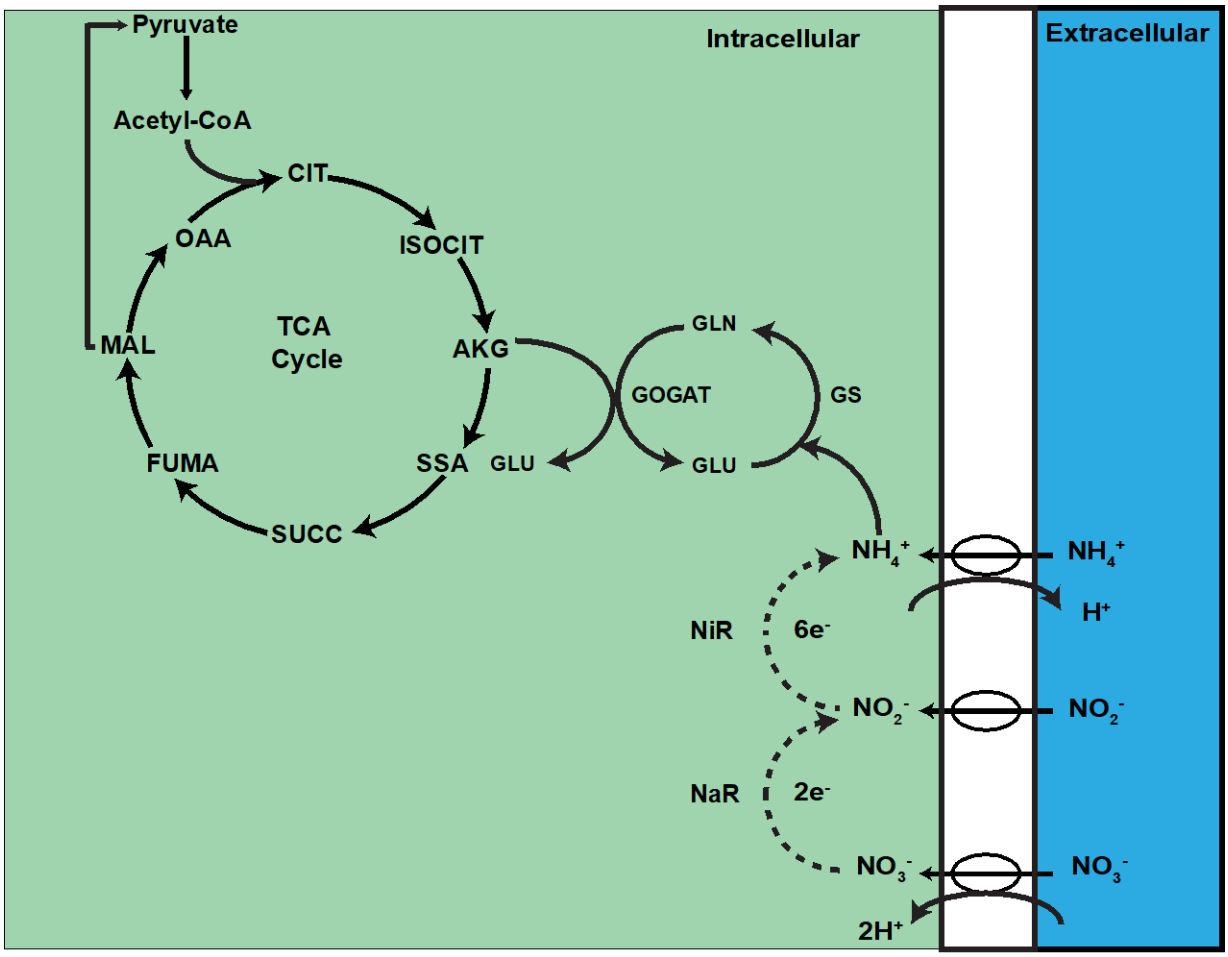

Figure 2-4. Uptake and Assimilation of Inorganic Nitrogen in Cyanobacteria.
Uptake in NO_3^- or NH_4^+ from the environment results in an increase or decrease in the extracellular pH, respectively. NO_3^- and NO_2^- require enzymatic reduction reactions to be converted into NH_4^+, which enters the GS-GOGAT cycle for assimilation and interaction of the TCA Cycle through AKG.

AKG levels vary as cells encounter different external nitrogen conditions (Muro-Pastor et al., 2001). AKG regulates the activity and/or binding of P_{II} signaling proteins (Forchhammer, 2004). (This regulatory partner swapping is summarized in **Fig. 2-5**). These proteins are thought to primarily regulate nitrogen uptake and metabolism in cyanobacteria (Schwarz et al., 2014), but have also been implicated in secondary interactions with carbon metabolism, such as fatty acid biosynthesis (Hauf et al., 2016). In conditions of NH_4^+ sufficiency (low AKG) and a low adenylate energy charge (AEC, an indicator of available metabolic energy) (Atkinson, 1968), P_{II} complexes with regulatory factor PipX, thereby sequestering PipX from interactions with the

global nitrogen transcriptional regulator NtcA. In this state of nitrogen abundance, P_{II} may also activate target enzyme N-acetylglutamate kinase (NAGK), which catalyzes the committed step in the arginine biosynthesis pathway to produce the nitrogen storage polymer, cyanophycin (Maheswaran et al., 2006). As cyanobacteria experience prolonged NH_4^+ limitation (moderate AKG), NtcA is activated and facilitates binding to target sites on the chromosome. NtcA overexpression in PCC 6803 significantly increased glycolytic flux (Koksharova et al., 1998), thereby increasing the pool size of several organic and amino acids (Osanai et al., 2014). This regulatory interaction was exploited in **Chapter 4** for enhanced production of L-Lactate. Severe NH_4^+ limitation (high AKG) and AEC lead to the phosphorylation and inactivation of P_{II}, thereby enhancing activated NtcA complex formation with PipX (Espinosa et al., 2014). The NtcA-PipX complex has been implicated in the strong activation of genes involved in inorganic and organic nitrogen transport, while repressing genes involved translation (Espinosa et al., 2014). As cyanobacteria experience extreme nitrogen limitation, degraded cyanophycin and phycobilisomes are recycled into the TCA cycle, resulting in a characteristic yellow-green color known as chlorosis (Krasikov et al., 2012).

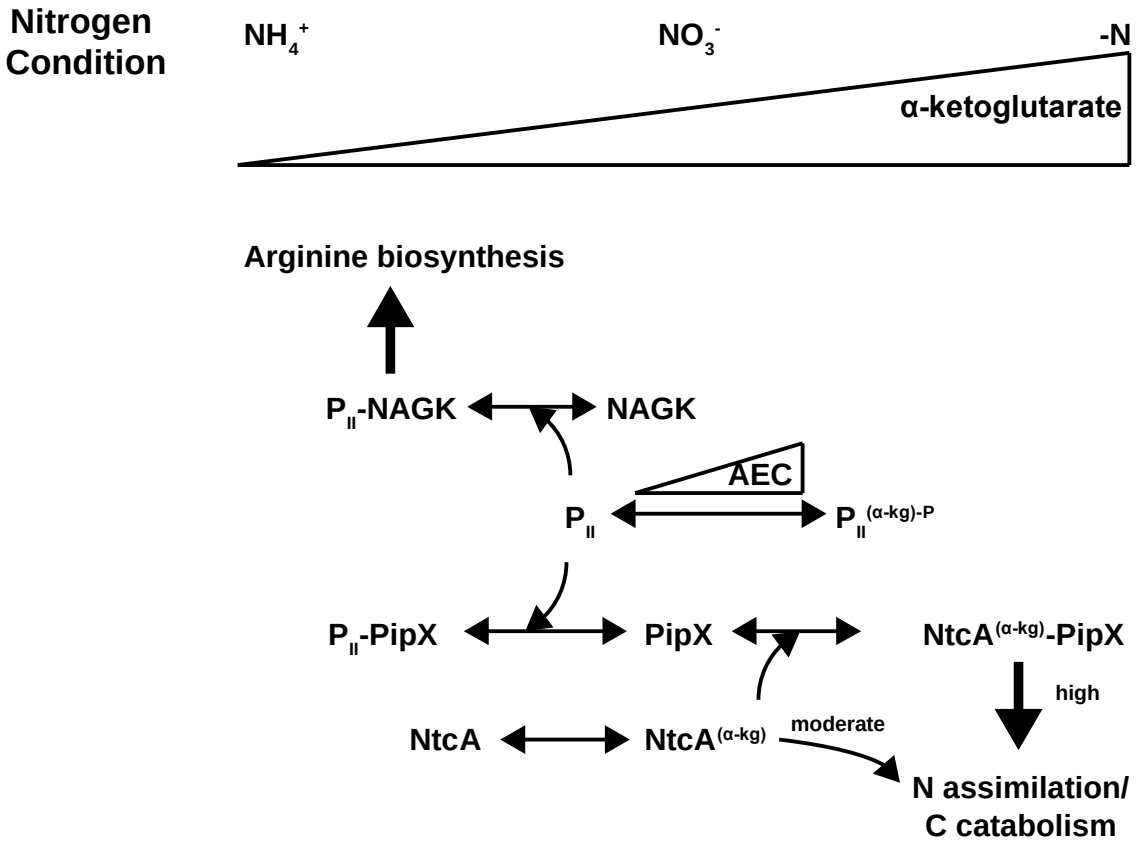

Figure 2-5. Regulation of Nitrogen Assimilation and Metabolism in Cyanobacteria.
As cyanobacteria assimilate NH_4^+, NO_3^-, or no nitrogen, intracellular levels of AKG are low, medium, and high, respectively. AKG levels and adenylate energy charge (AEC) control partner swapping with the P_{II} protein. With a high C:N ratio (low AKG), P_{II} interacts with and activates NAGK for the synthesis of cyanophycin. As AKG levels increase moderately, global nitrogen transcriptional regulator, NtcA, becomes activated and moderately effects genes involved in nitrogen assimilation and carbon catabolism. High intracellular levels of AKG facilitate complex formation of activated NtcA with regulatory factor, PipX, strongly inducing nitrogen assimilation genes and suppressing photosynthetic activity. Adapted from (Espinosa et al., 2014).

Direct assimilation of high concentrations of NH_4^+, like those found in centrate (Peccia et al., 2013), have also been demonstrated to accelerate photoinhibition and promote ROS formation in both microalgae and higher plants (Collos and Harrison, 2014; Dai et al., 2014). Studies comparing growth on a number of nitrogen sources in *Arabidopsis thaliana* have shown that NH_4^+ exposed plants have a higher NADPH/$NADP^+$ ratio, increased production of ROS (Podgórska et al., 2013), and upregulation in genes involved with the consumption of reducing equivalents (Hachiya et al., 2012), such as CO_2 fixation in PCC 7002 (Ludwig and Bryant, 2012b), consistent with the theory of reductive stress (Farhana et al., 2010; Lipinski, 2002).

However, cyanobacteria will preferentially uptake NH_4^+ over more oxidized nitrogen sources (Scherholz and Curtis, 2013), leading to a transporter imposed decrease in the external pH (Britto and Kronzucker, 2005). At high concentrations NH_4^+ may also interact with PSII and hinders the oxygen evolution process, thereby accelerating photoinhibition (Hou et al., 2011; Tsuno et al., 2011). The effect of NH_4^+ on the PSII activity of PCC 7002 has been not reported in the literature to date.

2.3 Literature Cited

Allahverdiyeva, Y., Mustila, H., Ermakova, M., Bersanini, L., Richaud, P., Ajlani, G., Battchikova, N., Cournac, L., Aro, E.-M., 2013. Flavodiiron proteins Flv1 and Flv3 enable cyanobacterial growth and photosynthesis under fluctuating light. Proc. Natl. Acad. Sci. U. S. A. 110, 4111–6. doi:10.1073/pnas.1221194110

Angermayr, S.A., Gorchs Rovira, A., Hellingwerf, K.J., 2015. Metabolic engineering of cyanobacteria for the synthesis of commodity products. Trends Biotechnol. 33, 352–361. doi:10.1016/j.tibtech.2015.03.009

Athanasiou, K., Dyson, B.C., Webster, R.E., Johnson, G.N., 2010. Dynamic acclimation of photosynthesis increases plant fitness in changing environments. Plant Physiol. 152, 366–73. doi:10.1104/pp.109.149351

Atkinson, D.E., 1968. The energy charge of the adenylate pool as a regulatory parameter. Interaction with feedback modifiers. Biochemistry 7, 4030–4034. doi:10.1021/bi00851a033

Baroukh, C., Muñoz-Tamayo, R., Steyer, J.-P., Bernard, O., 2015. A state of the art of metabolic networks of unicellular microalgae and cyanobacteria for biofuel production. Metab. Eng. 30, 49–60. doi:10.1016/j.ymben.2015.03.019

Beal, C.M., Hebner, R.E., Webber, M.E., Ruoff, R.S., Seibert, a. F., King, C.W., 2012. Comprehensive Evaluation of Algal Biofuel Production: Experimental and Target Results. Energies 5, 1943–1981. doi:10.3390/en5061943

Beal, C.M., Stillwell, A.S., King, C.W., Cohen, S.M., Berberoglu, H., Bhattarai, R.P., Connelly, R.L., Webber, M.E., Hebner, R.E., 2012. Energy Return on Investment for Algal Biofuel Production Coupled with Wastewater Treatment. Water Environ. Res. 84, 19.

Berg, I.A., 2011. Ecological aspects of the distribution of different autotrophic CO2 fixation pathways. Appl. Environ. Microbiol. 77, 1925–36. doi:10.1128/AEM.02473-10

Berla, B.M., Saha, R., Maranas, C.D., Pakrasi, H.B., 2015. Cyanobacterial Alkanes Modulate Photosynthetic Cyclic Electron Flow to Assist Growth under Cold Stress. Sci. Rep. 5, 14894. doi:10.1038/srep14894

Bersanini, L., Battchikova, N., Jokel, M., Rehman, A., Vass, I., Allahverdiyeva, Y., Aro, E.-M., 2014. Flavodiiron protein Flv2/Flv4-related photoprotective mechanism dissipates excitation pressure of PSII in cooperation with phycobilisomes in Cyanobacteria. Plant Physiol. 164, 805–18. doi:10.1104/pp.113.231969

Bozell, J.J., Petersen, G.R., 2010. Technology development for the production of biobased products from biorefinery carbohydrates—the US Department of Energy's "Top 10" revisited. Green Chem. 12, 539. doi:10.1039/b922014c

Britto, D.T., Kronzucker, H.J., 2005. Nitrogen acquisition, PEP carboxylase, and cellular pH homeostasis: new views on old paradigms. Plant, Cell Environ. 28, 1396–1409. doi:10.1111/j.1365-3040.2005.01372.x

Buchanan, B.B., Balmer, Y., 2005. Redox regulation: a broadening horizon. Annu. Rev. Plant Biol. 56, 187–220. doi:10.1146/annurev.arplant.56.032604.144246

Chen, X., Schreiber, K., Appel, J., Makowka, A., Fähnrich, B., Roettger, M., Hajirezaei, M., Sönnichsen, F., Schönheit, P., Martin, W.F., Gutekunst, K., 2016. The Entner-Doudoroff pathway is an overlooked glycolytic route in cyanobacteria and plants. Proc Natl Acad Sci U S A. doi:10.1073/pnas.1521916113

Chow, W.S., Melis, a, Anderson, J.M., 1990. Adjustments of photosystem stoichiometry in chloroplasts improve the quantum efficiency of photosynthesis. Proc. Natl. Acad. Sci. U. S. A. 87, 7502–7506. doi:10.1073/pnas.87.19.7502

Chubukov, V., Gerosa, L., Kochanowski, K., Sauer, U., 2014. Coordination of microbial metabolism. Nat. Rev. Microbiol. 12, 327–340. doi:10.1038/nrmicro3238

Clarens, A.F., Resurreccion, E.P., White, M. a, Colosi, L.M., 2010. Environmental life cycle comparison of algae to other bioenergy feedstocks. Environ. Sci. Technol. 44, 1813–9. doi:10.1021/es902838n

Collos, Y., Harrison, P.J., 2014. Acclimation and toxicity of high ammonium concentrations to unicellular algae. Mar. Pollut. Bull. 80, 8–23. doi:10.1016/j.marpolbul.2014.01.006

Dai, G.-Z., Qiu, B.-S., Forchhammer, K., 2014. Ammonium tolerance in the cyanobacterium Synechocystis sp. strain PCC 6803 and the role of the psbA multigene family. Plant. Cell Environ. 37, 840–51. doi:10.1111/pce.12202

Daley, S.M.E., Kappell, A.D., Carrick, M.J., Burnap, R.L., 2012. Regulation of the cyanobacterial CO2-concentrating mechanism involves internal sensing of NADP+ and α-ketogutarate levels by transcription factor CcmR. PLoS One 7, e41286. doi:10.1371/journal.pone.0041286

de Marsac, N.T., Lee, H.M., Hisbergues, M., Castets, A.M., Bedu, S., 2001. Control of nitrogen and carbon metabolism in cyanobacteria. J. Appl. Phycol. 13, 287–292.

Dickinson, K.E., Bjornsson, W.J., Garrison, L.L., Whitney, C.G., Park, K.C., Banskota, A.H., McGinn, P.J., 2015. Simultaneous remediation of nutrients from liquid anaerobic digestate and municipal wastewater by the microalga Scenedesmus sp. AMDD grown in continuous chemostats. J. Appl. Microbiol. 118, 75–83. doi:10.1111/jam.12681

Espinosa, J., Rodríguez-Mateos, F., Salinas, P., Lanza, V.F., Dixon, R., de la Cruz, F., Contreras, A., 2014. PipX, the coactivator of NtcA, is a global regulator in cyanobacteria. Proc. Natl. Acad. Sci. U. S. A. 111, E2423-30. doi:10.1073/pnas.1404097111

Fairley, P., 2011. Next generation biofuels. Nature 474, S2–S5.

Farhana, A., Guidry, L., Srivastava, A., Singh, A., Hondalus, M.K., Steyn, A.J.C., 2010. Reductive stress in microbes: implications for understanding Mycobacterium tuberculosis disease and persistence., Advances in microbial physiology. Elsevier Ltd. doi:10.1016/B978-0-12-381045-8.00002-3

Farooq, W., Suh, W.I., Park, M.S., Yang, J.W., 2015. Water use and its recycling in microalgae cultivation for biofuel application. Bioresour. Technol. 184, 73–81. doi:10.1016/j.biortech.2014.10.140

Flores, E., Herrero, A., 2004. Assimilatory Nitrogen Metabolism and Its Regulation, in: Bryant, D.A. (Ed.), The Molecular Biology of Cyanobacteria, Advances in Photosynthesis and Respiration. Springer Netherlands, Dordrecht, pp. 487–517. doi:10.1007/0-306-48205-3_16

Forchhammer, K., 2004. Global carbon/nitrogen control by PII signal transduction in cyanobacteria: From signals to targets. FEMS Microbiol. Rev. 28, 319–333. doi:10.1016/j.femsre.2003.11.001

Foyer, C.H., Neukermans, J., Queval, G., Noctor, G., Harbinson, J., 2012. Photosynthetic control of electron transport and the regulation of gene expression. J. Exp. Bot. 63, 1637–61. doi:10.1093/jxb/ers013

Hachiya, T., Watanabe, C.K., Fujimoto, M., Ishikawa, T., Takahara, K., Kawai-Yamada, M., Uchimiya, H., Uesono, Y., Terashima, I., Noguchi, K., 2012. Nitrate addition alleviates ammonium toxicity without lessening ammonium accumulation, organic acid depletion and inorganic cation depletion in Arabidopsis thaliana shoots. Plant Cell Physiol. 53, 577–91. doi:10.1093/pcp/pcs012

Hauf, W., Schmid, K., Gerhardt, E.C.M., Huergo, L.F., Forchhammer, K., 2016. Interaction of the nitrogen regulatory protein GlnB (PII) with biotin carboxyl carrier protein (BCCP) controls Acetyl-CoA levels in the cyanobacterium Synechocystis sp. PCC 6803. Front. Microbiol. 7, 1700. doi:10.3389/FMICB.2016.01700

Hendry, J.I., Prasannan, C., Ma, F., Möllers, K.B., Jaiswal, D., Digmurti, M., Allen, D.K., Frigaard, N.-U., Dasgupta, S., Wangikar, P.P., 2017. Rerouting of carbon flux in a glycogen mutant of cyanobacteria assessed via isotopically non-stationary 13C metabolic flux analysis. Biotechnol. Bioeng. n/a-n/a. doi:10.1002/bit.26350

Hihara, Y., Sonoike, K., Kanehisa, M., Ikeuchi, M., 2003. DNA Microarray Analysis of Redox-Responsive Genes in the Genome of the Cyanobacterium Synechocystis sp. Strain PCC 6803. J. Bacteriol. 185, 1719–1725. doi:10.1128/JB.185.5.1719

Hou, L.-H., Wu, C.-M., Huang, H.-H., Chu, H.-A., 2011. Effects of ammonia on the structure of the oxygen-evolving complex in photosystem II as revealed by light-induced FTIR difference spectroscopy. Biochemistry 50, 9248–54. doi:10.1021/bi200943q

Huergo, L.F., Dixon, R., 2015. The Emergence of 2-Oxoglutarate as a Master Regulator Metabolite. Microbiol. Mol. Biol. Rev. 79, 419–35. doi:10.1128/MMBR.00038-15

Keren, N., Krieger-Liszkay, A., 2011. Photoinhibition: molecular mechanisms and physiological significance. Physiol. Plant. 142, 1–5. doi:10.1111/j.1399-3054.2011.01467.x

Klementiev, K.E., Tsoraev, G. V, Tyutyaev, E. V, Zorina, A.A., Feduraev, P. V, Allakhverdiev, S.I., Paschenko, V.Z., 2017. Membrane fluidity controls redox-regulated cold stress responses in cyanobacteria. Photosynth. Res. 0, 0. doi:10.1007/s11120-017-0337-3

Koksharova, O., Schubert, M., Shestakov, S., Cerff, R., 1998. Genetic and biochemical evidence for distinct key functions of two highly divergent GAPDH genes in catabolic and anabolic carbon flow of the cyanobacterium. Plant Mol. Biol. 183–194.

Kramer, D.M., Evans, J.R., 2011. The importance of energy balance in improving photosynthetic productivity. Plant Physiol. 155, 70–78. doi:10.1104/pp.110.166652

Krasikov, V., Aguirre von Wobeser, E., Dekker, H.L., Huisman, J., Matthijs, H.C.P., 2012. Time-series resolution of gradual nitrogen starvation and its impact on photosynthesis in the

cyanobacterium Synechocystis PCC 6803. Physiol. Plant. 145, 426–39. doi:10.1111/j.1399-3054.2012.01585.x

Latifi, A., Ruiz, M., Zhang, C.-C., 2009. Oxidative stress in cyanobacteria. FEMS Microbiol. Rev. 33, 258–78. doi:10.1111/j.1574-6976.2008.00134.x

Laue, P., Bährs, H., Chakrabarti, S., Steinberg, C.E.W., 2014. Natural xenobiotics to prevent cyanobacterial and algal growth in freshwater: Contrasting efficacy of tannic acid, gallic acid, and gramine. Chemosphere 104, 212–220. doi:10.1016/j.chemosphere.2013.11.029

Lea-Smith, D.J., Bombelli, P., Vasudevan, R., Howe, C.J., 2016. Photosynthetic, respiratory and extracellular electron transport pathways in cyanobacteria. Biochim. Biophys. Acta - Bioenerg. 1857, 247–255. doi:10.1016/j.bbabio.2015.10.007

Leister, D., Shikanai, T., 2013. Complexities and protein complexes in the antimycin A-sensitive pathway of cyclic electron flow in plants. Front. Plant Sci. 4, 161. doi:10.3389/fpls.2013.00161

Lipinski, B., 2002. Evidence in support of a concept of reductive stress. Br. J. Nutr. 87, 93–4; discussion 94. doi:10.1079/BJN2001435

Liu, L.-N., Bryan, S.J., Huang, F., Yu, J., Nixon, P.J., Rich, P.R., Mullineaux, C.W., 2012. Control of electron transport routes through redox-regulated redistribution of respiratory complexes. Proc. Natl. Acad. Sci. U. S. A. 109, 11431–6. doi:10.1073/pnas.1120960109

Llácer, J.L., Espinosa, J., Castells, M.A., Contreras, A., Forchhammer, K., Rubio, V., 2010. Structural basis for the regulation of NtcA-dependent transcription by proteins PipX and PII. Proc. Natl. Acad. Sci. U. S. A. 107, 15397–402. doi:10.1073/pnas.1007015107

Ludwig, M., Bryant, D.A., 2012a. Synechococcus sp. Strain PCC 7002 Transcriptome: Acclimation to Temperature, Salinity, Oxidative Stress, and Mixotrophic Growth Conditions. Front. Microbiol. 3, 354. doi:10.3389/fmicb.2012.00354

Ludwig, M., Bryant, D.A., 2012b. Acclimation of the Global Transcriptome of the Cyanobacterium Synechococcus sp. Strain PCC 7002 to Nutrient Limitations and Different Nitrogen Sources. Front. Microbiol. 3, 145. doi:10.3389/fmicb.2012.00145

Ludwig, M., Bryant, D.A., 2011. Transcription Profiling of the Model Cyanobacterium Synechococcus sp. Strain PCC 7002 by Next-Gen (SOLiDTM) Sequencing of cDNA. Front. Microbiol. 2, 41. doi:10.3389/fmicb.2011.00041

Maheswaran, M., Ziegler, K., Lockau, W., Hagemann, M., Forchhammer, K., 2006. PII -Regulated Arginine Synthesis Controls Accumulation of Cyanophycin in Synechocystis sp . Strain PCC 6803. J. Bacteriol. 188, 2730–2734. doi:10.1128/JB.188.7.2730

Metcalf, L., Eddy, H., Tchobanoglous, G., 1972. Wastewater engineering: treatment, disposal, and reuse. McGraw-Hill Education.

Mizusawa, N., Wada, H., 2012. The role of lipids in photosystem II. Biochim. Biophys. Acta - Bioenerg. 1817, 194–208. doi:10.1016/j.bbabio.2011.04.008

Mostafa, S., Rosario-Ortiz, F., 2013. Singlet oxygen formation from wastewater organic matter. Environ. Sci. Technol.

Mueller-Cajar, O., Stotz, M., Bracher, A., 2014. Maintaining photosynthetic CO2 fixation via protein remodelling: the Rubisco activases. Photosynth. Res. 119, 191–201. doi:10.1007/s11120-013-9819-0

Mullineaux, C.W., 2014. Co-existence of photosynthetic and respiratory activities in cyanobacterial thylakoid membranes ☆. BBA - Bioenerg. 1837, 503–511. doi:10.1016/j.bbabio.2013.11.017

Mulo, P., Sakurai, I., Aro, E.-M., 2012. Strategies for psbA gene expression in cyanobacteria, green algae and higher plants: from transcription to PSII repair. Biochim. Biophys. Acta 1817, 247–57. doi:10.1016/j.bbabio.2011.04.011

Muro-Pastor, M.I., Florencio, F.J., 2003. Regulation of ammonium assimilation in cyanobacteria. Plant Physiol. Biochem. 41, 595–603. doi:10.1016/S0981-9428(03)00066-4

Muro-Pastor, M.I., Reyes, J.C., Florencio, F.J., 2001. Cyanobacteria Perceive Nitrogen Status by Sensing Intracellular 2-Oxoglutarate Levels. J. Biol. Chem. 276, 38320–38328. doi:10.1074/jbc.M105297200

Nagarajan, A., Pakrasi, H.B., 2001. Membrane-Bound Protein Complexes for Photosynthesis and Respiration in Cyanobacteria, in: eLS. John Wiley & Sons, Ltd. doi:10.1002/9780470015902.a0001670.pub2

Neilen, A., W. Hawker, D., R. O'Brien, K., Burford, M., 2017. Phytotoxic effects of terrestrial dissolved organic matter on a freshwater cyanobacteria and green algae species is affected by plant source and DOM chemical composition, Chemosphere. doi:10.1016/j.chemosphere.2017.06.063

Nishiyama, Y., Murata, N., 2014. Revised scheme for the mechanism of photoinhibition and its application to enhance the abiotic stress tolerance of the photosynthetic machinery. Appl. Microbiol. Biotechnol. 1. doi:10.1007/s00253-014-6020-0

Nomura, C., Bryant, D.A., 1999. Cytochrome c6 from synechococcus sp. PCC 7002, in: Peschek, G.A., Löffelhardt, W., Schmetterer, G. (Eds.), The Phototrophic Prokaryotes. Springer US, Boston, MA, pp. 269–274. doi:10.1007/978-1-4615-4827-0_31

Ogawa, T., Mi, H., 2007. Cyanobacterial NADPH dehydrogenase complexes. Photosynth. Res. 93, 69–77. doi:10.1007/s11120-006-9128-y

Olguín, E.J., Galicia, S., Camacho, R., Mercado, G., Pérez, T.J., 1997. Production of Spirulina sp. in sea water supplemented with anaerobic effluents in outdoor raceways under temperate climatic conditions. Appl. Microbiol. Biotechnol. 48, 242–247. doi:10.1007/s002530051045

Orfield, N.D., Fang, A.J., Valdez, P.J., Nelson, M.C., Savage, P.E., Lin, X.N., Keoleian, G.A., 2014. Life cycle design of an algal biorefinery featuring hydrothermal liquefaction: Effect of reaction conditions and an alternative pathway including microbial regrowth. ACS Sustain. Chem. Eng. 2, 867–874. doi:10.1021/sc4004983

Osanai, T., Oikawa, A., Iijima, H., Kuwahara, A., Asayama, M., Tanaka, K., Ikeuchi, M., Saito, K., Hirai, M.Y., 2014. Metabolomic Analysis Reveals Rewiring of Synechocystis sp. PCC 6803 Primary Metabolism by ntcA-overexpression., Environmental microbiology. doi:10.1111/1462-2920.12554

Parry, M.A.J., Andralojc, P.J., Scales, J.C., Salvucci, M.E., Carmo-Silva, A.E., Alonso, H., Whitney, S.M., 2012. Rubisco activity and regulation as targets for crop improvement. J. Exp. Bot. ers336-. doi:10.1093/jxb/ers336

Patzelt, D.J., Hindersin, S., Elsayed, S., Boukis, N., Kerner, M., Hanelt, D., 2015a. Hydrothermal gasification of Acutodesmus obliquus for renewable energy production and nutrient recycling of microalgal mass cultures. J. Appl. Phycol. 27, 2239–2250. doi:10.1007/s10811-014-0496-y

Patzelt, D.J., Hindersin, S., Kerner, M., Hanelt, D., 2015b. Responses of photosystems I and II of Acutodesmus obliquus to chemical stress caused by the use of recycled nutrients. Appl. Microb. CELL Physiol. doi:10.1007/s00253-015-7008-0

Peccia, J., Haznedaroglu, B., Gutierrez, J., Zimmerman, J.B., 2013. Nitrogen supply is an important driver of sustainable microalgae biofuel production. Trends Biotechnol. 31, 134–8. doi:10.1016/j.tibtech.2013.01.010

Pflugmacher, S., Pietsch, C., Rieger, W., Steinberg, C.E.W., 2006. Dissolved natural organic matter (NOM) impacts photosynthetic oxygen production and electron transport in coontail

Ceratophyllum demersum. Sci. Total Environ. 357, 169–175. doi:10.1016/j.scitotenv.2005.03.021

Pflugmacher, S., Spangenberg, M., Steinberg, C.E.W., 1999. Dissolved organic matter (DOM) and effects on the aquatic macrophyte Ceratophyllum demersum in relation to photosynthesis, pigmentpattern and activity of detoxication enzymes. J. Appl. Bot. 73, 184–190.

Podgórska, A., Gieczewska, K., Łukawska-Kuźma, K., Rasmusson, A.G., Gardeström, P., Szal, B., 2013. Long-term ammonium nutrition of Arabidopsis increases the extrachloroplastic NAD(P)H/NAD(P)(+) ratio and mitochondrial reactive oxygen species level in leaves but does not impair photosynthetic capacity. Plant. Cell Environ. 36, 2034–45. doi:10.1111/pce.12113

Price, G.D., 2011. Inorganic carbon transporters of the cyanobacterial CO2 concentrating mechanism, in: Photosynthesis Research. doi:10.1007/s11120-010-9608-y

Price, G.D., Badger, M.R., Woodger, F.J., Long, B.M., 2008. Advances in understanding the cyanobacterial CO2-concentrating-mechanism (CCM): functional components, Ci transporters, diversity, genetic regulation and prospects for engineering into plants. J. Exp. Bot. 59, 1441–61. doi:10.1093/jxb/erm112

Price, G.D., Woodger, F.J., Badger, M.R., Howitt, S.M., Tucker, L., 2004. Identification of a SulP-type bicarbonate transporter in marine cyanobacteria. Proc. Natl. Acad. Sci. 101, 18228–18233. doi:10.1073/pnas.0405211101

Razon, L., 2014. Life cycle analysis of an alternative to the haber-bosch process: Non-renewable energy usage and global warming potential of liquid ammonia from cyanobacteria. Environ. Prog. Sustain. Energy 33. doi:10.1002/ep

Rochaix, J.D., 2011. Reprint of: Regulation of photosynthetic electron transport. Biochim. Biophys. Acta - Bioenerg. 1807, 878–886. doi:10.1016/j.bbabio.2011.05.009

Rose, A.L., 2012. The influence of extracellular superoxide on iron redox chemistry and bioavailability to aquatic microorganisms. Front. Microbiol. 3, 124. doi:10.3389/fmicb.2012.00124

Ruiz-Martinez, A., Martin Garcia, N., Romero, I., Seco, A., Ferrer, J., 2012. Microalgae cultivation in wastewater: Nutrient removal from anaerobic membrane bioreactor effluent. Bioresour. Technol. 126, 247–253.

Scherholz, M.L., Curtis, W.R., 2013. Achieving pH control in microalgal cultures through fed-batch addition of stoichiometrically-balanced growth media. BMC Biotechnol. 13, 39. doi:10.1186/1472-6750-13-39

Schwarz, D., Orf, I., Kopka, J., Hagemann, M., 2014. Effects of Inorganic Carbon Limitation on the Metabolome of the Synechocystis sp. PCC 6803 Mutant Defective in glnB Encoding the Central Regulator PII of Cyanobacterial C/N Acclimation. Metabolites 4, 232–47. doi:10.3390/metabo4020232

Tabita, F.R., Satagopan, S., Hanson, T.E., Kreel, N.E., Scott, S.S., 2008. Distinct form I, II, III, and IV Rubisco proteins from the three kingdoms of life provide clues about Rubisco evolution and structure/function relationships. J. Exp. Bot. 59, 1515–1524. doi:10.1093/jxb/erm361

Takahashi, S., Milward, S.E., Fan, D.-Y., Chow, W.S., Badger, M.R., 2009. How does cyclic electron flow alleviate photoinhibition in Arabidopsis? Plant Physiol. 149, 1560–7. doi:10.1104/pp.108.134122

Tasaka, Y., Gombos, Z., Nishiyama, Y., Mohanty, P., Ohba, T., Ohki, K., Murata, N., 1996. Targeted mutagenesis of acyl-lipid desaturases in Synechocystis: evidence for the important roles of polyunsaturated membrane lipids in growth, respiration and photosynthesis. EMBO J. 15, 6416–25.

Tsuno, M., Suzuki, H., Kondo, T., Mino, H., Noguchi, T., 2011. Interaction and inhibitory effect of ammonium cation in the oxygen evolving center of photosystem II. Biochemistry 50, 2506–14. doi:10.1021/bi101952g

Voss, I., Sunil, B., Scheibe, R., Raghavendra, A.S., 2013. Emerging concept for the role of photorespiration as an important part of abiotic stress response. Plant Biol. (Stuttg). 15, 713–22. doi:10.1111/j.1438-8677.2012.00710.x

Wada, H., Murata, N., 1998. Membrane Lipids in Cyanobacteria, in: Paul-André, S., Norio, M. (Eds.), Lipids in Photosynthesis: Structure, Function and Genetics. Springer Netherlands, Dordrecht, pp. 65–81. doi:10.1007/0-306-48087-5_4

Wan, N., DeLorenzo, D.M., He, L., You, L., Immethun, C.M., Wang, G., Baidoo, E.E.K., Hollinshead, W., Keasling, J.D., Moon, T.S., Tang, Y.J., 2017. Cyanobacterial carbon metabolism: Fluxome plasticity and oxygen dependence. Biotechnol. Bioeng. 1–32. doi:10.1002/bit.26287

Wang, L., Min, M., Li, Y., Chen, P., Chen, Y., Liu, Y., Wang, Y., Ruan, R., 2010. Cultivation of green algae Chlorella sp. in different wastewaters from municipal wastewater treatment plant. Appl. Biochem. Biotechnol. 162, 1174–86. doi:10.1007/s12010-009-8866-7

White, D., Drummond, J., Fuqua, C., 2012. The Physiology and Biochemistry of Prokaryotes, 4th ed. Oxford University Press.

Williams, W.P., 1998. The Physical Properties of Thylakoid Membrane Lipids and Their Relation to Photosynthesis, in: Paul-André, S., Norio, M. (Eds.), Lipids in Photosynthesis: Structure, Function and Genetics. Springer Netherlands, Dordrecht, pp. 103–118. doi:10.1007/0-306-48087-5_6

Woodger, F.J., Bryant, D.A., Price, G.D., 2007. Transcriptional regulation of the CO2-concentrating mechanism in a euryhaline, coastal marine cyanobacterium, Synechococcus sp. Strain PCC 7002: role of NdhR/CcmR. J. Bacteriol. 189, 3335–47. doi:10.1128/JB.01745-06

Wright, A., Ansong, C., Sadler, N., 2014. Characterization of protein redox dynamics induced during light-to-dark transitions and nutrient limitation in cyanobacteria. Syst. … 5, 1–10. doi:10.6019/PXD000897.A

Yamamoto, Y., 2016. Quality Control of Photosystem II: The Mechanisms for Avoidance and Tolerance of Light and Heat Stresses are Closely Linked to Membrane Fluidity of the Thylakoids. Front. Plant Sci. 7, 1136. doi:10.3389/fpls.2016.01136

Young, J.D., Shastri, A. a, Stephanopoulos, G., Morgan, J. a, 2011. Mapping photoautotrophic metabolism with isotopically nonstationary (13)C flux analysis. Metab. Eng. 13, 656–65. doi:10.1016/j.ymben.2011.08.002

Yutthanasirikul, R., Nagano, T., Jimbo, H., Hihara, Y., Kanamori, T., Ueda, T., Haruyama, T., Konno, H., Yoshida, K., Hisabori, T., Nishiyama, Y., 2016. Oxidation of a cysteine residue in elongation factor EF-Tu reversibly inhibits translation in the cyanobacterium Synechocystis sp. PCC 6803. J. Biol. Chem. 291, 5860–5870. doi:10.1074/jbc.M115.706424

Zavafer, A., Cheah, M.H., Hillier, W., Chow, W.S., Takahashi, S., 2015. Photodamage to the oxygen evolving complex of photosystem II by visible light. Sci. Rep. 5, 16363. doi:10.1038/srep16363

Zhang, D., Yan, S., Song, W., 2014. Photochemically Induced Formation of Reactive Oxygen Species (ROS) from Effluents Organic Matter. Environ. Sci. Technol.

Zhang, P., Allahverdiyeva, Y., Eisenhut, M., Aro, E.-M., 2009. Flavodiiron proteins in oxygenic photosynthetic organisms: photoprotection of photosystem II by Flv2 and Flv4 in Synechocystis sp. PCC 6803. PLoS One 4, e5331. doi:10.1371/journal.pone.0005331

Zhang, Y., Kendall, A., Yuan, J., 2014. A comparison of on-site nutrient and energy recycling technologies in algal oil production. Resour. Conserv. Recycl. 88, 13–20. doi:10.1016/j.resconrec.2014.04.011

CHAPTER 3 CYANOBACTERIAL GROWTH ON MUNICIPAL WASTEWATER REQUIRES LOW TEMPERATURES

Travis C. Korosh[a,b], Andrew Dutcher[c], Brian F. Pfleger [a,d,], and Katherine D. McMahon [c,e]

[a] Department of Chemical and Biological Engineering, University of Wisconsin-Madison, Madison, WI 53706, United States
[b] Environmental Chemistry and Technology Program, University of Wisconsin-Madison, Madison, WI 53706, United States
[c] Department of Civil and Environmental Engineering, University of Wisconsin-Madison, Madison, WI 53706, United States
[d] Microbiology Doctoral Training Program, University of Wisconsin-Madison, Madison, WI 53706, United States
[e] Department of Bacteriology, University of Wisconsin-Madison, Madison, WI 53706, United States

Author Contributions:

Travis C. Korosh- constructed the strain used for experiments, performed EEM and UV-VIS analysis, oxygen evolution and fluorescence measurements, fatty acid methyl ester (FAME) derivatization and extraction, and drafting of the manuscript.
Andrew Dutcher- performed batch cultivations, flow cytometry, and GBF filtration and nutrient quantification.
Brian F. Pfleger-supervised research and provided critical feedback of the manuscript.
Katherine D. McMahon- supervised research and provided critical feedback of the manuscript.

Part of this chapter is adapted from *bioRxiv*, Travis C. Korosh, Andrew Dutcher, Brian F. Pfleger, Katherine D. McMahon, Cyanobacterial Growth on Municipal Wastewater Requires Low Temperatures, Copyright 2017.

3.1 Abstract

Side-streams in wastewater treatment plants can serve as concentrated sources of nutrients (i.e. nitrogen and phosphorus) to support the growth of photosynthetic organisms that ultimately serve as feedstock for production of fuels and chemicals. However, other chemical characteristics of these streams may inhibit growth in unanticipated ways. Here, we evaluated the use of liquid recovered from municipal anaerobic digesters via gravity belt filtration as a nutrient source for growing the cyanobacterium *Synechococcus* sp. strain PCC 7002. The gravity belt filtrate (GBF) contained high levels of complex dissolved organic matter (DOM), which seemed to negatively influence cells. We investigated the impact of GBF on physiological parameters such as growth rate, membrane integrity, membrane composition, photosystem composition, and oxygen evolution from photosystem II. At 37°C, we observed an inverse correlation between GBF concentration and membrane integrity. Radical production was also detected upon exposure to GBF at 37°C. However, at 27°C the dose dependent relationship between GBF concentration and lack of membrane integrity was abolished. Immediate resuspension of strains in high doses of GBF showed markedly reduced oxygen evolution rates relative to the control. Together, this suggests that one mechanism responsible for GBF toxicity to *Synechococcus* is the interruption of photosynthetic electron flow and subsequent phenomena. We hypothesize this is likely due to the presence of phenolic compounds within the DOM.

3.2 Introduction

The need to develop non-petroleum based platforms for fuel and chemical production is driving researchers to explore alternatives that harness renewable energy sources while minimizing other environmental impacts as freshwater depletion, eutrophication, and the use of

arable land for non-food production. Cyanobacteria are particularly attractive such platforms due to their genetic tractability, rapid growth rates, halotolerance, and ability to be grown on non-productive land with simple nutrient requirements (Oliver and Atsumi, 2014; Pate et al., 2011). According to published life cycle assessments, a large portion of the associated costs of culturing photoautotrophs are tied to upstream costs, such as CO_2 delivery and fertilizer application (Clarens et al., 2010). High phosphorus/nitrogen removal rates and energy efficiencies have been reported for photobioreactor and open pond cultivation systems using wastewater streams rich in nitrogen and phosphorus (Posadas et al., 2014; Sturm and Lamer, 2011). Therefore, it may be possible to offset the requirement for fertilizer by reclaiming nutrients from wastewater. This approach could yield the sought-after non-petroleum based alternative while also providing a more effective means of nutrient and metal removal than conventional wastewater treatment (de la Noüe et al., 1992; Hoffmann, 1998; Olguín, 2012). Side-streams from common wastewater treatment facilities such as supernatants or filtrates from solids-separation processes are particularly promising nutrient sources, assuming that cyanobacterial strains can efficiently use them.

Of the many streams available in common wastewater facilities, the liquid fraction of anaerobic digestate is thought to be the most attractive nutrient source (Olguín, 2012; Peccia et al., 2013; Rawat et al., 2011; Wang et al., 2010). Although digestate is rich in the inorganic constituents necessary for growth, it also contains dissolved organic matter (DOM) that has been shown to limit photosynthetic activity (Pflugmacher et al., 1999). DOM is a heterogenous mixture of aliphatic and aromatic compounds derived from the decomposition of living organisms (Zsolnay, 2003). The chemical nature of wastewater-derived DOM is largely governed by the type of treated waste and the treatment process, but it is largely comprised of

hydrophilic, fulvic, and humic substances (Akhiar et al., 2016; Imai et al., 2002). Humics can induce damaging permeability in model and bacterial membranes (Ojwang' and Cook, 2013; Vigneault et al., 2000). Various studies have also demonstrated that fulvic and humic acids can enhance the solubility of many organic compounds (Chiou et al., 1986), which in turn would augment their bioavailability and potential membrane permeability. Many of these compounds are also photo-reactive, producing toxic hydrogen peroxide and hydroxyl radicals (Lee et al., 2013; Zhang et al., 2014), which is of significant concern for phototroph cultivation.

The mode of DOM toxicity is thought to involve interactions with the protein-pigment complex of photosystem II (PSII) in photosynthetic organisms, although the exact molecular mechanism remains unclear (Laue et al., 2014). When the rate of light induced damage to PSII exceeds its rate of repair, growth suppression and chlorosis result from the phenomena known as photoinhibition (Keren and Krieger-Liszkay, 2011). When damage by photoinhibition is sufficient to hamper the natural ability to consume electrons generated by photosynthesis, reactive oxygen species (ROS) are concomitantly produced as an undesired by-product. Prolonged oxidative stress halts protein translation through oxidation of specific cysteine residues in the ribosomal elongation factors (Nagano et al., 2012). Given these findings, it is increasingly evident that under conditions of sustained stress, regulation of electron flow is critical to maintain homeostasis in photosynthetic organisms (Foyer et al., 2012; Voss et al., 2013). Thus, it is important to understand the mechanisms by which DOM may be interrupting electron flow in order to capitalize on the potential of cyanobacteria to remediate wastewater and generate high-value chemicals.

In this study, we tested the practicality of using combined streams from a municipal wastewater plant as a nutrient source for cyanobacterial cultivation. We used the euryhaline

cyanobacterium *Synechococcus* sp. strain PCC 7002 (PCC 7002) due to its exceptional tolerance to high light intensity, salt, and other environmental stresses (Ruffing, 2011; Xu et al., 2011). Initial attempts to grow PCC 7002 in this nutrient source under standard environmental conditions for this strain (1% (v/v) CO_2, a temperature of 37°C, and illumination of 200 µmol photons $m^{-2}s^{-1}$) resulted in photobleached (white-yellow) cultures. In an effort to explain this observation while developing more feasible cultivation conditions, we assessed the effects of many environmental parameters during PCC 7002 cultivation in wastewater-based media by monitoring changes in growth rate, photopigment abundance, oxygen evolution rates, membrane integrity, and membrane composition. High GBF concentrations were associated with elevated DOM levels. Decreased photosynthetic oxygen production rates were also noted upon exposure to high levels of GBF. We observed marked membrane permeability, photosystem degradation, low growth rates, in addition to ROS production for cultures exposed to GBF at 37°C. At 27°C, cultures grown on GBF had lessened membrane permeability, robust growth rates, as well as high levels of total fatty acids and an elevated unsaturated fatty acid content relative to control. This suggests tolerance to the photoinhibitory compound in GBF is governed by changes in membrane content and composition that occur during growth.

3.3 Materials and Methods

3.3.1 Medium and Growth Conditions

Wild type (WT) *Synechococcus* sp. strain PCC 7002 was obtained from the Pasteur Culture Collection of Cyanobacteria. Experiments were performed with a mutant strain of PCC 7002 harboring the *aaC1* gene encoding a gentamicin resistance marker in the A2842 locus to

maintain axenic cultures. Strains were grown and maintained on Medium A^+ (Stevens et al., 1973) supplemented with 5 µM $NiSO_4$ (Sakamoto and Bryant, 2001) with 1.5% Bacto-Agar. Strains were cultured in 250 ml baffled flasks with 50 mL media with 1% CO_2-enriched air at 150 rpm in a Kuhner ISF1-X orbital shaker. Temperature was maintained at 37°C or 27°C and light intensity was fixed at approximately 200 µmol photons $m^{-2}s^{-1}$ or 100 µmol photons $m^{-2}s^{-1}$ via a custom LED panel. Strains were pre-acclimated to the culture conditions overnight before inoculating in fresh media. Optical density at 730 nm was measured in a Tecan M1000 plate reader.

Wastewater-derived media was obtained from the Nine Springs Wastewater Treatment Plant (Dane County, Wisconsin, USA). The plant is configured for biological nutrient removal via a modified University of Cape Town process with no internal nitrate recycling and stable performance yielding high secondary effluent quality (total phosphorus < 1 mg P/L, ammonia < 1 mg N/L, nitrate ~ 15 mg N/L) (Flowers et al., 2013). Anaerobic digesters are used for solids stabilization and the resulting digested material is passed over a gravity belt filter for dewatering. The system includes an Ostara WASSTRIP process to recover phosphorus. This filtrate (GBF) served as the primary source of phosphorus and reduced nitrogen for our cultures, and effluent from the post-mainstream secondary treatment clarifier (secondary effluent) served as a diluent. GBF was filtered through a paper filter to remove any exceptionally large flocs, then stored at -80°C until use. Secondary effluent was collected one to four days before each experiment and held under refrigeration at approximately 2°C. Experimental media was comprised primarily of secondary clarifier effluent and GBF, combined in different proportions. Unless otherwise noted, GBF was used at a concentration of 12.5% (v/v) in secondary effluent, supplemented with trace metals and vitamin B12 at the concentrations found in Medium A^+, as well as KH_2PO_4 at a molar

ratio of 1:32 soluble reactive phosphorus (SRP) to bioavailable nitrogen (the sum of NH_4^+ and NO_3^-). All media was buffered with Tris-HCl and adjusted to pH 8.0 with potassium hydroxide or hydrochloric acid before sterilization by autoclaving, and gentamycin was added at working concentrations (30 μg/mL) after cooling.

3.3.2 Staining, Flow Cytometry, and Fluorescence Measurements

The membrane permeability of cyanobacteria cells was recorded by a flow cytometer (FACSCalibur, BD Biosciences, San Jose, CA, USA). After growth in the respective media, cells were centrifuged (2 minutes, 5000 RCF), decanted, and resuspended in 1 mL of Tris-Buffered Saline (TBS) solution (pH 8.0). To identify membrane-compromised cells, SYTOX Green (Life Technologies) was also added to each sample (1 μM). SYTO 59 (Life Technologies) was added to each sample (1 μM) as a nucleic acid counterstain. As a control for a permeabilized membrane, cells were resuspended in 190 proof ethanol. SYTOX green fluorescence was visualized using 488 nm laser excitation and emission area was read using a 530/30 nm bandpass filter. The 633-nm laser coupled with a 661/16 bandpass filter was used for SYTO 59 visualization. Analysis of the cytometric data was carried out with CellQuest Pro (BDBiosciences, San Jose,CA, USA) software.

To assess reactive oxygen species production, cells (OD_{730} = 1) were incubated overnight in Medium A^+, 12.5 % (v/v) GBF, 12.5 % (v/v) GBF + 1 mM Dithiothreitol (DTT), 12.5 % (v/v) GBF + 1 mM N-acetylcysteine (NAC), or Medium A^+ + 100 μM methyl viologen as a positive control at 37°C with 5% CO_2 at a light intensity of 200 μmol photons $m^{-2}s^{-1}$. Cells were washed in TBS, and either Sytox Green (1 μM) or CellROX Orange reagent (Life Technologies) (5 μM) was added. After 30 min incubation in darkness at 37°C, fluorescence was measured (Ex/Em 545/565

nm for Cell ROX Orange) and (Ex/Em 504/523 nm for Sytox Green) in a Tecan M1000 plate reader.

3.3.3 GBF Characterization

SRP, ammonia, nitrate, and nitrite concentrations were determined for all secondary clarifier effluent and GBF samples used in these experiments. In addition, the GBF was tested for total suspended solids (TSS), volatile suspended solids (VSS) total solids (TS), and chemical oxygen demand (COD). Ammonia, SRP, and COD concentrations were determined by colorimetric tests using reagents from Hach. Nitrate and nitrite were determined using high performance liquid chromatography (Shimadzu) with a C18 column and photodiode array detector (He and McMahon, 2011). TSS, VSS, and TS were measured according to Standard Method 2540 D, 2540 E, and 2540 B, respectively, with 47 mm diameter glass fiber filters (Whatman) used for TSS and VSS (Eaton and Franson, 2005). Fluorescence EEM measurements and UV-Vis absorbance scans were conducted using a M1000 Tecan plate reader using a UV-transparent plate (Costar 3635). Fluorescence intensity was normalized to quinine sulfate units (QSU), where 1 QSU is the maximum fluorescence intensity of 1 ppm of quinine sulfate in 0.1 N H_2SO_4 at Ex/Em = 350/450. Rayleigh scatter effects were removed from the data set.

3.3.4 Biochemical Analyses

Batch cultures were further assayed for fatty acid content, oxygen evolution rates, and chlorophyll a content. Cells were concentrated by centrifugation, washed in TBS, and lyophilized overnight to obtain dry cell weights (DCW). Fatty acids from approximately 10 mg of DCW with 10 mg/ml pentadecanoic acid as an internal standard were converted to methyl-

esters, extracted with n-hexane and analyzed by GC-FID on a Restek Stabilwax column (60m, 0.53 mm ID, 0.50 µm) (Lennen et al., 2010). Photosynthetic oxygen evolution from whole cells was measured with a Unisense MicroOptode oxygen electrode with 10 mM $NaHCO_3$ illuminated with a slide projector at photosynthetic photon flux densities ranging from 76-2700 µmol photons m^{-2} s^{-1} for 10 min at room temperature (Sakamoto and Bryant, 2002). Cells were collected by centrifugation and resuspended in the appropriate media to give an OD_{730} = 1.0. Chlorophyll a measurements were done via a 100% chilled methanol extraction procedure (Miyashita et al., 1997). Chlorophyll a was calculated via the following equation: $Chl_a = 16.29 * A^{665} - 8.54 * A^{652}$ (Porra et al., 1989).

3.4 Results

3.4.1 GBF and Secondary Effluent Characteristics

We measured nutrient concentrations from the batches of GBF collected over the 6-month experimental period (**Table 3-1** and **Table 3-2**), to ascertain if it was a stable and reliable nutrient source for cultivating the cyanobacteria. Sampling points from the Nine Springs Wastewater Treatment Plant (Dane County, Wisconsin, USA) are shown in **Fig. 3-1**. To calculate nutrient stoichiometries, we took the sum of NH_3-N and NO_3-N to be the bioavailable N. Nutrient levels in the GBF were markedly more variable than in the secondary effluent. The average molar ratio of bioavailable N to SRP was 35 ± 7 in GBF (12.5% v/v) diluted with secondary effluent, as compared to 32 in Medium A^+.

Table 3-1. Nutrient Composition of a Batch of 100% GBF Used for Subsequent Experiments.

Analyte	Concentration[a] (mg L^{-1}) (±SD)
NH_3–N	1180 ± 135
NO_3–N	7.5 ± 0.04
SRP	78 ± 10
COD	735 ± 4
TSS	467 ± 123
VSS	18 ± 2
TS	2350 ± 36
TS (Glass Fiber Filtered)	2030 ± 42
TS (0.45 um membrane filtered)	2000 ± 151

[a] Values shown represent the mean ± standard deviation (SD) of at least three technical replicates.

SRP-soluble reactive phosphorus
COD-chemical oxygen demand
TSS- total suspended solids
TS-total solids

Table 3-2. Characteristics of GBF and Secondary Effluent Over the 6-month Experimental Period.

Source	Analyte	Concentration[a] (mg L^{-1}) (±COV)
GBF	NH_3–N	920 ± 22%
	NO_3–N	3.9 ± 43%
	SRP	54 ± 27%
Secondary Effluent	NH_3–N	n.d.
	NO_3–N	19.3 ± 6.6%
	SRP	n.d.

[a] Values shown represent the mean ± coefficient of variation (COV) of at least three technical replicates**.**

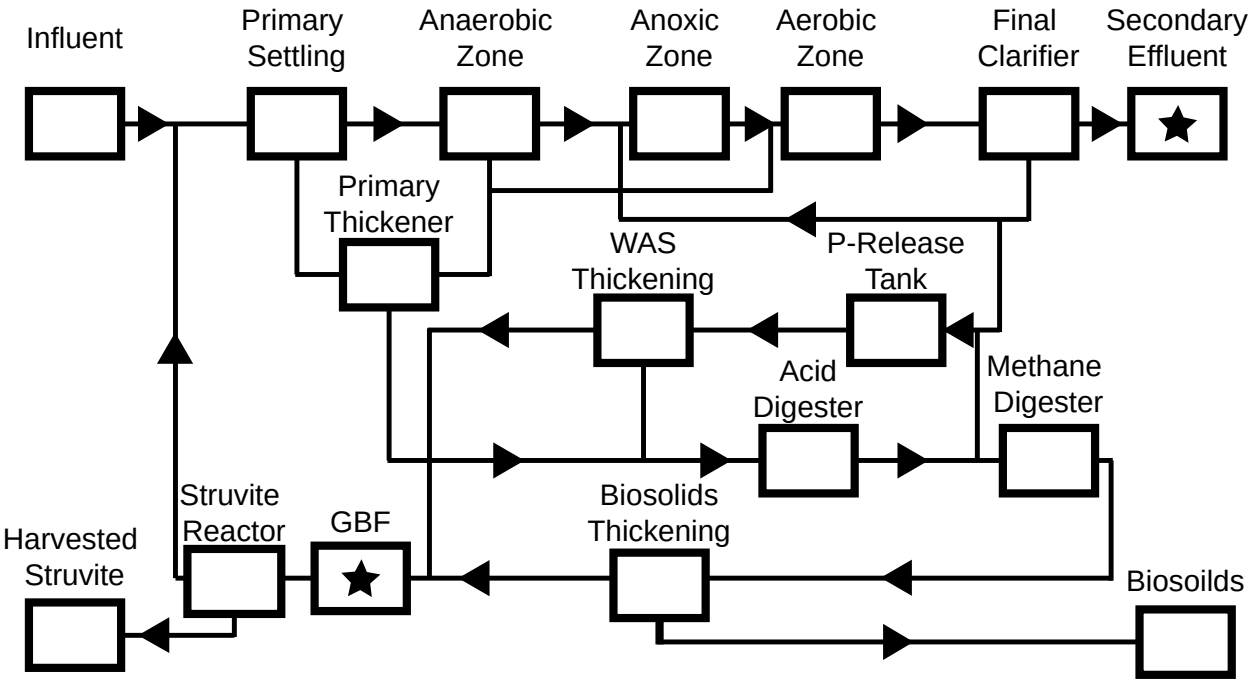

Figure 3-1. Flow Diagram and Nutrient Streams Obtained from the Nine Springs Wastewater Treatment Plant (Dane County, Wisconsin, USA).
Stars indicate sampling points.

We also measured DOM quality in the secondary effluent and GBF using UV-Vis absorbance scans and excitation−emission matrix (EEM) fluorescence spectroscopy (Chen et al., 2003) because we hypothesized that DOM was linked to toxicity during cultivation, as has been shown in prior studies (Neilen et al., 2017; Ojwang' and Cook, 2013; Vigneault et al., 2000). Relative to Medium A^+, absorbance scans of GBF (12.5% v/v) revealed high absorbance in the UV range (250-400 nm), indicative of aromatic hydrocarbons (Mayneord and Roe, 1935), which were diminished as the GBF was diluted to lower concentrations (**Fig. 3-2**). EEM fluorescence spectroscopy revealed that secondary effluent contained diffuse constituents, including humic [excitation wavelengths (>280 nm) and emission wavelengths (>380 nm)] and fulvic acid-like [excitation wavelengths (<250 nm) and emission wavelengths (>350 nm)] spectra relative to Medium A^+ (**Fig. 3-3**). The distinction between the two substances is historically based on solubility (Lehmann and Kleber, 2015), but compositionally, fulvic acids contain more acidic

functional groups than humic acids (Peña-méndez et al., 2005). The fulvic acid content in media preparations rose with increasing concentrations of GBF. Additionally, at high concentrations of GBF, a distinct region [excitation wavelengths (270 -290 nm) and emission wavelengths (340-400 nm)] was attributed to the presence of soluble microbial products, which include aromatic amino acids, carbohydrates, or phenols (Chen et al., 2003; Cowgill, 1963). The exact composition of these products varies with plant configuration, but they are refractory to microbial degradation (Dignac et al., 2000).

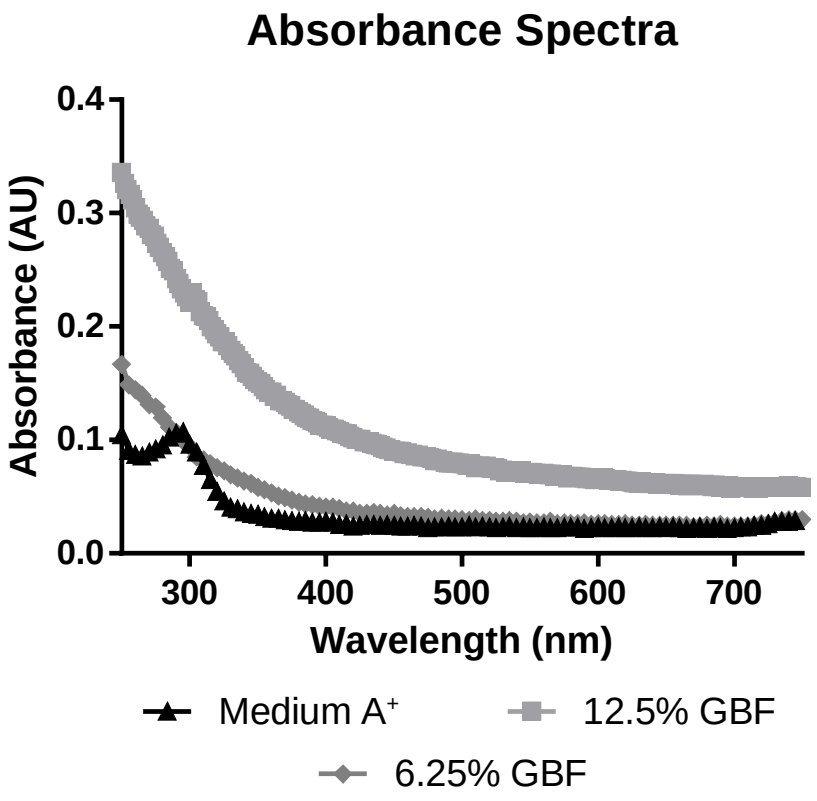

Figure 3-2. UV-VIS Absorption Spectra of Varying Concentrations of Tested Media.

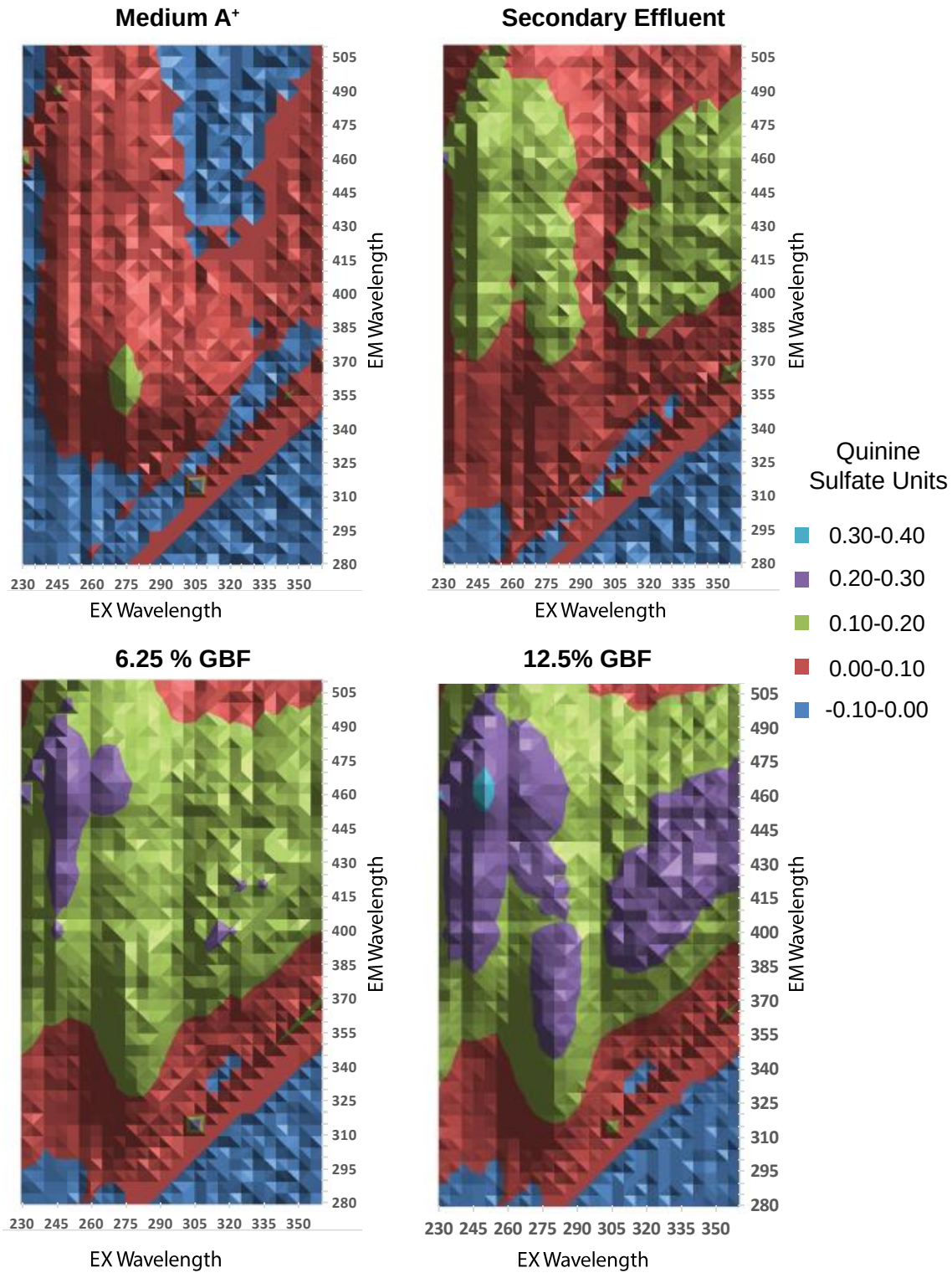

Figure 3-3. Excitation-Emission Matrix of tested medias.

Fluorescence values were normalized to 1 ppm of quinine sulfate in 0.1 N H_2SO_4 at Ex/Em = 350/450 nm.

3.4.2 Dose-Dependent Tolerance to GBF is a Function of Temperature

To evaluate the effects of GBF dosage on PCC 7002 physiology, we measured biomass accumulation (**Fig. 3-4**) and growth rates (**Table 3**) in GBF concentrations ranging from 6.25%-12.5% (v/v) as a function of temperature (27°C vs 37°C) and light intensity (100 μmol photons $m^{-2} s^{-1}$ vs 200 μmol photons $m^{-2} s^{-1}$). Medium A^+ served as a control. Higher temperatures depressed growth rates in GBF-based media. At 37°C, growth rates with 6.25% GBF at both 100 μmol photons $m^{-2} s^{-1}$ and 200 μmol photons $m^{-2} s^{-1}$ were most comparable to Medium A^+. Higher GBF concentrations had a more extreme effect on growth rates. However, this dose dependent effect of GBF on growth rate was abolished when the cultivation temperature was lowered to 27°C. At 200 μmol photons $m^{-2} s^{-1}$ and 27°C, GBF cultures grew twice as slowly as the control and there was no significant difference between the tested GBF concentrations. Under 100 μmol photons $m^{-2} s^{-1}$ and 27°C, growth rates were comparable across media conditions. Thus, successful cultivation using the more concentrated GBF media required adjusting both the light and temperature regimes.

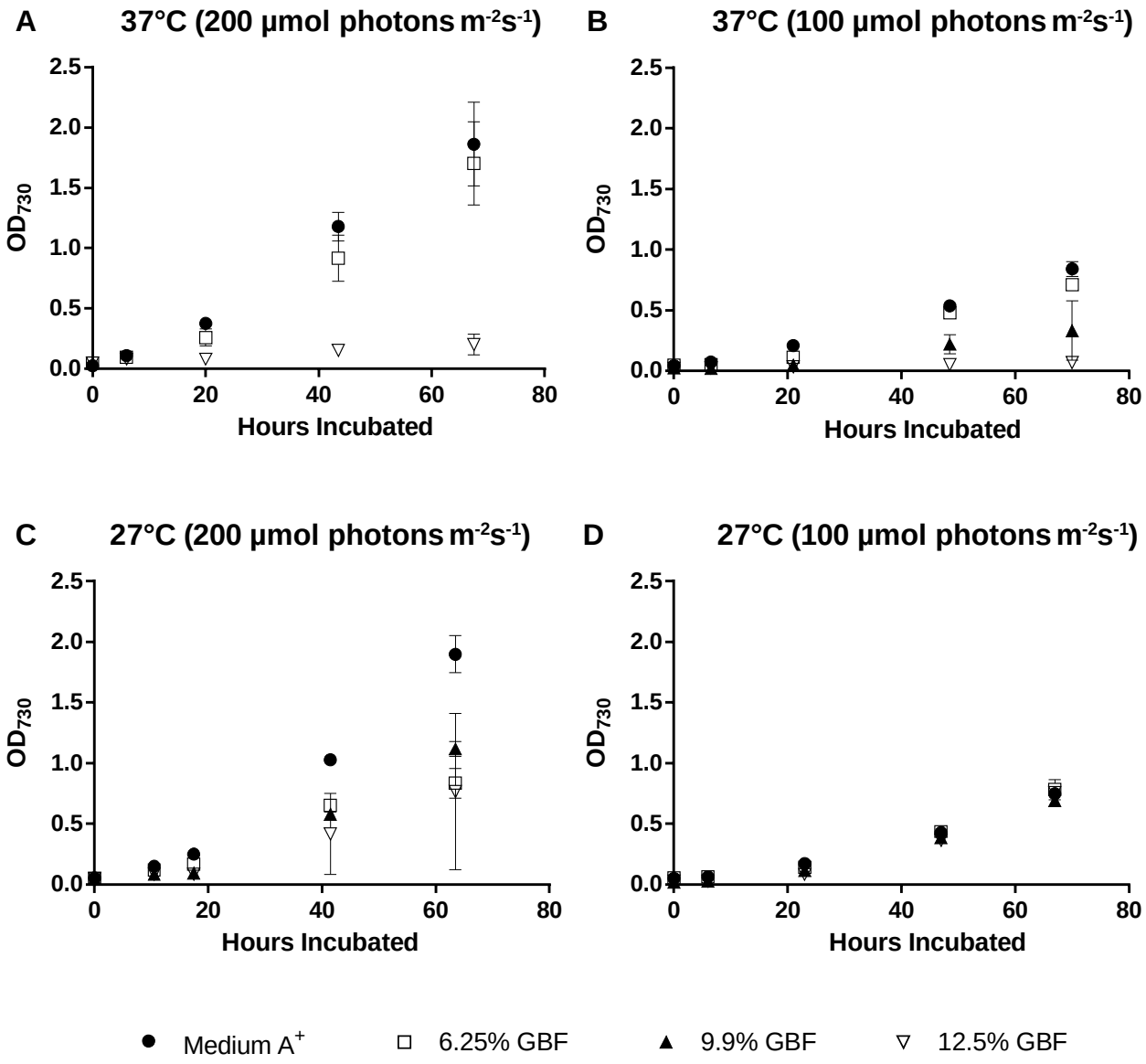

Figure 3-4. Biomass Accumulation for Cultures Grown in Medium A^+, 6.25 %, 9.9 %, or 12.5 % (v/v) GBF Media with 1 % CO_2.

(A) 37°C and 200 µmol photons m^{-2} s^{-1}, (B) 37°C and 100 µmol photons m^{-2} s^{-1}, (C) 27°C and 200 µmol photons m^{-2} s^{-1}, or (D) 27°C and 100 µmol photons m^{-2} s^{-1}. The values represent the mean ± SD of biological triplicates.

Table 3-3. Growth Rates with Varying Temperature and Light Intensity

Media	Light Intensity (μmol photons m^{-2} s^{-1})	Temperature (°C)	Growth Rate (±SD) ($OD\ day^{-1}$)
A^+	200	37	0.66 ± 0.04
6.25% GBF	200	37	0.58 ± 0.05
12.5% GBF	200	37	0.05 ± 0.01
A^+	100	37	0.28 ± 0.01
6.25% GBF	100	37	0.24 ± 0.01
9.9% GBF	100	37	0.11 ± 0.02
12.5% GBF	100	37	0.02 ± 0.00
A^+	200	27	0.73 ± 0.08
6.25% GBF	200	27	0.32 ± 0.03
9.9% GBF	200	27	0.42 ± 0.06
12.5% GBF	200	27	0.28 ± 0.04
A^+	100	27	0.25 ± 0.01
6.25% GBF	100	27	0.26 ± 0.02
9.9% GBF	100	27	0.24 ± 0.01
12.5% GBF	100	27	0.26 ± 0.02

Linear growth rates of cultures grown in Medium A^+ or GBF with the appropriate treatment under continuous illumination (200 μmol photons m^{-2} s^{-1} or 100 μmol photons m^{-2} s^{-1}) with 1 % CO2 at 37°C or 27°C. The values represent the mean ± SD of biological triplicates**.**

3.4.3 Dose-Dependent Membrane Permeability of GBF is a Function of Growth Temperature

We wondered whether the decreased growth rates in GBF at 37°C was a result of membrane permeability, given the known effect of humic acids on membrane integrity (Ojwang' and Cook, 2013; Vigneault et al., 2000). To track the dynamics of GBF induced membrane permeability, we employed forward scatter flow cytometry using SYTO 59 as a counterstain to identify cells, which were subsequently visualized for membrane permeability using Sytox Green. As Sytox Green is a membrane impermeable dye that fluoresces when binding to nucleic acids (Roth et al., 1997), fluorescence would indicate compromised outer membrane structures. Two distinct phases were identified upon exposure to GBF, which we interpreted as initial and chronic

membrane permeability (**Fig. 3-5**). Initial membrane permeability was defined as the Sytox Green positive events for samples analyzed within the first 10 hours of growth, while chronic membrane permeability accounted for the Sytox Green positive events during subsequent time points. As was the case for growth rate, a relationship between both initial and chronic membrane permeability and increasing GBF concentrations was found at 37°C (**Fig. 3-5A, 3-5B**). While we still detected considerable initial membrane permeability with GBF exposure at 27°C, chronic membrane permeability decreased over time, mostly likely to the increase in biomass (**Fig. 3-5C, 3-5D**). Altogether, this suggested that there was a temperature dependent adaptation that ameliorated the susceptibility of cultures to GBF induced membrane permeability.

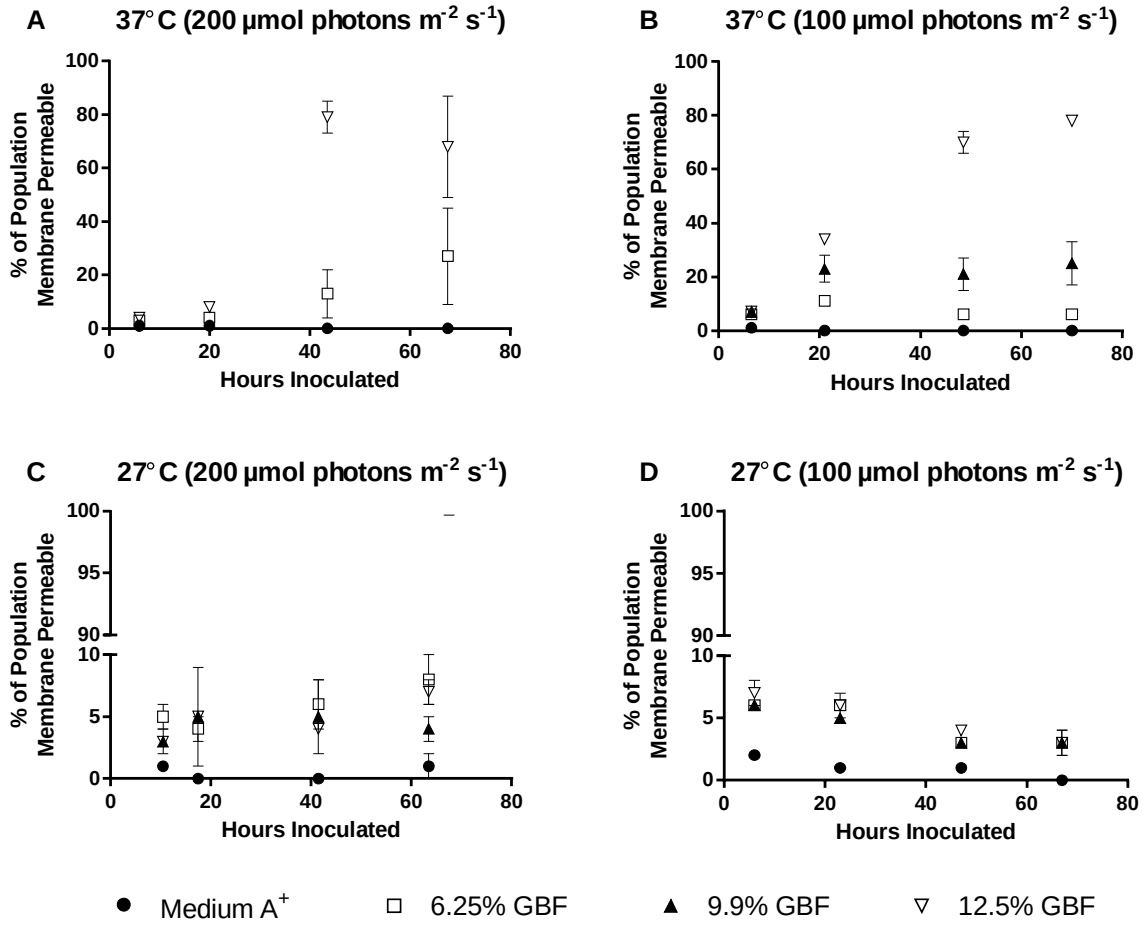

Figure 3-5. Membrane Permeability of Cultures Grown in Medium A^+, 6.25 %, 9.9 %, or 12.5 % (v/v) GBF Media with 1 % CO_2
(A) 37°C and 200 µmol photons m^{-2} s^{-1}, (B) 37°C and 100 µmol photons m^{-2} s^{-1}, (C) 27°C and 200 µmol photons m^{-2} s^{-1}, or (D) 27°C and 100 µmol photons m^{-2} s^{-1}. The values represent the mean ± SD of biological triplicates.

3.4.4 Exposure to GBF at High Temperatures Generates Radicals and Destroys Photosynthetic Pigments

We directly measured the ROS content and membrane permeability in response to overnight GBF exposure at 37°C using the fluorophores Sytox Green and CellROX Orange (**Fig. 3-6**). We examined the capacity of reducing agents Dithiothreitol (DTT) or N-acetylcysteine (NAC) to quench the media toxicity, since they have anti-oxidant properties due to the direct

reduction of disulfide bonds or as precursors for the anti-oxidant glutathione (Samuni et al., 2013). To measure their effect on the ROS production and culture viability after GBF exposure, we assessed ROS content and membrane integrity with either concurrent addition or preincubation of these quenching compounds in the diluted (12.5% v/v) GBF media. Addition of 100 µM methyl viologen to Medium A^+ served as a positive control for ROS production. Exposure of cells to 12.5%-GBF media resulted in marked ROS production and membrane permeability, which no thiol treatment alleviated.

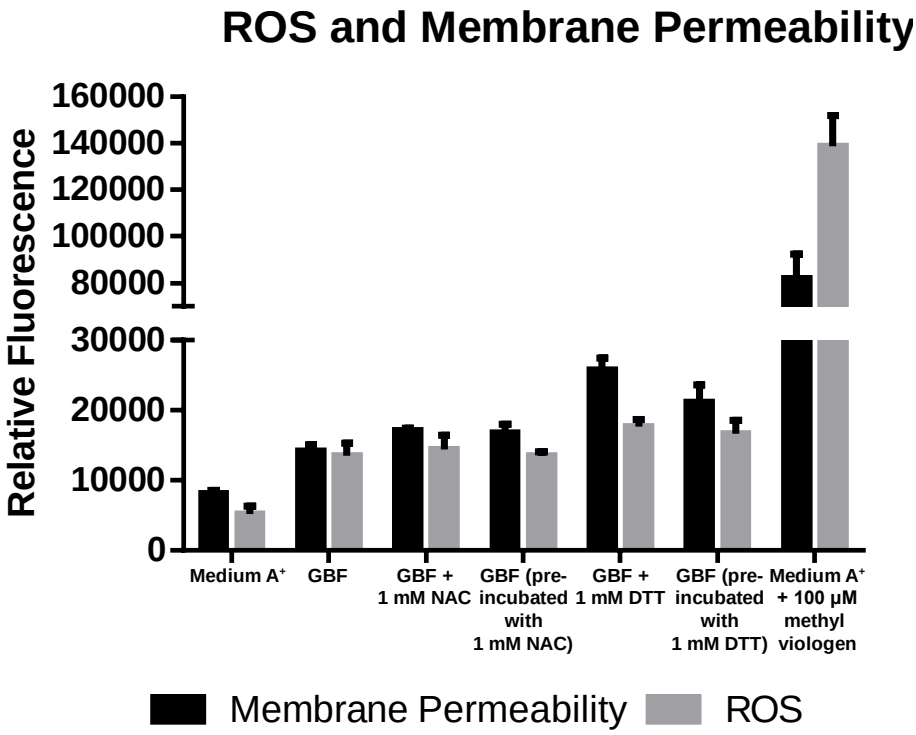

Figure 3-6. Reactive Oxygen Species and Membrane Permeability Assay.

Cells were grown to early linear phase in Medium A^+ or 12.5% GBF with the appropriate treatment under continuous illumination (200 µmol photons m^{-2} s^{-1}) with 1 % CO_2 at 37°C. Fluorescence values were normalized to OD_{730}. The values represent the mean ± SD of biological triplicates.

Photobleaching of the photosynthetic pigments is also a common symptom of oxidative stress in photosynthetic organisms and is caused by the accumulation of ROS (Latifi et al., 2009).

To investigate the effects of GBF media on the photosynthetic pigmentation, we performed whole cell absorbance scans of cultures cultivated at two different temperatures (27°C vs 37°C) at the same light intensity (200 μmol photons m^{-2} s^{-1}). High GBF concentrations yielded enhanced chlorophyll, phycobilisome, and carotenoid degradation at 37°C (**Fig. 3-7A**). At 27°C, photosynthetic pigments maintained intact relative to the control, regardless of GBF concentration, implying less ROS production at this temperature (**Fig. 3-7B**).

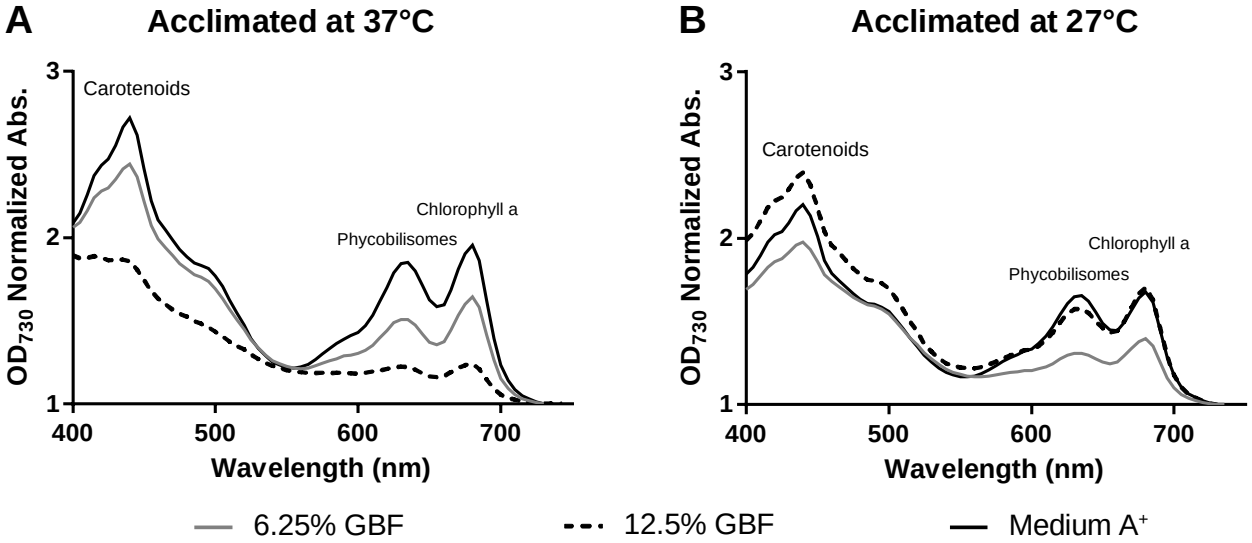

Figure 3-7. Absorption Spectra of Medium A^+ or GBF Exposed Strains as a Function of Temperature.

Cultures were grown in Medium A^+, 6.25 %, or 12.5 % (v/v) GBF media under continuous illumination (200 μmol photons m^{-2} s^{-1}) with 1 % CO_2 at (A) 37°C or (B) 27°C for 72 hours. The spectra were recorded in dilute cell suspensions and normalized to an OD_{730}. The peak at 438 nm is due to carotenoids, the peak at 637 nm is due to phycobilisomes, and the peak at 683 nm is due to chlorophyll a.

3.4.5 Exposure to GBF Retards Oxygen Evolution

To better delineate the cause of initial toxicity associated with high GBF concentrations, we measured maximal oxygen evolution rates for strains briefly exposed to diluted (12.5% v/v) GBF media while increasing the light intensity. Measurements of photosynthetic oxygen evolution would allow for an indirect assessment of PSII activity and electron transfer (van Gorkom and Gast, 1996). Cultures were grown to early linear phase in Medium A^+ or GBF media, washed, and

resuspended in the appropriate media. Resuspension media was saturated with HCO_3^- (10 mM) in order to prevent inorganic carbon limitation. As expected, cells grown and assayed in Medium A^+ at 37°C showed a clear increase in O_2 evolution rate as the light intensity approached saturation at 2700 μm photons $m^{-2} s^{-1}$, reaching a maximal rate of 240 ± 8 μmol O_2 (mg Chl a)$^{-1}$ h^{-1} (**Fig. 3-8A**). Cells grown in Medium A^+ at 37°C but assayed in 12.5% GBF had diminished O_2 evolution rates at all light intensities, plateauing with a rate of 79 ± 6 μmol O_2 (mg Chl a)$^{-1}$ h^{-1} at an intensity of 270 μmol photons $m^{-2} s^{-1}$ (**Fig. 3-8A**). Thus, exposure to GBF under these conditions immediately caused a decrease in O_2 production.

Next, we examined the effect of temperature in a similar experiment. Assays carried out in Medium A^+ after growth in Medium A^+ at 27°C showed much higher maximal O_2 evolution rates at all tested light intensities than with cells grown at 37°C (**Fig. 3-8B**), peaking at a rate 556 ± 102 μmol O_2 (mg Chl a)$^{-1}$ h^{-1}). This was expected because elevated O_2 evolution rates in low temperature grown PCC 7002 have been previously reported and were attributed to a substantial change in photosystem stoichiometry (Sakamoto and Bryant, 1998). The O_2 evolution rates of cells grown in Medium A^+ at 27°C and then resuspended in 12.5% GBF stayed relatively constant at all of the tested intensities and were roughly 5-fold lower than in controls, with a maximal rate of 109 ± 22 μmol O_2 (mg Chl a)$^{-1}$ h^{-1} at an intensity of 75 μmol photons $m^{-2} s^{-1}$. We compared the above rates to those from cultures grown in 12.5% GBF at 27°C to test if adaptation to GBF was met with changes in photosynthetic activity. At tested light intensities, O_2 evolution rates with 27°C GBF-adapted cultures were not statistically different than with unadapted cultures. Finally, we conducted the inverse experiment, using cultures grown in GBF Medium At 27°C but assayed in Medium A^+ under saturating light. Interestingly, they displayed the highest evolution rate of any tested condition, at 944 ± 96 μmol O_2 (mg Chl a)$^{-1}$ h^{-1} (**Fig. 3-8B**). This suggested that there is a

period of dynamic photosynthetic adaptation to overcome the stress of GBF, and that when the stress is alleviated the cells have an enhanced capacity for photosynthetic activity.

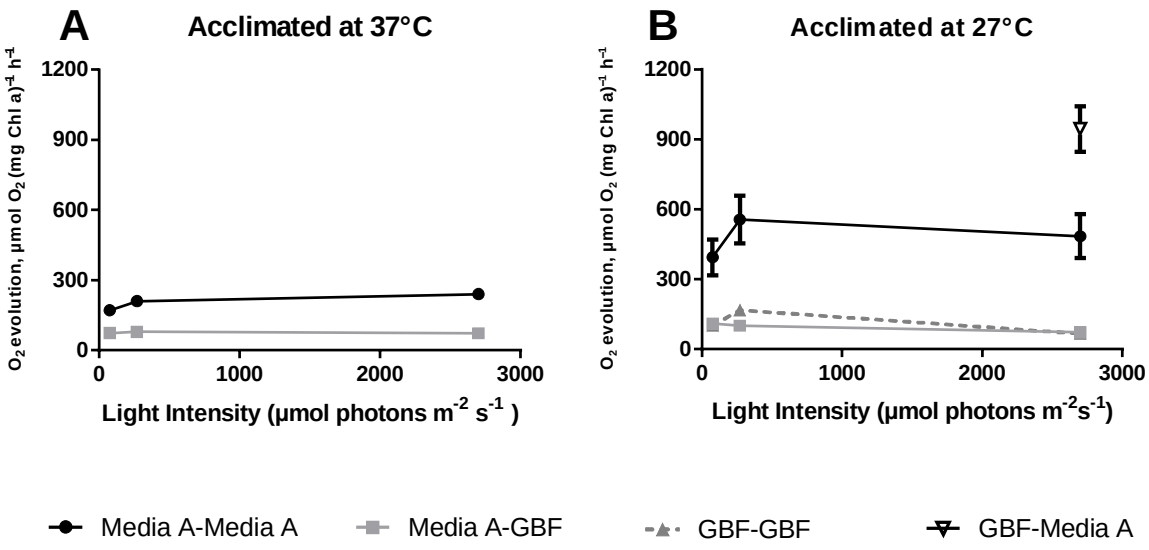

Figure 3-8. Rates of Oxygen Evolution as a Function of Acclimation temperature and Light Intensity.

Cells were grown to early linear phase in Medium A^+ or 12.5% GBF under continuous illumination (200 µmol photons m^{-2} s^{-1}) with 1 % CO_2 at (A) 37°C or (B) 27°C. Cells were pelleted, resuspended in Medium A^+ or 12.5% GBF, and the rate of maximal oxygen evolution was measured with 10 mM HCO_3^- as an electron acceptor at increasing light intensities. The values represent the mean ± SE of biological duplicates.

Additional assays were performed at light saturation (2700 µmol m^{-2} s^{-1}) with cultures adapted to 37°C (**Fig. 3-9A**) to highlight the effects of media conditions on oxygen evolution rates. As with other light intensities with 37°C adapted cultures, rates of oxygen evolution in GBF (73 ± 8 µmol O_2 (mg Chl a)$^{-1}$ h^{-1}) were much lower than Medium A^+ (248 ± 21 µmol O_2 (mg Chl a)$^{-1}$ h^{-1}). Increasing the osmolarity of the GBF medium by addition of equimolar concentrations of NaCl as Medium A^+ showed no statistical difference in oxygen evolution than without NaCl. Attempts to eliminate the inhibitory effect of GBF on oxygen evolution by gravity filtration through powdered activated carbon were unsuccessful. 10 µM DCMU in Medium A^+, or cultures pre-treated with 800 µg ml^{-1} Lincomycin in Medium A^+ and incubated at light saturation for 1 hour were used as controls for the inhibition of photosynthetic electron transfer

(Huber and Edwards, 1975) and de-novo protein synthesis (Tyystjärvi and Aro, 1996), respectively. However, evolution rates with these controls were higher than those treated with GBF, and no definitive conclusion on the mechanism of GBF induced reduction in oxygen evolution could be made. An additional experiment was done to examine the effects of NH_4 toxicity on oxygen evolution rates (**Fig. 3-9A**). Cultures were grown in Medium A^+ at 37°C, and resuspended in 12.5% GBF or default Medium A^+ as described above, or resuspended into Medium A^+ where NH_4Cl has been substituted at equimolar concentrations as the $NaNO_3$ normally present. As shown, there was no statistically significant effect of the presence of NH_4 on oxygen evolution rate, which differs from studies performed with other cyanobacterial strains (Dai et al., 2014).

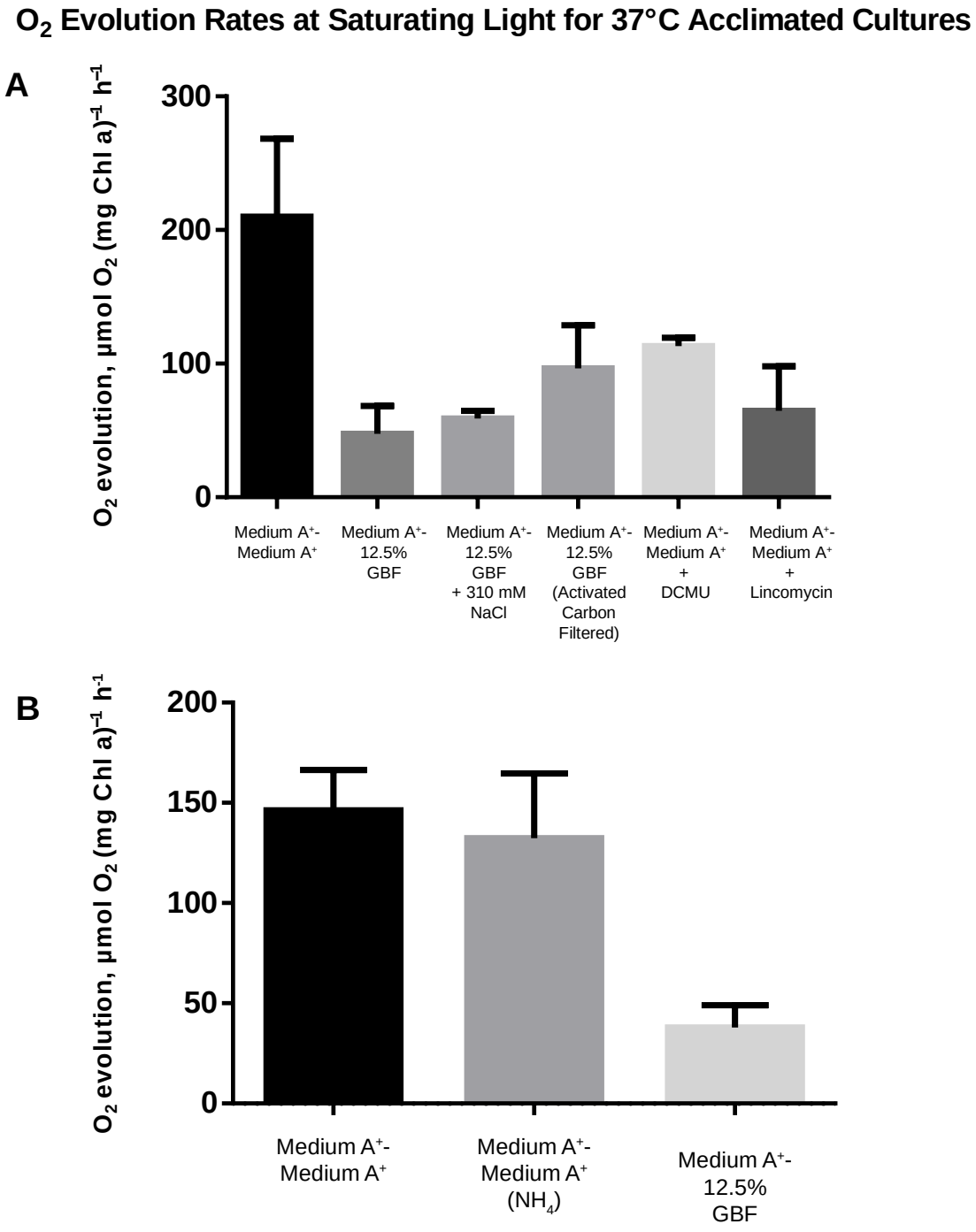

Figure 3-9. Photosynthetic Rates of Oxygen Evolution at Saturating Light Conditions.
Cells were grown to early linear phase in Medium A^+ under continuous illumination (200 µmol photons m^{-2} s^{-1}) with 1 % CO_2 at 37°C). (A) Cells were pelleted, resuspended in Medium A^+, 12.5% GBF, 12.5% GBF + 310 mM NaCl (control for osmolarity), 12.5% GBF prefiltered with activated carbon, Medium A^+ + 10 µM DCMU (control for inhibition for electron transport), or pre-treated with 800 µg ml^{-1} Lincomycin for 1 hour (control for the inhibition of protein synthesis.) (B) Cells were pelleted, resuspended in Medium A^+, Medium A^+ with 12 mM NH_4 as a nitrogen source, or 12.5% GBF. Maximal oxygen evolution rates were measured with 10 mM HCO_3 as an electron acceptor at 2700 µmol photons m^{-2} s^{-1}. The values represent the mean ± SE of biological duplicates.

3.4.6. Acclimation to GBF Changes Lipid Content and Composition

Based on the results described above, we hypothesized that the temperature dependent adaptation may be related to changes in membrane content and composition. We extracted total fatty acids of cultures grown at 27°C for 72 hours in 12.5% GBF or Medium A^+, and analyzed the content after derivatization. We could detect and resolve all major saturated and unsaturated fatty acid species (**Table 3-4**). Cultures grown in GBF had greater totals of assayed fatty acid species (27 ± 7 mg FAME $gDCW^{-1}$) when compared to cells grown in Medium A^+ (15 ± 1 mg FAME $gDCW^{-1}$). The most abundant fatty acid in all samples was 16:0 (42-45% of the total fatty acids). C18:2 Δ9,12 fatty acids comprised a significant fraction of Medium A^+ grown cultures with 22% of the total fatty acid species. However, in GBF-grown cells the amount of C18:2 Δ9,12 fatty acids were only 15%, while C18:3 Δ9,12,15 fatty acids were twice as high (p-value<0.0005) in GBF grown cells (16%) than in Medium A^+ grown cells (9%). Our fatty acid extraction suggests that cells were altering their membrane homeostasis when grown in GBF, as compared to standard growth in Medium A^+. While we did not differentiate the fatty acid content and composition between the outer, cytoplasmic, or thylakoid membranes in our study, prior work done with the cyanobacterium *Synechocystis* PCC 6803 found similar fatty acid composition between thylakoid and cytoplasmic membranes (Los and Murata, 1996).

Table 3-4. Fatty Acid Content and Composition of Cultures Grown in Medium A^+ or 12.5% GBF Media.

Growth Conditions[1]		Fatty Acids Species					
		C16:0	**C16:1 Δ9**	**C18:0**	**C18:1 Δ9**	**C18:2 Δ9,12**	**C18:3 Δ9,12,15**
Medium A^+	mg FA $gDCW^{-1}$	6.7 ± 0.7	2.0 ± 0.1	0.2 ± 0.1	1.5 ± 0.2	3.3 ± 0.2	1.4 ± 0.1
	% FA	44 ± 1	13 ± 1	2 ± 0	10 ± 0	22 ± 1	9 ± 1
GBF	mg FA $gDCW^{-1}$	11.6 ± 3.1	3.5 ± 0.8	1.3 ± 0.3	2.2 ± 0.7	3.9 ± 0.8	4.4 ± 1.6
	% FA	43 ± 0	13 ± 0	5 ± 0	8 ± 0	15 ± 1	16 ± 1***

[1] Strains were grown in the Medium A^+ or 12.5% GBF media under continuous illumination (200 μmol photons m^{-2} s^{-1}) at 27°C for 72 hours. Fatty acids were extracted and derivatized as previously described. The values represent the mean ± SD of two independent experiments. *** represent statistically significant differences from control (p-value<0.0005 using an unpaired t-test).

3.5 Discussion

The amount and distribution of arable land and potable water are projected to change over the next several decades due to climate change, while the rise in global population and standard of living are expected to increase demands (Parry et al., 2004). Integration of microalgal cultivation with industrial and municipal wastewater treatment circumvents many of the resource concerns raised over biofuel production (Pate et al., 2011), while simultaneously removing additional nutrients and pollutants present in the wastewater (Wang et al., 2016). However, under standard environmental conditions we were unable to obtain robust growth of PCC 7002 using a diluted municipal side stream as a nutrient source. We hypothesized that this effect may be due to the presence of DOM, which has been demonstrated to cause a decrease in photosynthetic performance in various strains of cyanobacteria (Gjessing et al., 1998; Shao et al., 2009; Sun et al., 2006). We investigated the effects of light intensity and temperature on the physiology of digestate grown cultures, in an effort to find conditions conducive to high growth rates and biomass generation and better understand the mechanisms of GBF toxicity.

We propose that the herbicidal effect of GBF is primarily due to PSII inhibition as shown in **Fig. 3-8** and **3-9**, brought about by quinone or phenolic compounds within the "soluble microbial products" found in our EEM scans (**Fig. 3-3**). Enrichment of humic material with quinone and phenolic compounds has been shown to be inhibitory to growth in cyanobacterial species (Bährs et al., 2013, 2012). Phenolic photosynthetic electron transfer inhibitors such as 2,5-Dibromo-3-methyl-6-isopropyl-p-benzoquinone (DBMIB), alter the redox potential of the PQ pool of PSII by blocking forward electron transfer to the cytochrome b_6/f complex (Schoepp et al., 1999). The immediate decrease in oxygen evolution (**Fig. 3-8**) and high rates of initial

membrane permeability (**Fig. 3-5**) upon GBF exposure suggests that the toxic compound(s) rapidly cross the outer membrane, where it interrupts photosynthetic electron flow. Chronic exposure to phenolic herbicides eventually leads to radical-catalyzed back reactions that trigger the formation of ROS (Pallett and Dodge, 1980) (**Fig. 3-6**) that facilitate complex destruction (**Fig. 3-7**) and cell death (Dominy and Williams, 1987; Idedan et al., 2011; Krieger-Liszkay et al., 2008; Latifi et al., 2009; Nishiyama et al., 2011). Some phenolic herbicides may also act as arylating agents, causing covalent binding to macromolecules via Michael addition and a depletion of thiol pools (Wang et al., 2006). The inability of the reducing agents we tested to maintain membrane integrity suggests that GBF-induced cytomembrane permeability is likely caused by redox cycling, and not arylation.

We found that cultivation temperature was an important factor that allowed for the growth of PCC 7002 under high GBF concentrations. Numerous physiological processes are altered at low temperatures (Morgan-Kiss et al., 2006). Notably, the fatty acyl chains in membranes undergo a transition from a fluid to nonfluid state (De Mendoza, 2014). Cyanobacterial membrane organization is complicated by the simultaneous existence of the outer, plasma, and thylakoid membranes, each with a designated physiological function (Pisareva et al., 2011). As part of the homeoviscous response upon a shift to a lower temperature, cyanobacteria alter the expression of desaturases in their plasma and thylakoid membranes (Mustardy et al., 1996) to increase unsaturated fatty acid content and maintain optimal membrane function (Singh et al., 2002). Optimal fluidity of thylakoid membranes is a critical factor in photosynthetic electron transport, due to the mobility of co-utilized redox components to both photosynthetic and respiratory complexes to ensure ideal electron flow (Liu, 2015; Mullineaux, 2014). It has been shown that temperature influences the kinetics governing the

redox state of plastiquinone (PQ) through alterations in thylakoid membrane composition and fluidity (Klementiev et al., 2017). We hypothesize that alteration of the thylakoid membrane to circumvent GBF induced changes in the redox state is also an important component of the adaptive response to lower temperatures, given the increase in total unsaturated fatty acids observed during cultivation in GBF-based media (**Table 3-4**).

The strong reduction of the PQ pool by phenolic herbicides also induces the phycobilisomes to physically move from PSII to PSI in a transition known as "state 2", thereby decreasing the ratio of reducing power to proton-motive force generated by photosynthesis (Mao et al., 2002). Marine *Synechococcus*, including PCC 7002, have also been shown to transition to state 2 upon shifts to lower temperature (Mackey et al., 2013). Mutant cells of the cyanobacterium *Synechocystis* PCC 6803 that lacked polyunsaturated fatty acids were unable to perform these state transitions at low temperatures (El Bissati et al., 2000). This change in photosystem arrangement at 27°C may also contribute to acclimation to the photoinhibitory compound. Future efforts to increase tolerance to these toxicants might include disruption of the inhibitor binding sites (Ajlani et al., 1989; Lee et al., 2001) or optimizing thylakoid membrane fluidity (Gombos et al., 1994).

3.6 Conclusions

Under standard cultivation conditions of 37°C with the cyanobacteria *Synechococcus* sp. strain PCC 7002, there was a dose-dependent relationship between liquid anaerobic digestate concentration and membrane permeability. This was met with ROS production and photopigment degradation. Digestate contained constituents of dissolved organic matter that were likely affecting photosynthetic electron transport. Decreasing the cultivation temperature to 27°C enabled robust

cultivation at high digestate concentrations, resulting in high biomass productivities. This temperature dependent tolerance may be due to changes in membrane properties. Our study highlights the contributions of dissolved organic matter to photosynthetic growth and physiology in wastewater based media, as well as a potential mechanism for tolerance in low temperatures.

3.7 Acknowledgements

This work was funded by the US National Science Foundation (EFRI-1240268). TCK is the recipient of a National Institutes of Health (NIH) Biotechnology Training Fellowship (NIGMS-5 T32 GM08349) and a fellowship from the UW-Madison College of Engineering's Graduate Engineering Research Scholars (GERS) program. The authors are grateful to Richard Mikel, Matthew Dysthe, and Derek Jacobs for help with routine sampling, and Andrew Maizel and Christina Remucal for advice on the excitation−emission matrix (EEM) fluorescence spectroscopy.

3.8 Literature Cited

Ajlani, G., Kirilovsky, D., Picaud, M., Astier, C., 1989. Molecular analysis of psbA mutations responsible for various herbicide resistance phenotypes in Synechocystis 6714. Plant Mol. Biol. 13, 469–79.

Akhiar, A., Torrijos, M., Battimelli, A., Carrère, H., 2016. Comprehensive characterization of the liquid fraction of digestates from full-scale anaerobic co-digestion. Waste Manag. doi:10.1016/j.wasman.2016.11.005

Bährs, H., Menzel, R., Kubsch, G., Stößer, R., Putschew, A., Heinze, T., Steinberg, C.E.W., 2012. Does quinone or phenol enrichment of humic substances alter the primary compound from a non-algicidal to an algicidal preparation? Chemosphere 87, 1193–1200. doi:10.1016/j.chemosphere.2012.01.009

Bährs, H., Putschew, A., Steinberg, C.E.W., 2013. Toxicity of hydroquinone to different freshwater phototrophs is influenced by time of exposure and pH. Environ. Sci. Pollut. Res. 20, 146–154. doi:10.1007/s11356-012-1132-5

Chen, W., Westerhoff, P., Leenheer, J.A., Booksh, K., 2003. Fluorescence Excitation-Emission Matrix Regional Integration to Quantify Spectra for Dissolved Organic Matter. Environ. Sci. Technol. 37, 5701–5710. doi:10.1021/es034354c

Chiou, C.T., Malcolm, R.L., Brinton, T.I., Kile, D.E., 1986. Water solubility enhancement of some organic pollutants and pesticides by dissolved humic and fulvic acids. Environ. Sci. Technol.;(United States) 20.

Clarens, A.F., Resurreccion, E.P., White, M. a, Colosi, L.M., 2010. Environmental life cycle comparison of algae to other bioenergy feedstocks. Environ. Sci. Technol. 44, 1813–9. doi:10.1021/es902838n

Cowgill, R.W., 1963. Fluorescence and the structure of proteins. I. Effects of substituents on the fluorescence of indole and phenol compounds. Arch. Biochem. Biophys. 100, 36–44. doi:10.1016/0003-9861(63)90031-6

Dai, G.-Z., Qiu, B.-S., Forchhammer, K., 2014. Ammonium tolerance in the cyanobacterium Synechocystis sp. strain PCC 6803 and the role of the psbA multigene family. Plant. Cell Environ. 37, 840–51. doi:10.1111/pce.12202

de la Noüe, J., Laliberté, G., Proulx, D., 1992. Algae and waste water. J. Appl. Phycol. 4, 247–254. doi:10.1007/BF02161210

De Mendoza, D., 2014. Temperature Sensing by Membranes. Annu. Rev. Microbiol 68, 101–16. doi:10.1146/annurev-micro-091313-103612

Dignac, M.F., Ginestet, P., Rybacki, D., Bruchet, A., Urbain, V., Scribe, P., 2000. Fate of wastewater organic pollution during activated sludge treatment: Nature of residual organic matter. Water Res. 34, 4185–4194. doi:10.1016/S0043-1354(00)00195-0

Dominy, P.J., Williams, W.P., 1987. Chlorophyll Photobleaching is Dependent on Photosystem II Inhibition, in: Biggins, J. (Ed.), Progress in Photosynthesis Research: Volume 4 Proceedings of the VIIth International Congress on Photosynthesis Providence, Rhode Island, USA, August 10--15, 1986. Springer Netherlands, Dordrecht, pp. 35–38. doi:10.1007/978-94-017-0519-6_6

Eaton, A.D., Franson, M.A.H., 2005. Standard Methods for the Examination of Water & Wastewater, 21st ed. American Public Health Association.

El Bissati, K., Delphin, E., Murata, N., Etienne, a, Kirilovsky, D., 2000. Photosystem II fluorescence quenching in the cyanobacterium Synechocystis PCC 6803: involvement of two different mechanisms. Biochim. Biophys. Acta 1457, 229–242. doi:10.1016/S0005-2728(00)00104-3

Flowers, J.J., Cadkin, T.A., McMahon, K.D., 2013. Seasonal bacterial community dynamics in a full-scale enhanced biological phosphorus removal plant. Water Res. 47, 7019–7031. doi:10.1016/j.watres.2013.07.054

Foyer, C.H., Neukermans, J., Queval, G., Noctor, G., Harbinson, J., 2012. Photosynthetic control of electron transport and the regulation of gene expression. J. Exp. Bot. 63, 1637–61. doi:10.1093/jxb/ers013

Gjessing, E.T., Alberts, J.., Bruchet, A., Egeberg, P.K., Lydersen, E., McGown, L.B., Mobed, J.J., Münster, U., Pempkowiak, J., Perdue, M., Ratnawerra, H., Rybacki, D., Takacs, M., Abbt-Braun, G., 1998. Multi-method characterisation of natural organic matter isolated from water: characterisation of reverse osmosis-isolates from water of two semi-identical dystrophic lakes basins in Norway. Water Res. 32, 3108–3124. doi:10.1016/S0043-1354(98)00060-8

Gombos, Z., Wada, H., Murata, N., 1994. The recovery of photosynthesis from low-temperature photoinhibition is accelerated by the unsaturation of membrane lipids: a mechanism of chilling tolerance. Proc. Natl. Acad. Sci. U. S. A. 91, 8787–91.

He, S., McMahon, K.D., 2011. "Candidatus Accumulibacter" gene expression in response to dynamic EBPR conditions. ISME J. 5, 329–40. doi:10.1038/ismej.2010.127

Hoffmann, J.P., 1998. Wastewater Treatment with Suspended and Nonsuspended Algae. J. Phycol. 34, 757–763. doi:10.1046/j.1529-8817.1998.340757.x

Huber, S.C., Edwards, G.E., 1975. Effect of DBMIB, DCMU and antimycin A on cyclic and noncyclic electron flow in C4 mesophyll chloroplasts. FEBS Lett. 58, 211–214. doi:10.1016/0014-5793(75)80261-4

Idedan, I., Tomo, T., Noguchi, T., 2011. Herbicide effect on the photodamage process of photosystem II: Fourier transform infrared study. Biochim. Biophys. Acta - Bioenerg. 1807, 1214–1220. doi:10.1016/j.bbabio.2011.06.006

Imai, A., Fukushima, T., Matsushige, K., Kim, Y.-H., Choi, K., 2002. Characterization of dissolved organic matter in effluents from wastewater treatment plants. Water Res. 36, 859–870. doi:10.1016/S0043-1354(01)00283-4

Keren, N., Krieger-Liszkay, A., 2011. Photoinhibition: molecular mechanisms and physiological significance. Physiol. Plant. 142, 1–5. doi:10.1111/j.1399-3054.2011.01467.x

Klementiev, K.E., Tsoraev, G. V, Tyutyaev, E. V, Zorina, A.A., Feduraev, P. V, Allakhverdiev, S.I., Paschenko, V.Z., 2017. Membrane fluidity controls redox-regulated cold stress responses in cyanobacteria. Photosynth. Res. 0, 0. doi:10.1007/s11120-017-0337-3

Krieger-Liszkay, A., Fufezan, C., Trebst, A., 2008. Singlet oxygen production in photosystem II and related protection mechanism. Photosynth. Res. 98, 551–564. doi:10.1007/s11120-008-9349-3

Latifi, A., Ruiz, M., Zhang, C.-C., 2009. Oxidative stress in cyanobacteria. FEMS Microbiol. Rev. 33, 258–78. doi:10.1111/j.1574-6976.2008.00134.x

Laue, P., Bährs, H., Chakrabarti, S., Steinberg, C.E.W., 2014. Natural xenobiotics to prevent cyanobacterial and algal growth in freshwater: Contrasting efficacy of tannic acid, gallic acid, and gramine. Chemosphere 104, 212–220. doi:10.1016/j.chemosphere.2013.11.029

Lee, E., Glover, C.M., Rosario-Ortiz, F.L., 2013. Photochemical formation of hydroxyl radical from effluent organic matter: Role of composition. Environ. Sci. Technol. 47, 12073–12080. doi:10.1021/es402491t

Lee, T.X., Metzger, S.U., Cho, Y.S., Whitmarsh, J., Kallas, T., 2001. Modification of inhibitor binding sites in the cytochrome bf complex by directed mutagenesis of cytochrome b6 in Synechococcus sp. PCC 7002. Biochim. Biophys. Acta - Bioenerg. 1504, 235–247. doi:10.1016/S0005-2728(00)00253-X

Lehmann, J., Kleber, M., 2015. The contentious nature of soil organic matter. Nature 1–9. doi:10.1038/nature16069

Lennen, R.M., Braden, D.J., West, R.A., Dumesic, J.A., Pfleger, B.F., 2010. A process for microbial hydrocarbon synthesis: Overproduction of fatty acids in Escherichia coli and catalytic conversion to alkanes. Biotechnol. Bioeng. 106, 193–202. doi:10.1002/bit.22660

Liu, L.-N., 2015. Distribution and dynamics of electron transport complexes in cyanobacterial thylakoid membranes. Biochim. Biophys. Acta - Bioenerg. doi:10.1016/j.bbabio.2015.11.010

Los, D.A., Murata, N., 1996. Characterization of the Fad12 mutant of Synechocystis that is defective in Δ12 acyl-lipid desaturase activity. Biochim. Biophys. Acta - Lipids Lipid Metab. 1299, 117–123. doi:10.1016/0005-2760(95)00204-9

Mackey, K.R.M., Paytan, A., Caldeira, K., Grossman, A.R., Moran, D., McIlvin, M., Saito, M.A., 2013. Effect of temperature on photosynthesis and growth in marine Synechococcus spp. Plant Physiol. 163, 815–29. doi:10.1104/pp.113.221937

Mao, H. Bin, Li, G.F., Ruan, X., Wu, Q.Y., Gong, Y.D., Zhang, X.F., Zhao, N.M., 2002. The redox state of plastoquinone pool regulates state transitions via cytochrome b6f complex in Synechocystis sp. PCC 6803. FEBS Lett. 519, 82–86. doi:10.1016/S0014-5793(02)02715-1

Mayneord, W. V, Roe, E.M.F., 1935. The Ultra-Violet Absorption Spectra of Some Complex Aromatic Hydrocarbons. I. Proc. R. Soc. Lond. A. Math. Phys. Sci. 152, 299–324.

Miyashita, H., Adachi, K., Kurano, N., Ikemot, H., Chihara, M., Miyach, S., 1997. Pigment composition of a novel oxygenic photosynthetic prokaryote containing chlorophyll d as the major chlorophyll. Plant cell Physiol. 38, 274–281.

Morgan-Kiss, R.M., Priscu, J.C., Pocock, T., Gudynaite-Savitch, L., Huner, N.P.A., 2006. Adaptation and Acclimation of Photosynthetic Microorganisms to Permanently Cold Environments. Microbiol. Mol. Biol. Rev. 70, 222–252. doi:10.1128/MMBR.70.1.222-252.2006

Mullineaux, C.W., 2014. Electron transport and light-harvesting switches in cyanobacteria. Front. Plant Sci. 5, 1–6. doi:10.3389/fpls.2014.00007

Mustardy, L., Los, D.A., Gombos, Z., Murata, N., 1996. Immunocytochemical localization of acyl-lipid desaturases in cyanobacterial cells: evidence that both thylakoid membranes and cytoplasmic membranes are sites of lipid desaturation. Proc. Natl. Acad. Sci. U. S. A. 93, 10524–7. doi:10.1073/pnas.93.19.10524

Nagano, T., Kojima, K., Hisabori, T., Hayashi, H., Morita, E.H., Kanamori, T., Miyagi, T., Ueda, T., Nishiyama, Y., 2012. Elongation factor G is a critical target during oxidative damage to the translation system of Escherichia coli. J. Biol. Chem. 287, 28697–704. doi:10.1074/jbc.M112.378067

Neilen, A., W. Hawker, D., R. O'Brien, K., Burford, M., 2017. Phytotoxic effects of terrestrial dissolved organic matter on a freshwater cyanobacteria and green algae species is affected by plant source and DOM chemical composition, Chemosphere. doi:10.1016/j.chemosphere.2017.06.063

Nishiyama, Y., Allakhverdiev, S.I., Murata, N., 2011. Protein synthesis is the primary target of reactive oxygen species in the photoinhibition of photosystem II. Physiol. Plant. 142, 35–46. doi:10.1111/j.1399-3054.2011.01457.x

Ojwang', L.M., Cook, R.L., 2013. Environmental Conditions That Influence the Ability of Humic Acids to Induce Permeability in Model Biomembranes. Environ. Sci. Technol. 47, 8280–8287. doi:10.1021/es4004922

Olguín, E.J., 2012. Dual purpose microalgae–bacteria-based systems that treat wastewater and produce biodiesel and chemical products within a Biorefinery. Biotechnol. Adv. 30, 1031–1046.

Oliver, J.W.K., Atsumi, S., 2014. Metabolic design for cyanobacterial chemical synthesis. Photosynth. Res. 120, 249–61. doi:10.1007/s11120-014-9997-4

Pallett, K.E., Dodge, A.D., 1980. Studies into the Action of Some Photosynthetic Inhibitor Herbicides. J. Exp. Bot. 31, 1051–1066. doi:10.1093/jxb/31.4.1051

Parry, M.L., Rosenzweig, C., Iglesias, A., Livermore, M., Fischer, G., 2004. Effects of climate change on global food production under SRES emissions and socio-economic scenarios. Glob. Environ. Chang. 14, 53–67. doi:10.1016/j.gloenvcha.2003.10.008

Pate, R., Klise, G., Wu, B., 2011. Resource demand implications for US algae biofuels production scale-up. Appl. Energy 88, 3377–3388. doi:http://dx.doi.org/10.1016/j.apenergy.2011.04.023

Peccia, J., Haznedaroglu, B., Gutierrez, J., Zimmerman, J.B., 2013. Nitrogen supply is an important driver of sustainable microalgae biofuel production. Trends Biotechnol. 31, 134–8. doi:10.1016/j.tibtech.2013.01.010

Peña-méndez, M.E., Havel, J., Patočka, J., 2005. Humic substances – compounds of still unknown structure : applications in agriculture , industry , environment , and biomedicine. J. Appl. Biomed. 3, 13–24. doi:https://assets.motherearthlabs.com/resources/4.humic_.substances.compnds.of_.unkwn_.structure2005.pdf

Pflugmacher, S., Spangenberg, M., Steinberg, C.E.W., 1999. Dissolved organic matter (DOM) and effects on the aquatic macrophyte Ceratophyllum demersum in relation to photosynthesis, pigmentpattern and activity of detoxication enzymes. J. Appl. Bot. 73, 184–190.

Pisareva, T., Kwon, J., Oh, J., Kim, S., Ge, C., Wieslander, A., Choi, J.-S., Norling, B., 2011. Model for membrane organization and protein sorting in the cyanobacterium Synechocystis sp. PCC 6803 inferred from proteomics and multivariate sequence analyses. J. Proteome Res. 10, 3617–31. doi:10.1021/pr200268r

Porra, R.J., Thompson, W.A., Kriedemann, P.E., 1989. Determination of accurate extinction coefficients and simultaneous equations for assaying chlorophylls a and b extracted with four different solvents: verification of the concentration of chlorophyll standards by atomic absorption spectroscopy. Biochim. Biophys. Acta (BBA)-Bioenergetics 975, 384–394.

Posadas, E., García-Encina, P.A., Domínguez, A., Díaz, I., Becares, E., Blanco, S., Muñoz, R., 2014. Enclosed tubular and open algal-bacterial biofilm photobioreactors for carbon and nutrient removal from domestic wastewater. Ecol. Eng. 67, 156–164. doi:10.1016/j.ecoleng.2014.03.007

Rawat, I., Ranjith Kumar, R., Mutanda, T., Bux, F., 2011. Dual role of microalgae: Phycoremediation of domestic wastewater and biomass production for sustainable biofuels production. Appl. Energy 88, 3411–3424.

Roth, B.L., Poot, M., Yue, S.T., Millard, P.J., 1997. Bacterial viability and antibiotic susceptibility testing with SYTOX green nucleic acid stain. Appl. Environ. Microbiol. 63, 2421–31.

Ruffing, A.M., 2011. Engineered cyanobacteria: Teaching an old bug new tricks. bioe 2, 136–149.

Sakamoto, T., Bryant, D.A., 2001. Requirement of Nickel as an Essential Micronutrient for the Utilization of Urea in the Marine Cyanobacterium Synechococcus sp. PCC 7002. Microbes Environ. 16, 177–184.

Sakamoto, T., Bryant, D. a, 2002. Synergistic effect of high-light and low temperature on cell growth of the Delta12 fatty acid desaturase mutant in Synechococcus sp. PCC 7002. Photosynth. Res. 72, 231–42. doi:10.1023/A:1019820813257

Sakamoto, T., Bryant, D. a, 1998. Growth at low temperature causes nitrogen limitation in the cyanobacterium Synechococcus sp. PCC 7002. Arch. Microbiol. 169, 10–9.

Samuni, Y., Goldstein, S., Dean, O.M., Berk, M., 2013. The chemistry and biological activities of N-acetylcysteine. Biochem. Biophys. 1830, 4117–4129. doi:10.1016/j.bbagen.2013.04.016

Schoepp, B., Brugna, M., Riedel, A., Nitschke, W., Kramer, D.M., 1999. The Qo-site inhibitor DBMIB favours the proximal position of the chloroplast Rieske protein and induces a pK-shift of the redox-linked proton. FEBS Lett. 450, 245–250. doi:10.1016/S0014-5793(99)00511-6

Shao, J., Wu, Z., Yu, G., Peng, X., Li, R., 2009. Allelopathic mechanism of pyrogallol to Microcystis aeruginosa PCC7806 (Cyanobacteria): From views of gene expression and antioxidant system. Chemosphere 75, 924–928. doi:10.1016/j.chemosphere.2009.01.021

Singh, S.C., Sinha, R.P., Häder, D., 2002. Role of Lipids and Fatty Acids in Stress Tolerance in Cyanobacteria. Acta Protozool. 41, 297–308. doi:citeulike-article-id:3906403

Stevens, S.E., Patterson, C.O.P., Myers, J., 1973. The Production of Hydrogen Peroxide by Blue-Green Algae: A Survey. J. Phycol. 9, 427–430. doi:10.1111/j.1529-8817.1973.tb04116.x

Sturm, B.S.M., Lamer, S.L., 2011. An energy evaluation of coupling nutrient removal from wastewater with algal biomass production. Appl. Energy 88, 3499–3506. doi:http://dx.doi.org/10.1016/j.apenergy.2010.12.056

Sun, B., Tanji, Y., Unno, H., 2006. Extinction of cells of cyanobacterium Anabaena circinalis in the presence of humic acid under illumination. Appl. Microbiol. Biotechnol. 72, 823–828. doi:10.1007/s00253-006-0327-4

Tyystjärvi, E., Aro, E.M., 1996. The rate constant of photoinhibition, measured in lincomycin-treated leaves, is directly proportional to light intensity. Proc. Natl. Acad. Sci. U. S. A. 93, 2213–2218. doi:10.1073/pnas.93.5.2213

van Gorkom, H.J., Gast, P., 1996. Measurement of Photosynthetic Oxygen Evolution, in: Amesz, J., Hoff, A.J. (Eds.), Biophysical Techniques in Photosynthesis. Springer Netherlands, Dordrecht, pp. 391–405. doi:10.1007/0-306-47960-5_24

Vigneault, B., Percot, A., Lafleur, M., Campbell, P.G.C., 2000. Permeability changes in model and phytoplankton membranes in the presence of aquatic humic substances. Environ. Sci. Technol. 34, 3907–3913. doi:10.1021/es001087r

Voss, I., Sunil, B., Scheibe, R., Raghavendra, A.S., 2013. Emerging concept for the role of photorespiration as an important part of abiotic stress response. Plant Biol. (Stuttg). 15, 713–22. doi:10.1111/j.1438-8677.2012.00710.x

Wang, L., Min, M., Li, Y., Chen, P., Chen, Y., Liu, Y., Wang, Y., Ruan, R., 2010. Cultivation of green algae Chlorella sp. in different wastewaters from municipal wastewater treatment plant. Appl. Biochem. Biotechnol. 162, 1174–86. doi:10.1007/s12010-009-8866-7

Wang, X., Thomas, B., Sachdeva, R., Arterburn, L., Frye, L., Hatcher, P.G., Cornwell, D.G., Ma, J., 2006. Mechanism of arylating quinone toxicity involving Michael adduct formation and induction of endoplasmic reticulum stress. Proc. Natl. Acad. Sci. U. S. A. 103, 3604–9. doi:10.1073/pnas.0510962103

Wang, Y., Ho, S.H., Cheng, C.L., Guo, W.Q., Nagarajan, D., Ren, N.Q., Lee, D.J., Chang, J.S., 2016. Perspectives on the feasibility of using microalgae for industrial wastewater treatment. Bioresour. Technol. 222, 485–497. doi:10.1016/j.biortech.2016.09.106

Xu, Y., Alvey, R.M., Byrne, P.O., Graham, J.E., Shen, G., Bryant, D.A., 2011. Expression of genes in cyanobacteria: adaptation of endogenous plasmids as platforms for high-level gene expression in Synechococcus sp. PCC 7002. Methods Mol. Biol. 684, 273–93. doi:10.1007/978-1-60761-925-3_21

Zhang, D., Yan, S., Song, W., 2014. Photochemically Induced Formation of Reactive Oxygen Species (ROS) from Effluents Organic Matter. Environ. Sci. Technol.

Zsolnay, Á., 2003. Dissolved organic matter: Artefacts, definitions, and functions, in: Geoderma. pp. 187–209. doi:10.1016/S0016-7061(02)00361-0

CHAPTER 4 METABOLIC ENGINEERING OF *SYNECHOCOCCUS* SP. STRAIN PCC7002 FOR L-LACTATE PRODUCTION

Travis C. Korosh[a,b], Gina C. Gordon[a,c], Jeffrey C. Cameron[d,e], Andrew L. Markley[a], Matthew B. Begemann[a,c], Brian F. Pfleger[a,c]

[a] Department of Chemical and Biological Engineering, University of Wisconsin-Madison, 1415 Engineering Drive, Madison, WI 53706
[b] Environmental Chemistry and Technology Program, University of Wisconsin-Madison, 660 N Park St, Madison, WI 53706
[c] Microbiology Doctoral Training Program, University of Wisconsin-Madison, 1550 Linden Drive, Madison, WI 53706
[d] Department of Chemistry and Biochemistry, University of Colorado-Boulder, 596 UCB, Boulder, CO 80309
[e] Renewable and Sustainable Energy Institute, University of Colorado-Boulder, 27 UCB, Boulder, CO 80309

Author Contributions:

Travis C. Korosh- constructed all strains used for experiments, performed batch cultivations and organic acid quantification, and drafting of the manuscript.
Gina C. Gordon- constructed pCas2F, pCas034, and pCas39 and provided critical feedback of the manuscript.
Jeffrey C. Cameron- provided critical feedback of the manuscript.
Andrew L. Markley- provided critical feedback of the manuscript.
Matthew B. Begemann- provided critical feedback of the manuscript.
Brian F. Pfleger-supervised research and provided critical feedback of the manuscript.

Part of this chapter is adapted from *Metabolic Engineering*, Vol. 38, Gina C. Gordon, Travis C. Korosh, Jeffrey C. Cameron, Andrew L. Markley, Matthew B. Begemann, Brian F. Pfleger, CRISPR interference as a titratable, trans-acting regulatory tool for metabolic engineering in the cyanobacterium Synechococcus sp. strain PCC 7002, p. 170-179, https://doi.org/10.1016/j.ymben.2016.07.007, Copyright 2016, with permission from Elsevier.

4.1 Abstract

L-lactate is a model organic acid to investigate metabolic engineering principles in a cyanobacterial host, due to its proximity to central metabolism and low toxicity. In this chapter. we report the development of a cyanobacterium, *Synechococcus* sp. strain PCC 7002, capable of producing L-lactate at high carbon flux. We found that matching enzymatic cofactor preference with cofactor availability increased carbon partitioning three-fold. Removal of glycogen synthesis in L-lactate producing strain backgrounds had a pleiotropic effect on fitness and caused metabolic spillover. Repressing a key enzyme involved in the coordination nitrogen and carbon metabolism via CRISPRi led to highest reported volumetric productivity to date. Overexpression of a glycolytic transcriptional regulator also increased carbon flux to L-lactate.

4.2 Introduction

Cyanobacterial strains have been metabolically engineered to produce a variety of compounds including sugars, alcohols, hydrocarbons, and organic acids (Angermayr et al., 2014; Ducat et al., 2011; Mendez-Perez et al., 2011; Oliver et al., 2013) While these works demonstrate the versatility of cyanobacteria as chemical production platforms, the utility of these strains for industrial chemical production is limited by their relatively low volumetric productivities. The cyanobacterial strains which have been traditionally used in metabolic engineering, *Synechococcus* sp. PCC 7942 (PCC 7942) and *Synechocystis* sp. PCC 6803 (PCC 6803), can double every 6-24 hrs (Berla et al., 2013). In contrast, the cyanobacterium *Synechococcus* sp. PCC 7002 (PCC 7002) is a relatively fast-growing strain, capable of doubling every 3-5 hrs (Heidorn et al., 2011). The faster growth rate of PCC 7002 can be attributed to its high inorganic carbon transport flux (Clark et al., 2014) and the resulting high flux of carbon

fixation. Harnessing the carbon fixation potential of PCC 7002 could result in higher productivities, which may offset the current high costs of photosynthetic chemical production.

L-Lactate is an excellent model compound for studying metabolic engineering strategies in photoautotrophic bacteria because its synthesis pathway is short (one step removed from central metabolism) and consumes cofactors within the range generated by photosynthesis during linear electron transport (Oliver and Atsumi, 2014). Therefore, any design principles that translate to greater productivity for L-lactate, should hold true for more valuable products. L-lactate is traditionally produced though the fermentation of yeast and/or lactic acid bacteria for use in the food and polymer industries at volumetric productivities reaching 4 g L^{-1} h^{-1} (Okano et al., 2010). The cyanobacteria PCC 6803 and PCC 7942 have both been engineered to produce lactate using lactate dehydrogenase (LDH) enzymes obtained from a wide range of microbial sources to convert the central metabolite pyruvate to L-lactate using NAD(P)H as a source of reducing power (Angermayr et al., 2014; Niederholtmeyer et al., 2010). PCC 7002 has an endogenous LDH, but wild-type (WT) cultures produce negligible levels of lactate under standard laboratory conditions.

In this work, a synthetic biology toolbox (Markley et al., 2015) was used to control expression of heterologous enzymes that increased the ability of PCC7002 to produce the industrially-attractive organic acid, L-lactic acid. Here, we report the effects of enzymatic cofactor preference, and deletion of a competitive carbon sinks on overall lactate productivity rates for PCC 7002. We demonstrated novel strategies for increasing carbon flux by conditionally downregulating a key node in nitrogen assimilation, or by overexpression of a transcriptional regulator. The resulting strains produced 2-fold more lactate than a baseline

engineered cell line, representing the highest photosynthetically generated productivity to date, 2.2 ± 0.029 mM day^{-1}.

4.3 Materials and Methods

4.3.1 Chemicals, Reagents, and Media

Strains were grown and maintained on Medium A^+ (Stevens et al., 1973) with 1.5% (w/v) Bacto-Agar (Fisher). Strains with antibiotic resistance markers were selected on media with antibiotics (kanamycin, 100 μg/mL; gentamicin, 30 μg/mL) and strains with cassettes introduced in the A1838 (*acsA)* locus were plated on 100 μM acrylic acid. Optical density at 730 nm was measured in a Genesys 20 spectrophotometer (Thermo Scientific) in 1-cm cuvette or in a Tecan M1000 plate reader. Dry cell weight conversions using OD_{730nm} obtained from Tecan M1000 were determined from cell pellets washed in distilled water and then lyophilized (1 OD_{730nm} = 1.056 gDCW/L). (Note that in (Gordon et al., 2016), cell pellets were washed with Tris-buffered saline before determining dry weight rather than distilled water. To correct for this, those dry weight measurements were multiplied by 0.75, the ratio of the dry weight of a distilled water washed pellet to a Tris-buffered saline washed pellet). Dry cell weight conversions using OD_{730nm} obtained from Genesys 20 spectrophotometer were determined from cell pellets washed in distilled water and then lyophilized (1 OD_{730nm} = 0.26 gDCW/L).

4.3.2 Mutant Construction

Heterologous genes were integrated onto the chromosome of wild-type PCC 7002 using homologous recombination and screened for homozygous integration (Davies et al., 2014). The

udhA gene was amplified with the primers using *E. coli* K12 MG1655 DNA genomic DNA. The *BsLDH* gene was amplified with the primers using *Bacillus subtilis* genomic DNA. The design of point mutations in the nucleotide sequences of the LDH enzymes was based on the V39R mutation described for the L-LDH of *B. subtilis* strain 168 (Richter et al., 2011). The *sll1330* gene (Rre37) was amplified with the primers using *Synechocystis* (strain PCC 6803) genomic DNA. Expression cassettes were cloned into *E. coli* plasmids containing 500-1000 bp of homology targeting sequences to one of three PCC 7002 loci SYNPCC7002_A1838, SYNPCC7002_A2842 and/or NS1 (Ruffing et al., 2016) (**Table 4-1**). In these cassettes, genes were placed under control of the $P_{cLac094}$ (Markley et al., 2015) or the P_{EZtet} (Zess et al., 2016) inducible promoter system. Selection was performed by expression of an antibiotic resistance marker or using the acrylic acid counterselection system (Begemann et al., 2013). All plasmids were constructed using *in vitro* recombination assembly with overlapping primers using the *Phusion* DNA polymerase and sequence verified before transformation (Gibson et al., 2009).

Table 4-1. Plasmids Used in This Study

Name	**Expression Cassette**	Ref.
pTK004	ΔSYNPCC7002_A0095::aphII	This work
pTK011	ΔSYNPCC7002_A1838::$P_{clac143}$-BsLDH-udhA	This work
pTK013	ΔSYNPCC7002_A1838::$P_{clac143}$-BsLDHV39R-udhA	This work
pTK015	ΔSYNPCC7002_A1838:: $P_{clac143}$-BsLDH	This work
pTK017	ΔSYNPCC7002_A1838:: $P_{clac143}$-BsLDHV39R	This work
pTK035	ΔSYNPCC7002_A2842:: $P_{clac143}$-BsLDHV39R-aacC1	(Gordon et al., 2016)
pCas2F	ΔSYNPCC7002_A1838:: P_{EZtet}-dCas9 F RBS	(Gordon et al., 2016)
pCas034	ΔNS1:: P_{EZtet}-sgRNA YFP- aphII	(Gordon et al., 2016)
pCas039	ΔNS1:: P_{EZtet}-sgRNA glnA- aphII	(Gordon et al., 2016)
pTK036	ΔSYNPCC7002_A2842:: $P_{clac143}$-BsLDHV39R-rre37-aacC1	This work

4.3.3 Cultivation Conditions

Throughout the course of the experiments described in this chapter, several cultivation apparatuses were utilized depending on the equipment available. All experiments were performed with Medium A^+ (Stevens et al., 1973) supplemented with 1 µM $NiSO_4$ to avoid Ni-limitation (Sakamoto and Bryant, 2001), with greater than ambient concentrations of CO_2 at 37-38°C, and similar illuminated surface to volume ratios. For initial experiments assessing WT PCC 7002 and strains TK.001-TK.004, triplicate cultures were grown in flasks containing 200-mL of media. Cultures were grown at 37˚C with continuous illumination at 325 µmol photons m^{-2} s^{-1} and were sparged with 0.4% (v/v) CO_2 in air. Experiments with strains TK.005-TK.009 were grown in triplicate using tubes containing 15-mL of media grown at 37˚C with continuous illumination at 325 µmol photons m^{-2} s^{-1} sparged with 0.4% (v/v) CO_2 in air. Cultures utilizing the CRISPRi system (CC130-CC142) were sparged with either air (0.04% CO_2) or high CO_2 (1% CO_2) in duplicate using tubes containing 15-mL of media and induced with 1000 ng ml-1 anhydrous tetracycline (aTc). Temperature was maintained at 38°C and light intensity was approximately 250 umol photons $m^{-2}s^{-1}$. Strains TK.041, CC133, and TK.029 were grown in 250 ml baffled flasks with 50 mL of media with 1% CO_2-enriched air at 150 rpm in a custom Kuhner ISF1-X orbital shaker with continuous illumination at 200 µmol photons m^{-2} s^{-1}. Prior to each run, cultures were grown to early stationary phase with the appropriate antibiotics (OD_{730} of approximately 1), and then re-diluted to OD_{730} of 0.05, and induced with IPTG at time zero.

4.3.4 Analytical Procedures

Samples were withdrawn periodically for biomass and lactate measurements, centrifuged, and the supernatant was stored at -20°C until quantification. Biomass productivity was calculated over the time course using a linear fit assuming 50% carbon by mass (Thomas, 2015). Glycogen content was assayed using an enzymatic kit (Cayman Chemical) according to the manufacturer's instructions. Organic acids in the supernatant were quantified by comparison of refractive index peaks with peaks generated by known amounts of lactate, α-ketoglutaric acid, and pyruvate sodium salts (Sigma) in Medium A^+ after analysis by HPLC (Shimadzu Co., Columbia, MD, USA) system equipped with a quaternary pump, autosampler, vacuum degasser, photodiode array and refractive index detector. Throughout the course of the experiments described in this chapter, several HPLC methods were utilized depending on the equipment available. Initial HPLC separations were performed using an Aminex HPX-87H column. The HPLC operating conditions were as follows: Mobile phase: 5 mM H_2SO_4, Flow rate 0.600 mL/min, Column Temperature 50C, refractive index Detector Temperature 50C, photodiode array Detector at 210 nm Run time: 25 minutes, Injection volume 20 µL. Later HPLC separations were performed using an Ultra Aqueous C18 column (Restek). The HPLC operating conditions were as follows: mobile phase: 50 mM KH_2PO_4 (pH 2.5 with 1% Acetonitrile), flow rate 0.100 mL/min, column temperature 30°C, photodiode array detector at 210 nm, run time: 10 minutes, injection volume 10 µL.

4.4 Results

4.4.1 LDH Cofactor Affinity Enhances Productivity

It has become apparent that cofactor usage can have large effects on the overall titer of fermentation products such as ethanol, 1-butanol, 1,2-propanediol, and lactate (Angermayr et al., 2014; Lan and Liao, 2012; Li and Liao, 2013; Oliver et al., 2013). Cyanobacteria have a ten-fold higher intracellular concentration of NADPH than NADH under photoautotrophic growth (Bennette et al., 2011) and most lactate dehydrogenases (LDH) prefer NADH. Therefore, metabolic engineering strategies for producing L-lactate in cyanobacteria have employed the soluble and bidirectional transhydrogenase (*uhdA)* from *E. coli* (Sauer et al., 2004) to convert NAPDH to NADH, or have expressed a NADPH-utilizing LDH. The *B. subtilis* lactate dehydrogenase (BsLDH) natively uses NADH as source of reductant. An engineered version of the *B. subtilis* LDH with a single amino acid substitution (BsLDHV39R) has been demonstrated to utilize NADPH at very high specific activities compared to other LDH enzymes (Richter et al., 2011). This engineered enzyme has been used previously for L-lactate production in PCC 6803 (Angermayr et al., 2014). To resolve the effects of the enzymatic cofactor usage on productivity, both BsLDH and BsLDHV39R with or without an additional soluble transhydrogenase (*udhA)* were placed in an artificial operon under control of the $P_{cLac143}$ IPTG-inducible system (Markley et al., 2015) in the chromosomal SYNPCC7002_A1838 locus (Begemann et al., 2013) of PCC 7002, generating strains TK.001-TK.004. WT PCC 7002 was used as a negative control.

As shown in **Fig. 4-1**, WT PCC 7002, TK.001 (BsLDH), TK.002 (BsLDH udhA), TK.003 (BsLDHV39R), and TK.004 (BsLDHV39R udhA), all grew at relatively similar linear

growth rates under conditions of 200-ml cultures at 325 µmol photons m^{-2} s^{-1} and 0.4% (v/v) CO_2 in air at 37˚C with 0.5 mM IPTG. However, there were prominent differences in lactate productivity between strains. WT PCC 7002 produced no detectable quantities of lactate during the sampling period, indicating that the native copy of *ldh* is not sufficient for producing lactate under these conditions. As has reported in other studies (Angermayr et al., 2012), introduction of the BsLDH to a WT strain increased L-lactate production as shown in TK.001(productivity: 0.005 ± 0.002 mM h^{-1}, 3% carbon flux). Addition of the transhydrogenase in strain TK.002 increased the saturation of the wild-type BsLDH with NADH, and moderately increased L-lactate production (productivity: 0.008 ± 0.001 mM h^{-1}, 3% carbon flux). Lactate productivities from the TCK003 strain (0.023 ± 0.002 mM h^{-1}, 10% carbon flux) and the TCK004 strain (0.024 ± 0.002 mM h^{-1}, 11% carbon flux) were significantly higher, suggesting that the NADPH preferring LDH was a superior strategy for producing L-lactate, as has been previously reported (Angermayr et al., 2014) (see **Table 4-2**). No detectable amounts of pyruvate or α-ketoglutarate could be found in the media for any of the tested strains under these conditions.

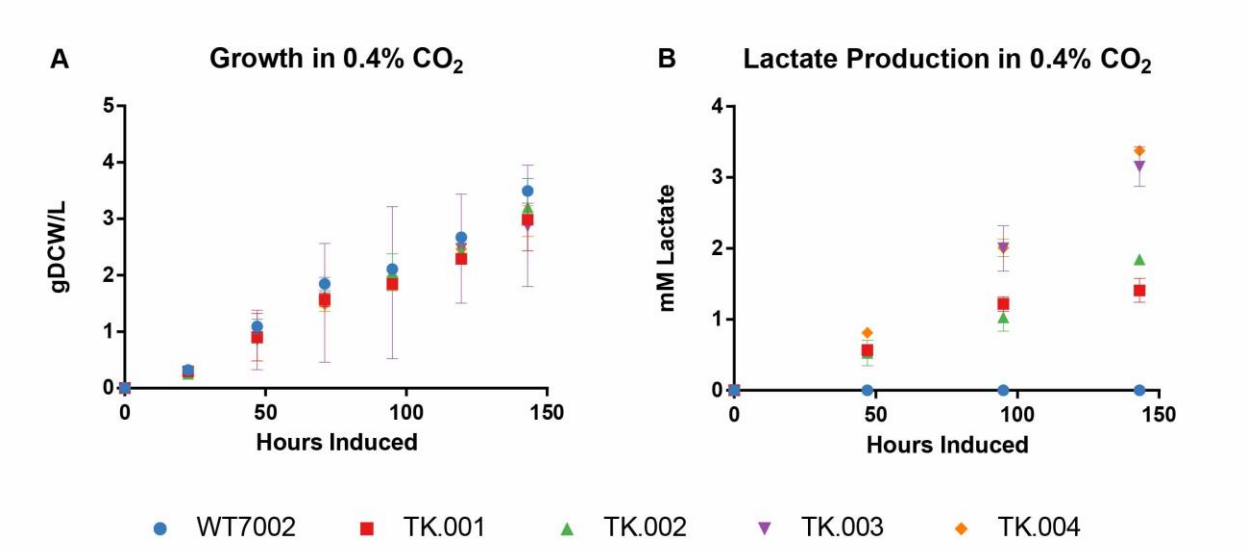

Figure 4-1. Changing the Cofactor Preference of the LDH to NADPH Increases L-lactate Productivity.

(A) Growth and (B) L-Lactate production of strains cultivated in 200-ml cultures at 325 μmol photons m^{-2} s^{-1} and 0.4% (v/v) CO_2 in air at 37˚C with 0.5 mM IPTG.

4.4.2 Removal of a Competing Carbon Sink Has Pleiotropic Effects

Glycogen is a storage polymer of α-1,4 linked, α-1,6 branched glucose that can be found in a wide variety of species (Ball and Morell, 2003). During photoautotrophic growth glycogen has been reported to account for 10-20% of the total fixed carbon in PCC 7002 (Hendry et al., 2017) and its biosynthesis is tightly regulated in response to environmental conditions (Xu et al., 2013). Deletion of the *glgC* gene, which encodes the enzyme ADP-pyrophosphorylase, removes the ability for PCC 7002 to synthesize glycogen, but reroutes carbon flux to synthesize greater amounts of soluble sugars (Guerra et al., 2013) and metabolites involved in fermentation, including pyruvate (Davies et al., 2014), the precursor to lactate. This phenomenon has been attributed to be a broad feature of metabolism under conditions of a high carbon supply and unrestricted carbon uptake (Paczia et al., 2012). A similar strategy has been used to improve L-lactate productivity in PCC 6803 under nitrogen limitation (van der Woude et al., 2014). To examine the effect of the removal of this competing carbon sink on growth rates and lactate productivity, the *glgC* gene was disrupted with the kanamycin resistance gene, *aphII* in WT PCC 7002 and strains TK.001-TK.004, yielding strains TK.005-TK.009.

Initially, we directly compared the glycogen content of WT PCC 7002 and its ΔglgC counterpart, strain TK.005 after 24 hours of growth in ambient CO_2. As shown in **Fig. 4-2A**, the intracellular concentration of glycogen in strain TK.005 was negligible. WT PCC 7002, TK.003, and TK.004 were also further assessed to TK.005, TK.008, and TK.009 (their ΔglgC counterparts) in terms of growth rates and final biomass titers in the same cultivation conditions (**Fig. 4-2B).** All tested ΔglgC strains of PCC 7002 had remarkably lower growth rates and appeared to reach

stationary phase sooner when compared to their parent strains. Additional experiments were performed comparing biomass accumulation as well as lactate, pyruvate, and α-ketoglutarate excretion in strains TK.005-TK.009 with 15-ml cultures at 325 µmol photons m^{-2} s^{-1} and 0.4% (v/v) CO_2 in air at 37˚C (**Fig. 4-3)**. As glycogen synthesis was disrupted, lag times were exacerbated in strains presumably consuming NADPH at high rates, either though expression the soluble transhydrogenase or the V39R LDH. Model fitting of a PCC 7002 mutant deficient in glycogen synthesis has suggested a mismatch between the supply and demand of ATP and NADPH (Hendry et al., 2017), which may explain the intensified lag times. At the onset of stationary phase, we also saw excretion of α-ketoglutarate and pyruvate in strains TK.005-TK.009 as reported by prior studies (Guerra et al., 2013). L-lactate was only found in strains containing an LDH, representing up to 6% of the total fixed carbon in strain TK.006. L-lactate volumetric productivities in strains TK.007-TK.009 were significantly lower due to lower growth rates (**Table 4-2**). Pyruvate accumulation in the media of strains TK.006-TK.009 also suggested that expression of LDH was not optimized in this experiment.

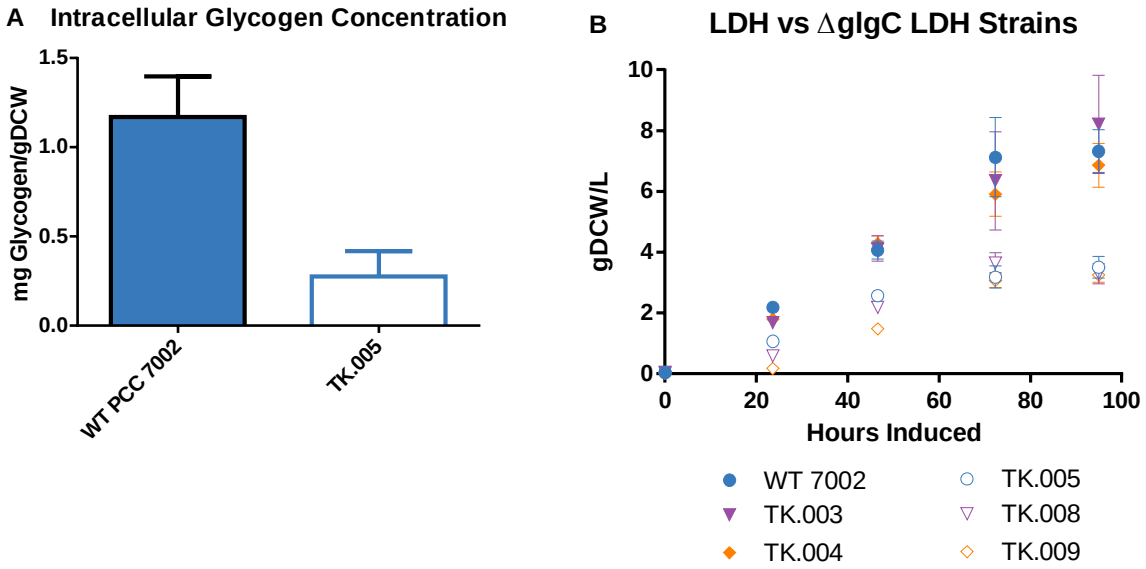

Figure 4-2. Deletion of *glgC* Drastically Decreases Intracellular Glycogen, Lowers Growth Rates, and Causes Cells to Reach Stationary Phase Sooner.

(A) Intracellular glycogen as measured by an enzymatic kit (B) Growth of strains cultivated in 15-ml cultures at 325 µmol photons m^{-2} s^{-1} and 0.4% (v/v) CO_2 in air at 37˚C with 0.5 mM IPTG.

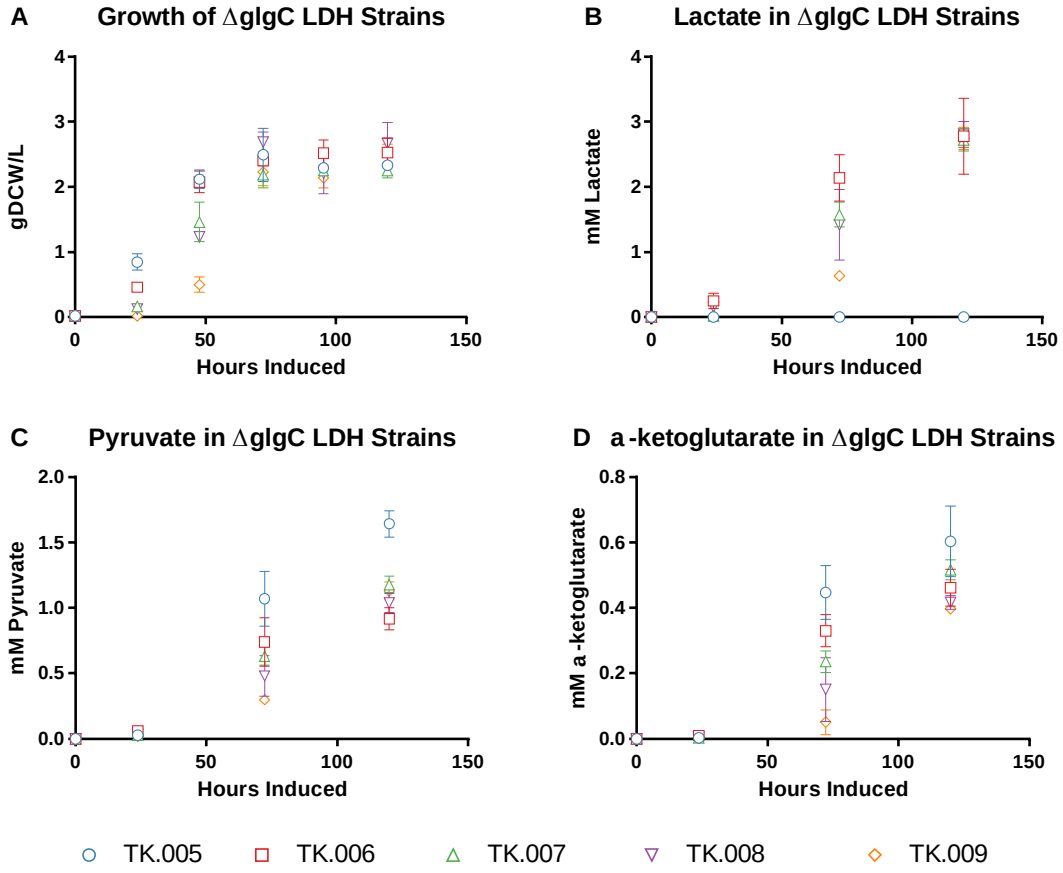

Figure 4-3. Removal of Glycogen Synthesis Does Not Enhance L-lactate Productivity Under Standard Conditions.
(A) Growth (B) L-Lactate production (C) Pyruvate production (D) α-ketoglutarate production in ΔglgC strains cultivated in 15-ml cultures at 325 µmol photons m^{-2} s^{-1} and 0.4% (v/v) CO_2 in air at 37˚C with 0.5 mM IPTG.

4.4.3 Conditionally Downregulating *glnA* via CRISPRi Improves L-lactate Production

Trans-acting regulators also have the potential to implement elegant regulatory strategies in cell factories. We used the CRISPRi tools described in (Gordon et al., 2016) to increase the production of lactate. An expression cassette with V39R LDH under the control of the $P_{cLac143}$ IPTG-inducible system (Markley et al., 2015) was integrated into the chromosome at the A2842 (*glpK)* locus along with a gentamicin resistance marker to generate the base strain, CC133. In conjunction with elevated expression of the optimized LDH, we predicted that limited flux from

carbon fixation to pyruvate would limit lactate production. Enhanced pyruvate excretion and attenuation of phycobilisome and chlorophyll *a* degradation has been demonstrated under nitrogen starvation in several strains of cyanobacteria when glycogen synthesis is disrupted (Davies et al., 2014, Gründel et al., 2012; Hickman et al., 2013). We hypothesized that moderate reduction of glutamine synthetase I (*glnA*) expression would slow the rate of nitrogen assimilation though the GS-GOGAT pathway (Muro-Pastor and Florencio, 2003). Slowing the rate of nitrogen assimilation would thereby lead to increased intracellular accumulation of α-ketoglutarate, activating the global nitrogen transcriptional activator, NtcA, a transcription factor from the cyclic AMP receptor protein class (Herrero et al., 2001). This in turn, modulates a suite of metabolic processes related to glycogen degradation and glycolysis, thereby enhancing the flux of fixed carbon to pyruvate (Osanai et al., 2006). However, severe nitrogen limitation will further increase intracellular α-ketoglutarate levels, facilitating complex formation between active NtcA and regulatory factor, PipX (Espinosa et al., 2006), negatively affecting de-novo protein synthesis and overall photosynthesis rates (Espinosa et al., 2014; Krasikov et al., 2012). Therefore, we chose to titrate the degree of repression of *glnA* using the CRISPRi approached described above (**Fig. 4-4**). As additional controls, a sgRNA targeting YFP or *glnA* were integrated in the NS1 locus under the control of the aTc-inducible system, to create strains CC142 and CC130, respectively. dCas9 with the F RBS was integrated in CC130 to create strain CC131.

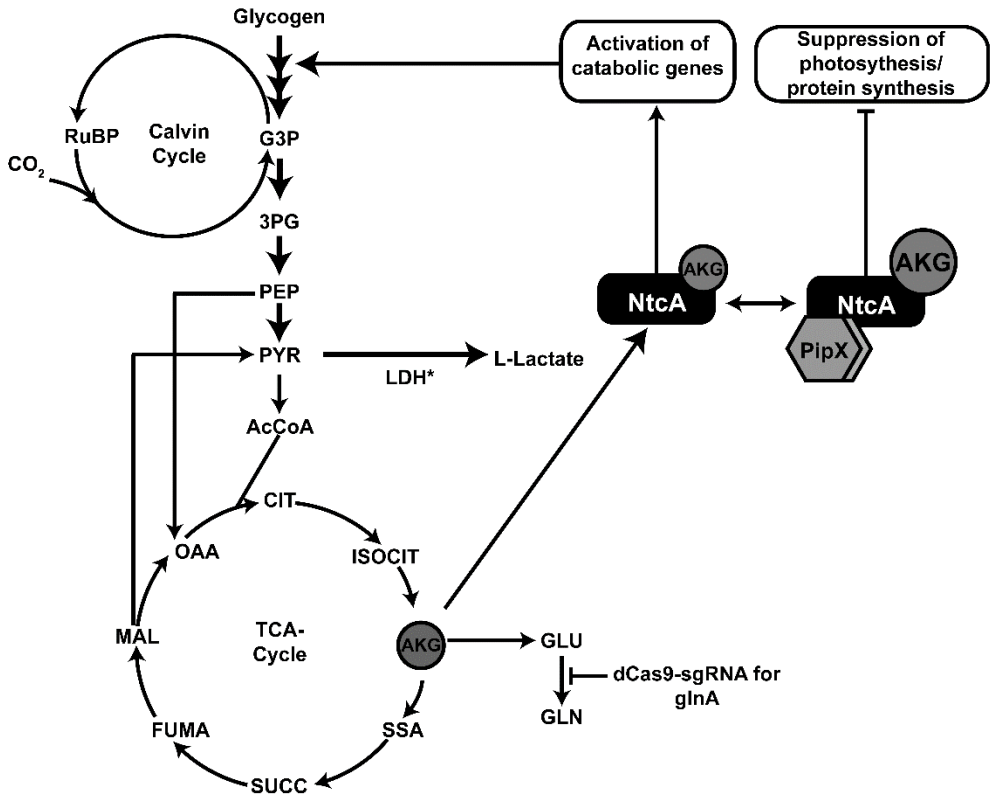

Figure 4-4. Schematic of Proposed Mechanism for Increased L-lactate Production.
Moderate accumulation of α-ketoglutarate by *glnA* repression leads to NtcA activation and subsequent activation of catabolic genes.

Interestingly, we found enhanced lactate production, as well as delayed phycobilisome and chlorophyll *a* degradation (**Fig. 4-5E, Fig. 4-5F)**, in both strains harboring the *glnA* sgRNA when compared to the control strains in 1% CO_2 or air. This inhibition of phycobilisome degradation had been previously reported for PCC 7942 treated with a chemical inhibitor of glutamine synthetase (Sauer et al., 1999). Integration of *glnA* sgRNA improved production rates (productivity: 0.079 ± 0.001 mM h^{-1}, carbon flux: 14%) in CC130 and (productivity: 0.092 ± 0.001 mM h^{-1}, carbon flux: 16%) in CC131, both significantly improved to control strains CC133 (productivity: 0.045 ± 0.002 mM h^{-1}, carbon flux: 8%) and CC142 (productivity: 0.029 ± 0.002 mM h^{-1}, carbon flux: 5%), indicating that this effect was *glnA* sgRNA specific (**Fig. 4-5B)**. This *glnA* sgRNA mediated effect may be due to a basal level of repression though cross-talk with the native CRISPR-Cas systems, unlike the other native genes targeted previously, given the

difference in transcript abundance between *glnA, ccmK,* and *cpcB* (Ludwig and Bryant, 2012, 2011). There was no apparent difference in growth rate between the any of the producing strains in 1% CO_2 (**Fig. 4-5A**) or air (**Fig. 4-5C**). *glnA* has previously been shown to be non-essential for ammonium assimilation in PCC 7002 (Wagner et al., 1993). This suggests that *glnA* repression or LDH expression did not severely impact amino acid synthesis or biomass generation. Given the significant increase in carbon products, the data also suggests that carbon storage polymers were rerouted to product, or carbon fixation rates were enhanced in CC131, analogous to cells engineered to secrete sucrose (Ducat et al., 2012).

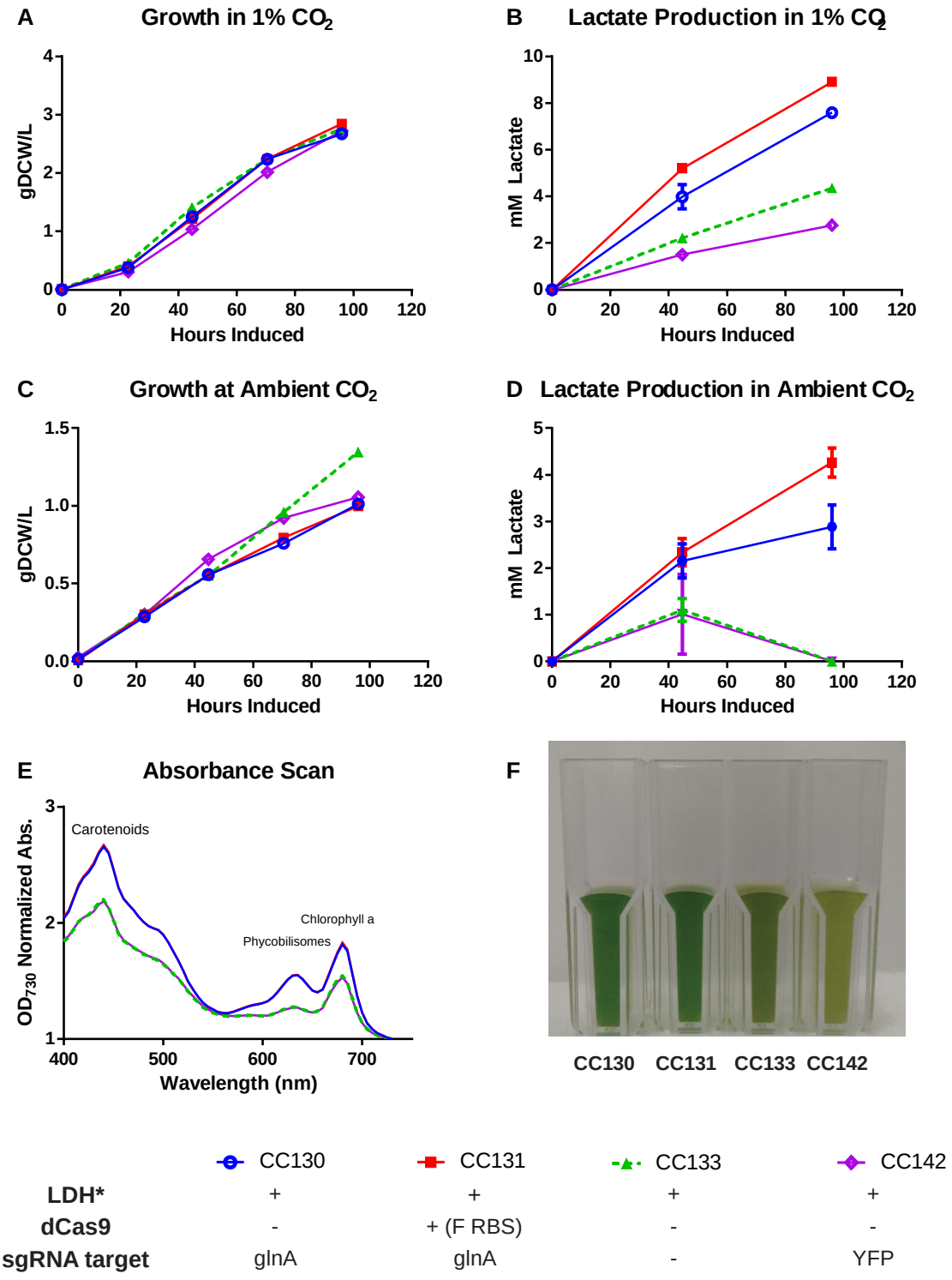

Figure 4-5. Repression of Glutamine Synthetase Improves L-lactate Production and Halts Phycobilisome (635 nm) and Chlorophyll *a* (680 nm) Degradation.
(A) Growth and (B) L-Lactate production of strains grown in 1% CO_2. Growth (C) and (D) L-Lactate production of strains grown in air. Averages of strains grown in duplicate are shown (error bars show standard deviation). Representative (E) spectra and (F) image are of cultures grown in air at 96 hs of induction, normalized to OD_{730nm}.

4.4.4 Overexpression of a Glycolytic Transcriptional Regulator Enhances L-lactate production

High glycolytic flux has been shown to enhance the synthesis of pyruvate in metabolically engineered strains of *E. coli* (Zhu et al., 2008). Glycolytic flux is primarily controlled by the demands for cofactors, such as NADH and ATP, and has been enhanced in *E. coli* by creating futile cycles (Holm et al., 2010). An alternative strategy to increase glycolytic flux would be enhance expression of a regulator. For example, overexpression of the NtcA transcriptional regulator has been used to enhance production of ethylene in engineered strains of PCC 6803 (Mo et al., 2017). In cyanobacteria, *sll1330* (Rre37*)* has been shown to positively regulate glycolytic flux (Tabei et al., 2007) and glycogen catabolism (Osanai et al., 2014) as part of the OmpR-type two component regulatory system. Rre37 expression is also enhanced under nitrogen depletion though activation of the NtcA regulon (Azuma et al., 2011). It is presumed that stimulation of this regulator is the main driver of the high productivity of strain CC131. Direct overexpression of Rre37 would be advantageous to the CRISPRi strategy employed with strain CC131 in environments where the intracellular concentration of α-ketoglutarate is low, such as in $NH4^+$ containing media. To test the effect of Rre37 on lactate productivity, an operon with the engineered V39R LDH and Rre37 under the control of the $P_{cLac143}$ IPTG-inducible system (Markley et al., 2015) was integrated into the chromosome at the A2842 (*glpK)* locus along with a gentamicin resistance marker to generate the strain TK.029. Attempts to solely integrate Rre37 failed to generate viable colonies. Strain CC133 and TK.041 (gentamicin resistance marker in the A2842 locus) served as positive and negative controls, respectively. As shown in **Fig. 4-6,** simultaneous expression of V39R LDH and Rre37 in strain TK.029 enhanced L-lactate production (productivity: 0.066 ± 0.019 mM h^{-1}, 19% carbon flux) relative to CC133 (productivity: 0.039 ± 0.015 mM h^{-1},

13% carbon flux). Both LDH expressing strains had a minor growth defect relative to the antibiotic cassette control, TK.041.

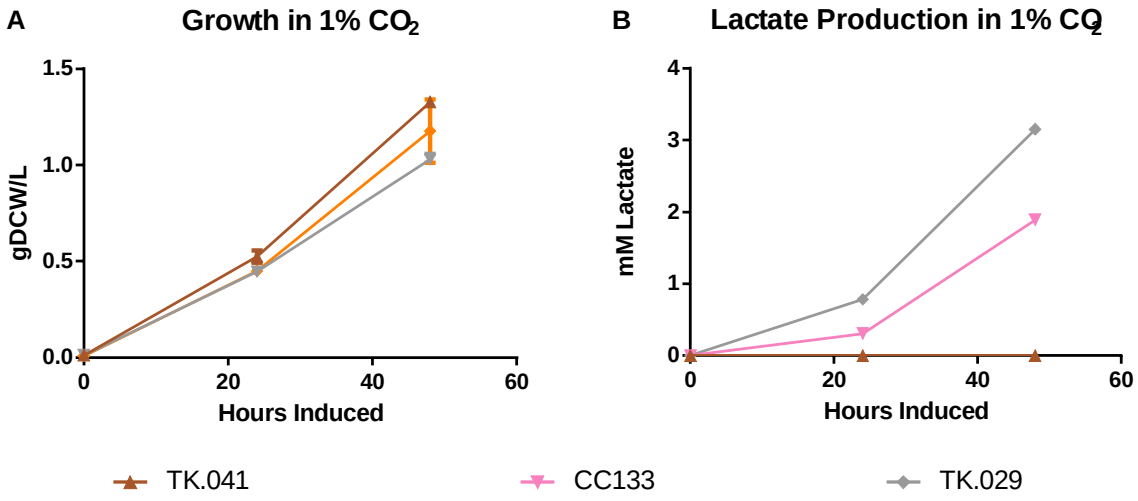

Figure 4-6. Simultaneous Overexpression of Optimized LHD and Glycolytic Regulator Rre37 Increases L-lactate Productivity.
(A) Growth and (B) L-Lactate production of strains cultivated in 50-ml cultures at 200 µmol photons m^{-2} s^{-1} and 1% (v/v) CO_2 in air at 37˚C with 1 mM IPTG.

Table 4-2. Genotypes and Performance Metrics of Lactate Producing Strains of *Synechococcus* sp. strain PCC 7002

Strain	Genotype	IPTG (mM)	Linear Growth Rate (±SD) gDCW h^{-1}	Production Rate (±SD) mM L-lactate h^{-1}	% Carbon Partitioning
WT	WT PCC 7002	0	0.018 ± 0.002	0	0
TK.001	ΔA1838::$P_{cLac143}$-BsLDH	0.5	0.018 ± 0.001	0.005 ± 0.002	2 ± 0.7
TK.002	ΔA1838::$P_{cLac143}$-BsLDH udhA	0.5	0.018 ± 0.001	0.008 ± 0.001	3 ± 0.4
TK.003	ΔA1838::$P_{cLac143}$-BsLDHV39R	0.5	0.018 ± 0.001	0.022 ± 0.002	9 ± 0.7
TK.004	ΔA1838::$P_{cLac143}$-BsLDHV39R udhA	0.5	0.016 ± 0.002	0.023 ± 0.001	11 ± 1.1
TK.005[a]	ΔA0095::aphII	0	0.036 ± 0.005	0	0
TK.006[a]	ΔA0095::aphII ΔA1838::$P_{cLac143}$-BsLDH	1	0.036 ± 0.007	0.031 ± 0.003	6 ± 0.9
TK.007[a]	ΔA0095::aphII ΔA1838::$P_{cLac143}$-BsLDH udhA	1	0.032 ± 0.006	0.023 ± 0.003	5 ± 0.9
TK.008[a]	ΔA0095::aphII ΔA1838::$P_{cLac143}$-BsLDHV39R	1	0.038 ± 0.009	0.021 ± 0.004	4 ± 0.9
TK.009[a]	ΔA0095::aphII ΔA1838::$P_{cLac143}$-BsLDHV39R udhA	1	0.029 ± 0.011	0.009 ± 0.001	2 ± 0.6
CC130	ΔA2842::$P_{cLac143}$-BsLDHV39R-aacC1 ΔNS1:: P_{EZtet} sgRNA glnA- aphII	1	0.040 ± 0.002	0.079 ± 0.001	14 ± 0.7
CC131	ΔA2842::$P_{cLac143}$-BsLDHV39R-aacC1 ΔA1838::$P_{EZtet\ F\ RBS}$ dCas9 ΔNS1:: P_{EZtet} sgRNA glnA- aphII	1	0.042 ± 0.002	0.092 ± 0.001	16 ± 1.3
CC133	ΔA2842::$P_{cLac143}$-BsLDHV39R-aacC1	1	0.040 ± 0.002	0.045 ± 0.002	8 ± 1.2
CC142	ΔA2842::$P_{cLac143}$-BsLDHV39R-aacC1 ΔNS1:: P_{EZtet} sgRNA YFP- aphII	1	0.040 ± 0.002	0.025 ± 0.005	5 ± 0.4
TK.041[b]	ΔA2842::aacC1	0	0.027 ± 0.002	0	0
CC133[b]	ΔA2842::$P_{cLac143}$-BsLDHV39R-aacC1	1	0.021 ± 0.001	0.039 ± 0.015	13 ± 5.2
TK.029[b]	ΔA2842::$P_{cLac143}$-BsLDHV39R rre37-aacC1	1	0.024 ± 0.002	0.066 ± 0.019	19 ± 5.8

Blocked rows report data from experiments run at the same time. [a]Data calculated using 72 hours of growth and production, due to non-linear fit in stationary phase. [b]Data calculated using 48 hours of growth and production

4.5 Discussion

PCC 7002 was metabolically engineered to excrete L-lactate by heterologous expression of an engineered *B. subtilis* LDH. Production rates were further enhanced by stimulating glycolytic flux, resulting in a maximum volumetric productivity of 0.092 ± 0.001 mM h^{-1} and carbon flux of 16% in strain CC131. This is the highest L-lactate productivity for a cyanobacteria to date, and was achieved with no significant growth defect. Prior attempts to increase pyruvate supply in PCC 6803 have overexpressed a pyruvate kinase or partially limited PEP carboxylase activity (Angermayr et al., 2014), but these attempts left mutant strains with a lowered growth rate. The approaches to increase pyruvate availability using CRISPRi or Rre37 as described in this chapter most likely resulted from indirect upregulation of the enzyme glyceraldehyde-3-phosphate dehydrogenase (GAPDH-1), which is the rate limiting enzyme for lower glycolysis in PCC 7002 (Kumaraswamy et al., 2013). GAPDH-1 has shown to be upregulated during nitrogen starvation (Osanai et al., 2006) and Rre37 overexpression (Osanai et al., 2014) in PCC 6803. GAPDH-1 overexpression in PCC 7002 resulted in an increased redox poise and lower-glycolytic catabolic rate during fermentative conditions, with no noted growth defect under photoautotrophic conditions (Kumaraswamy et al., 2013). GAPDH-1 is also allosterically feedback-regulated by the $NADH/NAD^+$ ratio (Koksharova et al., 1998), so it may be possible that the engineered LDH overexpression significantly alters the redox state of the cell, such that the native regulation is relieved. It is worth noting that optimization of LDH expression was not performed in these experiments, so future work should investigate if significant carbon partitioning to L-lactate results in enhanced carbon fixation, as was reported for sucrose production (Ducat et al., 2012) or a fitness reduction. The effects of long-term carbon

partitioning to another pyruvate derived product, ethanol, were recently described for PCC 7002 cultivated under diurnal cycles (Kopka et al., 2017). There, it was reported that significant a pyruvate pool depletion gradually decreased productivity in mutant strains, and should be overcome by increasing photosynthetic efficiency.

Disruption of glycogen synthesis resulted in strains of PCC 7002 that excreted large amounts of overflow metabolites and reached stationary phase sooner than counterparts with an intact biosynthetic pathway, as has been reported for other cyanobacterial strains (Benson et al., 2016; Gründel et al., 2012). It was interesting to note that lag times increased and L-lactate productivities fell in any NADPH consuming strain in the ΔglgC background. Activity of the ADP-pyrophosphorylase (glgC) has been demonstrated to be redox regulated in PCC 6803 (Díaz-Troya et al., 2014), and glycogen synthesis has been shown to be an integral response to various stresses in cyanobacteria (Gründel et al., 2012). This work adds to the growing body of research that suggests disruption of polyglucan biosynthesis should be avoided in cyanobacteria due to its broad metabolic role in photosynthetic organisms (Baran et al., 2017).

4.6 Conclusions

Synechococcus sp. PCC 7002 was initially metabolically engineered to excrete L-lactate by heterologous expression of an engineered *B. subtilis* lactate dehydrogenase. Removal of glycogen synthesis did not increase productivity under tested conditions. L-lactate production rates were improved roughly two-fold by stimulating glycolytic flux, either by downregulation of a key enzyme involved in nitrogen assimilation or overexpression of a transcriptional regulator. We could partition 16% of fixed carbon into product without any notable effects on fitness. We

anticipate that this approach could be similarly effective in increasing photosynthetic flux to other chemical products, especially those derived from pyruvate.

4.7 Acknowledgements

This work was supported by the US Department of Energy though grant DE-SC0010329; the National Science Foundation grant EFRI-1240268; and the William F. Vilas Trust. GCG and TCK are recipients of NIH Biotechnology Training Fellowships (NIGMS - 5 T32 GM08349).

4.7 Literature Cited

Angermayr, S.A., Paszota, M., Hellingwerf, K.J., 2012. Engineering a cyanobacterial cell factory for production of lactic acid. Appl. Environ. Microbiol. 78, 7098–106. doi:10.1128/AEM.01587-12

Angermayr, S.A., van der Woude, A.D., Correddu, D., Vreugdenhil, A., Verrone, V., Hellingwerf, K.J., 2014. Exploring metabolic engineering design principles for the photosynthetic production of lactic acid by Synechocystis sp. PCC6803, Biotechnology for Biofuels. doi:10.1186/1754-6834-7-99

Azuma, M., Osanai, T., Hirai, M.Y., Tanaka, K., 2011. A response regulator Rre37 and an RNA polymerase sigma factor SigE represent two parallel pathways to activate sugar catabolism in a cyanobacterium Synechocystis sp. PCC 6803. Plant Cell Physiol. 52, 404–12. doi:10.1093/pcp/pcq204

Ball, S.G., Morell, M.K., 2003. From Bacterial Glycogen to Starch: Understanding the Biogenesis of the Plant Starch Granule. Annu. Rev. Plant Biol. doi:10.1146/annurev.arplant.54.031902.134927

Baran, R., Lau, R., Bowen, B.P., Diamond, S., Jose, N., Garcia-Pichel, F., Northen, T.R., 2017. Extensive Turnover of Compatible Solutes in Cyanobacteria Revealed by Deuterium Oxide (D2O) Stable Isotope Probing. ACS Chem. Biol. 12, 674–681. doi:10.1021/acschembio.6b00890

Begemann, M.B., Zess, E.K., Walters, E.M., Schmitt, E.F., Markley, A.L., Pfleger, B.F., 2013. An organic acid based counter selection system for cyanobacteria. PLoS One 8, e76594.

doi:10.1371/journal.pone.0076594

Bennette, N., Eng, J., Dismukes, G., 2011. An LC–MS-based chemical and analytical method for targeted metabolite quantification in the model cyanobacterium Synechococcus sp. PCC 7002. Anal. Chem. 3808–3816.

Benson, P.J., Purcell-Meyerink, D., Hocart, C.H., Truong, T.T., James, G.O., Rourke, L., Djordjevic, M.A., Blackburn, S.I., Price, G.D., 2016. Factors Altering Pyruvate Excretion in a Glycogen Storage Mutant of the Cyanobacterium, Synechococcus PCC7942. Front. Microbiol. 7, 475. doi:10.3389/fmicb.2016.00475

Berla, B.M., Saha, R., Immethun, C.M., Maranas, C.D., Moon, T.S., Pakrasi, H.B., 2013. Synthetic biology of cyanobacteria: unique challenges and opportunities. Front. Microbiol. 4, 246. doi:10.3389/fmicb.2013.00246

Clark, R.L., Cameron, J.C., Root, T.W., Pfleger, B.F., 2014. Insights into the industrial growth of cyanobacteria from a model of the carbon-concentrating mechanism. AIChE J. 60, 1269–1277. doi:10.1002/aic.14310

Davies, F.K., Work, V.H., Beliaev, A.S., Posewitz, M.C., 2014. Engineering Limonene and Bisabolene Production in Wild Type and a Glycogen-Deficient Mutant of Synechococcus sp. PCC 7002. Front. Bioeng. Biotechnol. 2, 1–11. doi:10.3389/fbioe.2014.00021

Díaz-Troya, S., López-Maury, L., Sánchez-Riego, A.M., Roldán, M., Florencio, F.J., 2014. Redox regulation of glycogen biosynthesis in the cyanobacterium synechocystis sp. PCC 6803: Analysis of the AGP and glycogen synthases. Mol. Plant 7, 87–100. doi:10.1093/mp/sst137

Ducat, D.C., Avelar-Rivas, J.A., Way, J.C., Silver, P.A., 2012. Rerouting carbon flux to enhance photosynthetic productivity. Appl. Environ. Microbiol. 78, 2660–8. doi:10.1128/AEM.07901-11

Ducat, D.C., Way, J.C., Silver, P.A., 2011. Engineering cyanobacteria to generate high-value products. Trends Biotechnol. 29, 95–103.

Espinosa, J., Forchhammer, K., Burillo, S., Contreras, A., 2006. Interaction network in cyanobacterial nitrogen regulation: PipX, a protein that interacts in a 2-oxoglutarate dependent manner with PII and NtcA. Mol. Microbiol. 61, 457–69. doi:10.1111/j.1365-2958.2006.05231.x

Espinosa, J., Rodríguez-Mateos, F., Salinas, P., Lanza, V.F., Dixon, R., de la Cruz, F., Contreras, A., 2014. PipX, the coactivator of NtcA, is a global regulator in cyanobacteria. Proc. Natl. Acad. Sci. U. S. A. 111, E2423-30. doi:10.1073/pnas.1404097111

Gibson, D.G., Young, L., Chuang, R.-Y., Venter, J.C., Hutchison, C.A., Smith, H.O., 2009. Enzymatic assembly of DNA molecules up to several hundred kilobases. Nat. Methods 6, 343–5. doi:10.1038/nmeth.1318

Gordon, G.C., Korosh, T.C., Cameron, J.C., Markley, A.L., Begemann, M.B., Pfleger, B.F., 2016. CRISPR interference as a titratable, trans-acting regulatory tool for metabolic engineering in the cyanobacterium Synechococcus sp. strain PCC 7002. Metab. Eng. 38, 170–179. doi:10.1016/j.ymben.2016.07.007

Gründel, M., Scheunemann, R., Lockau, W., Zilliges, Y., 2012. Impaired glycogen synthesis causes metabolic overflow reactions and affects stress responses in the cyanobacterium Synechocystis sp. PCC 6803. Microbiology 158, 3032–43. doi:10.1099/mic.0.062950-0

Guerra, L.T., Xu, Y., Bennette, N., McNeely, K., Bryant, D. a, Dismukes, G.C., 2013. Natural osmolytes are much less effective substrates than glycogen for catabolic energy production in the marine cyanobacterium Synechococcus sp. strain PCC 7002. J. Biotechnol. 166, 65–75. doi:10.1016/j.jbiotec.2013.04.005

Heidorn, T., Camsund, D., Huang, H.-H., Lindberg, P., Oliveira, P., Stensjö, K., Lindblad, P., 2011. Chapter Twenty-Four - Synthetic Biology in Cyanobacteria: Engineering and Analyzing Novel Functions, in: Enzymology, C.V.B.T.-M. in (Ed.), Synthetic Biology, Part A. Academic Press, pp. 539–579. doi:http://dx.doi.org/10.1016/B978-0-12-385075-1.00024-X

Hendry, J.I., Prasannan, C., Ma, F., Möllers, K.B., Jaiswal, D., Digmurti, M., Allen, D.K., Frigaard, N.-U., Dasgupta, S., Wangikar, P.P., 2017. Rerouting of carbon flux in a glycogen mutant of cyanobacteria assessed via isotopically non-stationary 13C metabolic flux analysis. Biotechnol. Bioeng. n/a-n/a. doi:10.1002/bit.26350

Herrero, A., Muro-Pastor, A.M., Flores, E., 2001. Nitrogen control in cyanobacteria. J. Bacteriol. 183, 411–25.

Hickman, J.W., Kotovic, K.M., Miller, C., Warrener, P., Kaiser, B., Jurista, T., Budde, M., Cross, F., Roberts, J.M., Carleton, M., 2013. Glycogen synthesis is a required component of the nitrogen stress response in Synechococcus elongatus PCC 7942. Algal Res. 2, 98–106. doi:10.1016/j.algal.2013.01.008

Holm, A.K., Blank, L.M., Oldiges, M., Schmid, A., Solem, C., Jensen, P.R., Vemuri, G.N., 2010. Metabolic and transcriptional response to cofactor perturbations in Escherichia coli. J. Biol. Chem. 285, 17498–17506. doi:10.1074/jbc.M109.095570

Koksharova, O., Schubert, M., Shestakov, S., Cerff, R., 1998. Genetic and biochemical evidence for distinct key functions of two highly divergent GAPDH genes in catabolic and anabolic

carbon flow of the cyanobacterium. Plant Mol. Biol. 183–194.

Kopka, J., Schmidt, S., Dethloff, F., Pade, N., Berendt, S., Schottkowski, M., Martin, N., Dühring, U., Kuchmina, E., Enke, H., Kramer, D., Wilde, A., Hagemann, M., Friedrich, A., 2017. Systems analysis of ethanol production in the genetically engineered cyanobacterium Synechococcus sp. PCC 7002. Biotechnol. Biofuels 10, 56. doi:10.1186/s13068-017-0741-0

Krasikov, V., Aguirre von Wobeser, E., Dekker, H.L., Huisman, J., Matthijs, H.C.P., 2012. Time-series resolution of gradual nitrogen starvation and its impact on photosynthesis in the cyanobacterium Synechocystis PCC 6803. Physiol. Plant. 145, 426–39. doi:10.1111/j.1399-3054.2012.01585.x

Kumaraswamy, G.K., Guerra, T., Qian, X., Zhang, S., Bryant, D. a., Dismukes, G.C., 2013. Reprogramming the glycolytic pathway for increased hydrogen production in cyanobacteria: metabolic engineering of NAD+-dependent GAPDH. Energy Environ. Sci. 6, 3722. doi:10.1039/c3ee42206b

Lan, E.E.I., Liao, J.C.J., 2012. ATP drives direct photosynthetic production of 1-butanol in cyanobacteria. Proc. Natl. Acad. Sci. U. S. A. 109, 6018–23. doi:10.1073/pnas.1200074109/-/DCSupplemental.www.pnas.org/cgi/doi/10.1073/pnas.1200074109

Li, H., Liao, J.C., 2013. Engineering a cyanobacterium as the catalyst for the photosynthetic conversion of CO2 to 1,2-propanediol. Microb. Cell Fact. 12, 4. doi:10.1186/1475-2859-12-4

Ludwig, M., Bryant, D.A., 2012. Acclimation of the Global Transcriptome of the Cyanobacterium Synechococcus sp. Strain PCC 7002 to Nutrient Limitations and Different Nitrogen Sources. Front. Microbiol. 3, 145. doi:10.3389/fmicb.2012.00145

Ludwig, M., Bryant, D.A., 2011. Transcription Profiling of the Model Cyanobacterium Synechococcus sp. Strain PCC 7002 by Next-Gen (SOLiD^{TM}) Sequencing of cDNA. Front. Microbiol. 2, 41. doi:10.3389/fmicb.2011.00041

Markley, A.L., Begemann, M.B., Clarke, R.E., Gordon, G.C., Pfleger, B.F., 2015. A synthetic biology toolbox for controlling gene expression in the cyanobacterium Synechococcus sp. PCC 7002. ACS Synth. Biol. 4, 595–603. doi:10.1021/sb500260k

Mendez-Perez, D., Begemann, M.B., Pfleger, B.F., 2011. Modular synthase-encoding gene involved in α-olefin biosynthesis in Synechococcus sp. strain PCC 7002. Appl. Environ. Microbiol. 77, 4264–7. doi:10.1128/AEM.00467-11

Mo, H., Xie, X., Zhu, T., Lu, X., 2017. Effects of global transcription factor NtcA on

photosynthetic production of ethylene in recombinant Synechocystis sp. PCC 6803. Biotechnol. Biofuels 10, 145. doi:10.1186/s13068-017-0832-y

Muro-Pastor, M.I., Florencio, F.J., 2003. Regulation of ammonium assimilation in cyanobacteria. Plant Physiol. Biochem. 41, 595–603. doi:10.1016/S0981-9428(03)00066-4

Niederholtmeyer, H., Wolfstädter, B.T., Savage, D.F., Silver, P. a, Way, J.C., 2010. Engineering cyanobacteria to synthesize and export hydrophilic products. Appl. Environ. Microbiol. 76, 3462–6. doi:10.1128/AEM.00202-10

Okano, K., Tanaka, T., Ogino, C., Fukuda, H., Kondo, A., 2010. Biotechnological production of enantiomeric pure lactic acid from renewable resources: recent achievements, perspectives, and limits. Appl. Microbiol. Biotechnol. 85, 413–23. doi:10.1007/s00253-009-2280-5

Oliver, J.W.K., Atsumi, S., 2014. Metabolic design for cyanobacterial chemical synthesis. Photosynth. Res. 120, 249–61. doi:10.1007/s11120-014-9997-4

Oliver, J.W.K., Machado, I.M.P., Yoneda, H., Atsumi, S., 2013. Cyanobacterial conversion of carbon dioxide to 2,3-butanediol. Proc. Natl. Acad. Sci. U. S. A. 110, 1249–54. doi:10.1073/pnas.1213024110

Osanai, T., Imamura, S., Asayama, M., Shirai, M., Suzuki, I., Murata, N., Tanaka, K., 2006. Nitrogen induction of sugar catabolic gene expression in Synechocystis sp. PCC 6803. DNA Res. 13, 185–95. doi:10.1093/dnares/dsl010

Osanai, T., Oikawa, A., Numata, K., Kuwahara, A., Iijima, H., Doi, Y., Saito, K., Hirai, M.Y., 2014. Pathway-level acceleration of glycogen catabolism by a response regulator in the cyanobacterium Synechocystis species PCC 6803. Plant Physiol. 164, 1831–41. doi:10.1104/pp.113.232025

Paczia, N., Nilgen, A., Lehmann, T., Gätgens, J., Wiechert, W., Noack, S., 2012. Extensive exometabolome analysis reveals extended overflow metabolism in various microorganisms. Microb. Cell Fact. 11, 122. doi:10.1186/1475-2859-11-122

Richter, N., Zienert, A., Hummel, W., 2011. A single-point mutation enables lactate dehydrogenase from Bacillus subtilis to utilize NAD+ and NADP+ as cofactor. Eng. Life Sci. 11, 26–36. doi:10.1002/elsc.201000151

Ruffing, A.M., Jensen, T.J., Strickland, L.M., 2016. Genetic tools for advancement of Synechococcus sp. PCC 7002 as a cyanobacterial chassis. Microb. Cell Fact. 15, 190. doi:10.1186/s12934-016-0584-6

Sakamoto, T., Bryant, D.A., 2001. Requirement of Nickel as an Essential Micronutrient for the Utilization of Urea in the Marine Cyanobacterium Synechococcus sp. PCC 7002. Microbes Environ. 16, 177–184.

Sauer, J., Görl, M., Forchhammer, K., 1999. Nitrogen starvation in Synechococcus PCC 7942: Involvement of glutamine synthetase and NtcA in phycobiliprotein degradation and survival. Arch. Microbiol. 172, 247–255. doi:10.1007/s002030050767

Sauer, U., Canonaco, F., Heri, S., Perrenoud, A., Fischer, E., 2004. The Soluble and Membrane-bound Transhydrogenases UdhA and PntAB Have Divergent Functions in NADPH Metabolism of Escherichia coli. J. Biol. Chem. 279, 6613–6619. doi:10.1074/jbc.M311657200

Stevens, S.E., Patterson, C.O.P., Myers, J., 1973. The Production of Hydrogen Peroxide by Blue-Green Algae: A Survey. J. Phycol. 9, 427–430. doi:10.1111/j.1529-8817.1973.tb04116.x

Tabei, Y., Okada, K., Tsuzuki, M., 2007. Sll1330 controls the expression of glycolytic genes in Synechocystis sp. PCC 6803. Biochem. Biophys. Res. Commun. 355, 1045–1050. doi:10.1016/j.bbrc.2007.02.065

Thomas, E., 2015. Microbial growth and physiology: A call for better craftsmanship. Front. Microbiol. 6, 1–12. doi:10.3389/fmicb.2015.00287

van der Woude, A.D., Angermayr, S.A., Veetil, V.P., Osnato, A., Hellingwerf, K.J., 2014. Carbon sink removal: Increased photosynthetic production of lactic acid by Synechocystis sp. PCC6803 in a glycogen storage mutant. J. Biotechnol. doi:10.1016/j.jbiotec.2014.04.029

Wagner, S.J., Thomas, S.P., Kaufman, R.I., Nixon, B.T., Stevens, S.E., 1993. The glnA gene of the cyanobacterium Agmenellum quadruplicatum PR-6 is nonessential for ammonium assimilation. J. Bacteriol. 175, 604–12.

Xu, Y., Guerra, L.T., Li, Z., Ludwig, M., Dismukes, G.C., Bryant, D. a, 2013. Altered carbohydrate metabolism in glycogen synthase mutants of Synechococcus sp. strain PCC 7002: Cell factories for soluble sugars. Metab. Eng. 16, 56–67. doi:10.1016/j.ymben.2012.12.002

Zess, E.K., Begemann, M.B., Pfleger, B.F., 2016. Construction of new synthetic biology tools for the control of gene expression in the cyanobacterium Synechococcus sp. strain PCC 7002. Biotechnol. Bioeng. 113, 424–432. doi:10.1002/bit.25713

Zhu, Y., Eiteman, M.A., Altman, R., Altman, E., 2008. High Glycolytic Flux Improves Pyruvate Production by a Metabolically Engineered Escherichia coli Strain . Appl. Environ.

Microbiol. 74, 6649–6655. doi:10.1128/AEM.01610-08

CHAPTER 5 ENGINEERING PHOTOSYNTHETIC PRODUCTION OF L-LYSINE

Travis C. Korosh[a,b], Andrew L. Markley[a], Ryan L. Clark[a], Laura L. McGinley[a], Katherine D. McMahon[b,c,d,e], and Brian F. Pfleger [a,c,]

[a] Department of Chemical and Biological Engineering, University of Wisconsin-Madison, Madison, WI 53706, United States
[b] Environmental Chemistry and Technology Program, University of Wisconsin-Madison, Madison, WI 53706, United States
[c] Microbiology Doctoral Training Program, University of Wisconsin-Madison, Madison, WI 53706, United States
[d] Department of Civil and Environmental Engineering, University of Wisconsin-Madison, Madison, WI 53706, United States
[e] Department of Bacteriology, University of Wisconsin-Madison, Madison, WI 53706, United States

Author Contributions:

Travis C. Korosh- constructed TK strains used for experiments, performed batch cultivations and amino acid quantification, and drafting of the manuscript.
Andrew L. Markley- constructed AM strains used for experiments and provided critical feedback of the manuscript.
Ryan L. Clark- performed photobioreactor experiments and provided critical feedback of the manuscript.
Laura L. McGinley- performed photobioreactor experiments.
Katherine D. McMahon- supervised research and provided critical feedback of the manuscript.
Brian F. Pfleger-supervised research and provided critical feedback of the manuscript.

This chapter is adapted from *Metabolic Engineering*, Vol. 44, Travis C. Korosh, Andrew L. Markley, Ryan L. Clark, Laura L. McGinley, Brian F. Pfleger, Katherine D. McMahon, Engineering photosynthetic production of L-lysine, p. 273-283, https://doi.org/10.1016/j.ymben.2017.10.010, Copyright 2017, with permission from Elsevier.

5.1 Abstract

L-lysine and other amino acids are commonly produced through fermentation using strains of heterotrophic bacteria such as *Corynebacterium glutamicum*. Given the large amount of sugar this process consumes, direct photosynthetic production is intriguing alternative. In this study, we report the development of a cyanobacterium, *Synechococcus* sp. strain PCC 7002, capable of producing L-lysine with CO_2 as the sole carbon-source. We found that heterologous expression of a lysine transporter was required to excrete lysine and avoid intracellular accumulation that correlated with poor fitness. Simultaneous expression of a feedback inhibition resistant aspartate kinase and lysine transporter were sufficient for high productivities, but this was also met with a decreased chlorophyll content and reduced growth rates. Increasing the reductant supply by using NH_4^+, a more reduced nitrogen source relative to NO_3^-, resulted in a two-fold increase in productivity directing 18% of fixed carbon to lysine. Given this advantage, we demonstrated lysine production from media formulated with a municipal wastewater treatment sidestream as a nutrient source for increased economic and environmental sustainability. Based on our results, we project that *Synechococcus* sp. strain PCC 7002 could produce lysine at areal productivities approaching that of sugar cane to lysine via fermentation using non-agricultural lands and low-cost feedstocks.

5.2 Introduction

L-lysine is one of the essential amino acids required for human and animal growth. As demand for meat (e.g. poultry, swine, cattle) has grown, so has demand for essential amino acids, especially lysine (Eggeling and Bott, 2015). Lysine and other amino acids are commonly produced by fermentation using strains of heterotrophic bacteria, such as *Escherichia coli* and

Corynebacterium glutamicum (Brautaset and Ellingsen, 2011). *C. glutamicum glutamicum* has been engineered to produce lysine with a yield of 0.31 g lysine/g sugar. At this yield, current lysine demand (~1.85 million tons per year) would consume approximately 3% of world sugar production (~200 million tons per year – USDA-ERS). For this reason, it is important to consider alternative feedstocks and production strategies for essential amino acids. Direct photosynthetic production of L-lysine is an attractive process because it circumvents the need for harvesting, processing and fermentation of plant-derived sugars, by directly coupling lysine biosynthesis to photosynthesis. Cyanobacteria are attractive photosynthetic organisms for L-lysine production due to the availability of genetic tools, rapid growth rates, halotolerance, and ability to be grown on non-productive land with simple nutrient requirements (Oliver and Atsumi, 2014; Pate et al., 2011) or wastestreams (Korosh et al., 2017). Here, we report successful metabolic engineering strategies for production of L-lysine from a strain of the fast-growing *Synechococcus* sp. strain PCC 7002.

The structure and regulation of amino acid biosynthesis has been well studied and used to design metabolic engineering strategies in various bacteria. For example, a lysine producing *C. glutamicum* strain was rationally designed by overexpressing feedback-resistant enzyme variants that increased flux in relevant anaplerotic and biosynthetic reactions (Becker et al., 2011). L-lysine is a part of the aspartate-family of amino acids that also includes L-isoleucine, L-methionine, and L-threonine (Kirma et al., 2012). The precursors and metabolites in this amino acid family are interconnected to several parts of central metabolism and are homeostatically controlled by several transcriptional and/or post-translational mechanisms (Wittmann and Becker, 2007). In cyanobacteria, the anaplerotic reaction of phosphoenolpyruvate carboxylase (PEPC) combines PEP with HCO_3^- to generate oxaloacetate (**Fig. 5-1**). Oxaloacetate, a

component of the modified cyanobacteria TCA cycle (Zhang and Bryant, 2011), is then converted to L-aspartate by aspartate aminotransferase where it enters the lysine biosynthetic pathway. High levels of L-aspartate negatively affect PEPC activity (O'Regan et al., 1989). L-aspartate is further converted to L-aspartyl-phosphate by aspartate kinase (AK), an enzyme that is subject to feedback inhibition by L-lysine and L-threonine at regulatory subunits. L-aspartyl-phosphate is then converted by aspartate semialdehyde dehydrogenase into L-aspartate semialdehyde. From this branch point, L-aspartate semialdehyde may either be converted into L-homoserine, which is used for biosynthesis of the other members of the aspartate family of amino acids; or into L-2,3 dihydropicolinate by dihydrodipicolinate synthase (DHDPS) in the lysine biosynthetic pathway. Like AK, DHDPS is also subject to feedback regulation by L-lysine and L-threonine. The variant of the lysine biosynthetic pathway in plants and cyanobacteria is distinct in that it uses a L, L-diaminopimelate aminotransferase to convert L-2,3,4,5 tetrahydrodipicolinate to L,L-diaminopimelate as opposed to the dehydrogenase, acetylase, and succinylase pathways found in most other organisms (Hudson et al., 2006). From L, L-diaminopimelate, subsequent epimerization and decarboxylation reactions are used to ultimately generate L-lysine, which then is then excreted by the transporter, *lysE,* in *C. glutamicum* (Kelle et al., 1996). A corresponding transporter in *Synechococcus* sp. strain PCC 7002 has not been identified.

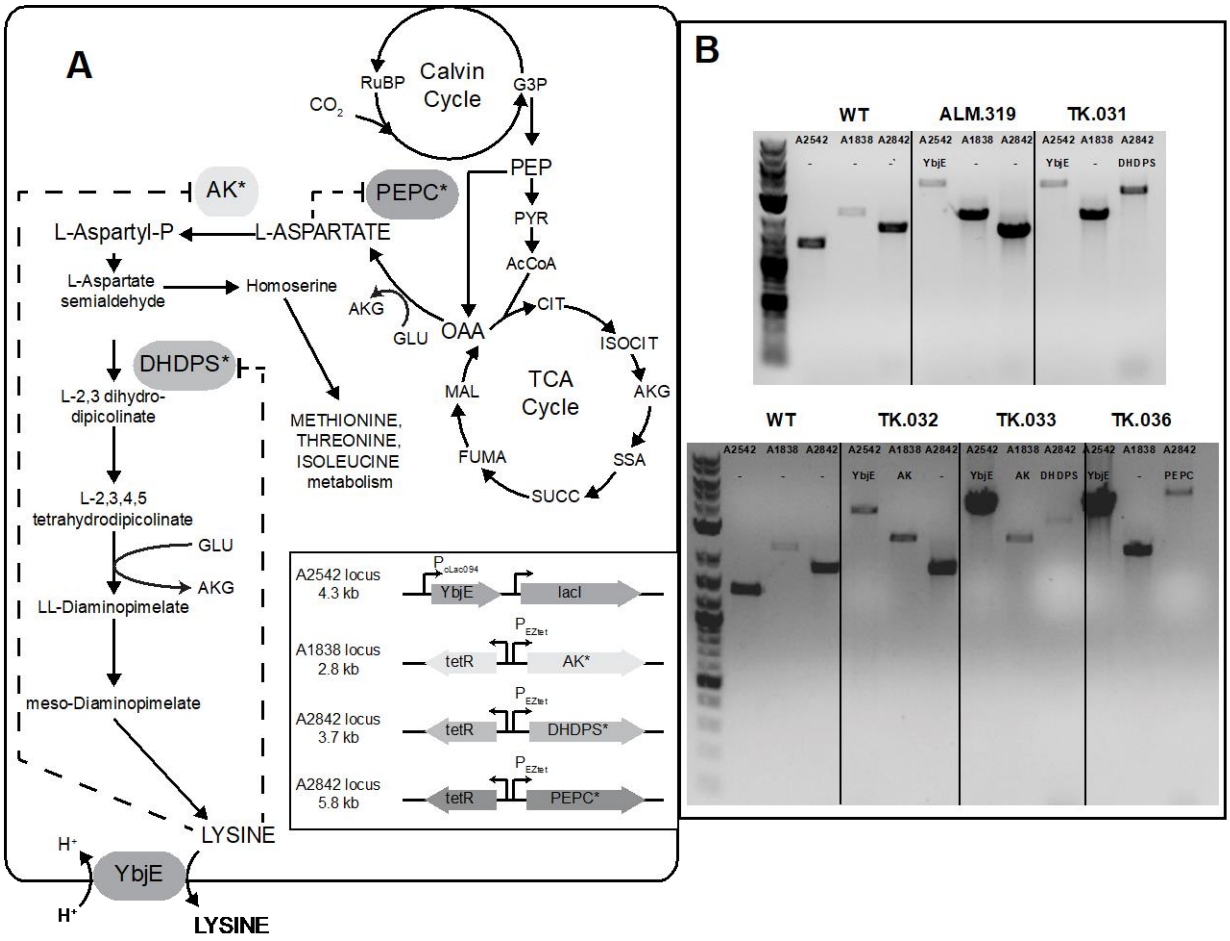

Figure 5-1. Overview of the L-lysine biosynthetic pathway in *Synechococcus* sp. strain PCC 7002 and verification of chromosomal segregation of heterologous genes.
(A)Insert shows a schematic representation of the integration and induction systems of the heterologous genes introduced into the listed genomic loci. Dashed arrows indicate the presence of allosteric regulation of the native enzymes. (B) Gels show bands corresponding to PCR products created from colonies of each strain using primers flanking each loci. The length of each expected band is listed in the inset of panel A.

Here, we report increased L-lysine excretion in the cyanobacterium *Synechococcu*s sp. strain PCC 7002 (hereafter PCC 7002) with heterologous expression of the amino acid exporter *ybjE* from *Escherichia coli.* We also examined the effects of feedback-resistant AK, DHDPS, and PEPC variants on L-lysine productivity. The best producing strain was cultivated in laboratory photobioreactors to study L-lysine production dynamics during growth to a light-limited stationary phase. We examined the effects of media composition on L-lysine production and cellular growth rates by using nitrate, ammonia, and a N-/P-rich sidestream from a municipal

wastewater treatment facility as a nutrient source. Our work demonstrates the potential of engineered photoautotrophic amino acid production in cyanobacteria.

5.3 Materials and Methods

5.3.1 Reagents and Media

Enzymes were purchased from New England Biolabs (Ipswich, MA). Nucleic acid purification materials were purchased from Qiagen (Venlo, Netherlands). Chemicals were purchased from Sigma-Aldrich (St. Louis, MO) or Fisher Scientific (Hampton, NH) unless otherwise specified.

5.3.2 Strain Construction

Heterologous genes were integrated onto the chromosome of wild-type PCC 7002 using homologous recombination (Davies et al., 2014). Expression cassettes were cloned into *E. coli* plasmids containing 500-1000 bp of homology targeting sequences to one of three PCC 7002 loci SYNPCC7002_A1838, SYNPCC7002_A2542, and/or SYNPCC7002_A2842 (Table 1). In these cassettes, genes were placed under control of the $P_{cLac094}$ (Markley et al., 2015) or the P_{EZtet} (Zess et al., 2016) inducible promoter system. Selection was performed by expression of an antibiotic resistance marker or using the acrylic acid counterselection system (Begemann et al., 2013). Plasmids were made using Gibson assembly (Gibson et al., 2009) with regions of homology added in the 5’ end of the primers. The feedback resistant *C. glutamicum* dapA gene (DHDPS) was codon optimized for PCC 7002 expression and chemically synthesized (Invitrogen) (Cremer et al., 1991). The ppc gene (PEPC) was amplified with the primers using

Synechococcus elongatus (strain PCC 7942) genomic DNA. The site-specific mutation in PEPC (N1015G) to remove feedback inhibition were based on (Chen et al., 2014). The lysC gene (AK) from *Xenorhabdus bovienii* (strain SS-2004) was codon optimized for PCC 7002 expression and chemically synthesized. The site-specific mutation in AK (T369I) to remove feedback inhibition made to the original protein sequence was based on (Qi et al., 2011). Descriptions of plasmids used in this study are shown in **Table 5-1**.

Table 5-1. Plasmids Used in this study

Name	**Expression Cassette**	Ref.
pADC181	ΔSYNPCC7002_A2542::P_{clac94}-ybjE-aphII	This work
pTK043	ΔSYNPCC7002_A2842::P_{tetO2}-DHDPS-aacC1	This work
pALM285	ΔSYNPCC7002_A1838::P_{tetO2}-AK	This work
pALM287	ΔSYNPCC7002_A2842::P_{tetO2}-PEPC- aacC1	This work

5.3.3 Cultivation Conditions

Strains were grown and maintained on Medium A^+ (Jr et al., 1973) with 1.5% Bacto-Agar. Strains with antibiotic resistance markers were selected on media with antibiotics (kanamycin, 100 μg/mL; gentamicin, 30 μg/mL) and strains with cassettes introduced in the SYNPCC7002_A1838 (*acsA)* locus were plated on 100 μM acrylic acid. Strains were grown in 250 ml baffled flasks with 50 mL Medium A^+ with 1% CO_2-enriched air at 150 rpm in a Kuhner ISF1-X orbital shaker. Growth on wastewater-derived nutrients was accomplished as described elsewhere (Korosh et al., 2017). Briefly, filtrate from the anaerobic digester gravity belt filter (GBF), and effluent from the post-mainstream secondary treatment clarifier (secondary effluent) served as a diluent which was obtained from Nine Springs Wastewater Treatment Plant (Dane County, Wisconsin). To ensure complete nutrient requirements, the GBF media was supplemented with trace metals and vitamin B12 at the concentrations found in Medium A^+, as

well as KH_2PO_4 at a molar ration of 1:32 soluble reactive phosphorus to bioavailable nitrogen due to the WASSTRIP process employed. GBF was used at a concentration of 12.5% (v/v) in secondary effluent. Temperature was maintained at 37°C or 27°C and light intensity was approximately 200 µmol photons $m^{-2}s^{-1}$ via a custom LED panel. Optical density was measured in a Genesys 20 spectrophotometer (Thermo Scientific) in 1-cm cuvette. Unless otherwise noted, 1 mM IPTG was used and/or 10-1000 ng ml^{-1} anhydrous tetracycline was used for induction studies.

5.3.4 Photobioreactor Cultivation of Strain TK.032

A homemade photobioreactor system (Clark et al., 2017) was used for these experiments for growth with excess nutrients and CO_2. The reactor vessels were 1 L Corning wide mouth bottles (10 cm diameter, surface area to volume ratio of 40 m^{-1}). Radially averaged irradiance was 350 µmol PAR m^{-2} s^{-1} from cool white fluorescent tubes (4000K color temperature). Three photobioreactors were inoculated with TK.032 to an OD_{730} of 0.05 with a working volume of 930 mL of Medium A supplemented with 110 mM $NaNO_3$, 1.1 mM $FeCl_3$, 5.2 mM KH_2PO_4, 100 µg mL^{-1} kanamycin, 1 mM IPTG, and 100 ng mL^{-1} anhydrous tetracycline. The temperature controller was set to maintain the reactors at 37°C. A gas phase containing 5% CO_2 was introduced at a flow rate of 0.3 L min^{-1} and the system was given 1 hour to equilibrate, at which point the pH was adjusted to 7 by adding 1.7mL of 5 M NaOH. Time zero for the data reported (beginning of linear growth phase) was taken to be 48 hours after inoculation (OD_{730}~1). Samples were taken approximately every 24 hours after adjusting the reactor volume with sterile MilliQ filtered water to make up for evaporation and the pH and OD_{730} were measured. An OD_{730} to g DCW L^{-1} conversion was determined to be 0.26 g DCW L^{-1} OD_{730}^{-1} by weighing cell

pellets washed three times with MilliQ filtered water and then lyophilized. Samples were centrifuged and the supernatant was saved for lysine quantification (stored at -20°C until measurement). Additional KH_2PO_4 was added in 5.2mM aliquots on days 2 and 6 (pH fluctuated between 6.7 and 7.2 as KH_2PO_4 was added and subsequently consumed).

5.3.5 Analytical Measurements

Samples were withdrawn periodically for biomass and lysine measurements, centrifuged, and the supernatant was stored at -20°C until quantification by HPLC (Shimadzu Co., Columbia, MD, USA) equipped with a quaternary pump, autosampler, vacuum degasser, photodiode array and fluorescence detector. HPLC separations were performed using a Xbridge C18 column (2.1 X 150 mM, 3.5 µm, Waters). The method employed a 20-minute linear gradient starting with 100% Buffer A: [925 ml of 100 mM Acetate (pH 6.95); 50 ml of HPLC Grade Methanol: 25 ml of HPLC Grade Tetrahydrofuran] to 100% Buffer B: [975 ml of HPLC Grade Methanol: 25 ml of HPLC Grade Tetrahydrofuran] before returning to the initial conditions for 10 mins. The flow rate was 0.400 mL/min, column temperature 40°C, and injection volume 10 µL. Amino acid samples and standards were quantified by comparison with peaks generated by monitoring the fluorescence (Ex 320 nm/ Em 450 nm) of known amounts of standards in Medium A^+, after precolumn derivatization with 3 mg/ml o-phthalaldehyde with 3-mercaptopropionic acid in 0.4 M borate buffer.

Linear regression (excluding t_0) was used to calculate rates of lysine production and growth. Carbon partitioning was calculated assuming 50% carbon by mass (Thomas, 2015). Chlorophyll a measurements were performed via a 100% chilled methanol extraction procedure

(Miyashita et al., 1997). Chlorophyll a was calculated via the following equation: $Chl_a = 16.29 * A^{665} - 8.54 * A^{652}$ (Porra et al., 1989).

5.4 Results

5.4.1 Lysine Export is the First Barrier to Increased Flux

Amino acid biosynthesis is a highly regulated cellular process (Umbarger, 1978) and metabolic engineering strategies to increase production depend on by-passing native regulation. For example, expression of the feedback-insensitive DHDPS from *C. glutamicum* has been used to increase the free lysine content of canola seed (Falco et al., 1995). Therefore, for our first attempt at increasing lysine production, we integrated a modified DHDPS gene in the ΔSYNPCC7002_A1838 locus under control of the $P_{cLac094}$ induction system (Markley et al., 2015), yielding strain AM.183. When this strain was cultured photoautotrophically, we observed a significant growth defect with increasing inducer concentration, as well as intracellular lysine accumulation (**Fig. 5-2**). Attempts to integrate other deregulated genes (e.g. PEPC, AK) from the lysine biosynthetic pathway and DHDPS under the control of strong P_{cLac} promoters into wild type PCC 7002 failed to generate viable colonies. Therefore, we speculated that the increased intracellular lysine concentration could result from the lack of a lysine exporter and cause cellular toxicity by feedback inhibition of other amino acid pathways. A prior study indicated that L-lysine could be excreted from PCC 7002 into the media by an endogenous transport system (Baran et al., 2011), but homologs to known lysine transporters were not identifiable in the PCC 7002 genome. Our data suggested that if a native lysine efflux system existed it was a potential bottleneck. Therefore, we integrated the *ybjE* (*lysO*) transporter from *E. coli* in the

SYNPCC7002_A2842 locus under the $P_{cLac094}$ induction system, yielding strain AM.273. Cultures of AM.273 grew rapidly (no defect relative to WT) and generated a large pool of lysine in the extracellular media. From these experiments, we concluded that PCC7002 requires increased export flux to produce elevated levels of lysine. All subsequent experiments were based off a strain (AM.319) expressing *ybjE* in the SYNPCC7002_A2542 locus under P_{clac94}.

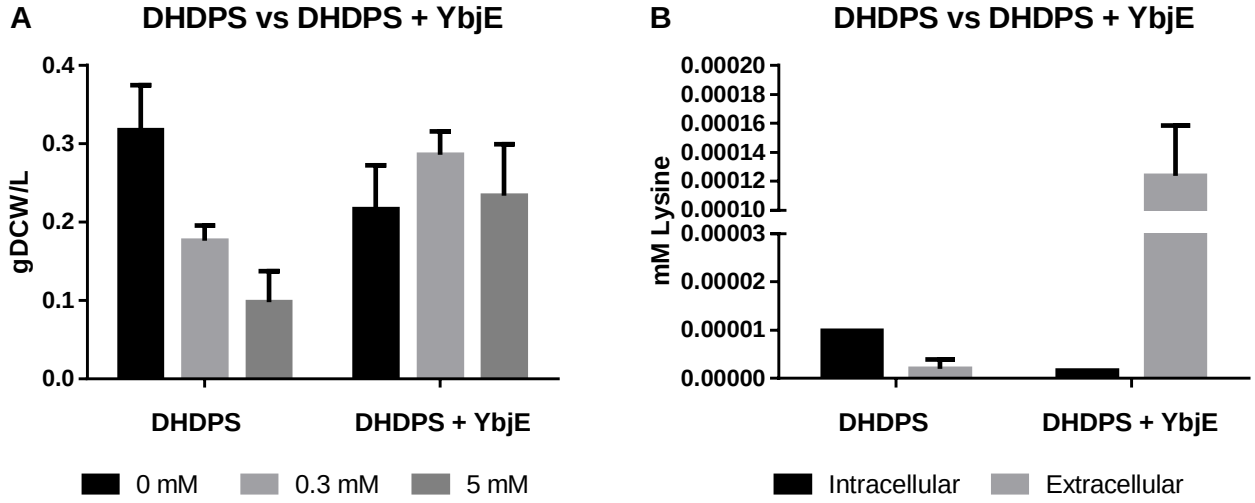

Figure 5-2. (A) Growth and (B) Lysine Production of ALM.183 (DHDPS) and ALM.273 (DHDPS + YbjE)
Samples were induced with 0, 0.3, or 5 mM IPTG for 48 hrs under continuous illumination (200 µmol photons m^{-2} s^{-1}) with 1 % CO_2 at 37°C. The data shown for intracellular and extracellular lysine are for samples induced with 0.3 mM IPTG. The values represent the mean ± SD of biological triplicates.

5.4.2 Modifying the Flux to the Aspartate Family of Amino Acids

Having addressed the export barrier, we next explored the impact of known regulatory points in lysine biosynthesis by expressing feedback-resistant variants of key enzymes, AK, DHDPS, and PEPC (Cremer et al., 1991). Aspartate kinase (AK) plays a central role regulating the biosynthesis of the aspartate family of amino acids (Malumbres and Martín, 1996). Many natural AK are subject to feedback inhibition by lysine. To circumvent this regulation, AK variants have been engineered to remove this mechanism of control (Qi et al., 2011). Here, we

integrated a gene encoding a feedback-insensitive variant of AK into the SYNPCC7002_A1838 locus of the base strain (AM.319) under control of the P_{EZtet} induction system (strain TK.032). Attempts to integrate the AK under control of the stronger P_{clac94} induction system were unsuccessful. To commit flux towards lysine and away from the other members of the aspartate family of amino acids, we integrated a feedback insensitive DHDPS into the SYNPCC7002_A2842 locus of AM.319 under the control of the P_{EZtet} induction system to catalyze the conversion of aspartate semialdehyde to L-2,3 dihydropicolinate, generating strain TK.031. Phosphoenolpyruvate carboxylase (PEPC) fixes CO_2 to generate oxaloacetate used in the modified TCA cycle and as a precursor to amino acids. We integrated PEPC into the SYNPCC7002_A2842 locus under the control of the P_{EZtet} induction system to generate strain TK.036. The PEPC variant was cloned from *Synechococcus elongatus (strain PCC* 7942) and engineered to be feedback insensitive based off a point mutation that improved lysine production by 37% in *C. glutamicum* (Chen et al., 2014). Lastly, we assembled a DHDPS and AK overexpression strain by integrating the DHDPS cassette into TK.032 at the SYNPCC7002_A2842 locus to generate strain TK.033. Attempts to make other double and triple mutants failed to fully segregate or generate viable colonies. We cultivated each of these strains photoautotrophically in 250 ml baffled shake flasks under standard laboratory conditions of continuous illumination of 200 µmol photons m^{-2} s^{-1} with 1 % CO_2 at 37°C to compare growth rates and lysine productivity. Each strain was induced with 1 mM IPTG (to express ybjE) and varying levels of anhydrotetracycline (aTc is used to express enzymes linked to P_{EZtet}). Relevant genotypes and performance metrics for strains used in these experiments are shown in **Table 5-2.**

Table 5-2. Overview of L-lysine Producing Strains of *Synechococcus* sp. strain PCC 7002

Strain	Genotype			T (°C)	Media	[aTc] (ng ml^{-1})	Linear Growth Rate (±SD) (gDCW L^{-1} h^{-1})	Productivity (±SE) (mmol lysine h^{-1})	%Carbon to Lysine (±SE)	Titer (±SD) (mM lysine)
	A2542	A1838	A2842							
AM.319	ybjE			37	A^+	-	0.027 ± 0.001	0.004 ± 0.002	2 ± 0.8	0.78 ± 0.13
TK.032	ybjE	AK		37	A^+	10	0.021 ± 0.001	0.010 ± 0.001	7 ± 0.8	1.19 ± 0.14
TK.032	ybjE	AK		37	A^+	100	0.025 ± 0.001	0.010 ± 0.002	6 ± 1.2	1.25 ± 0.12
TK.032	ybjE	AK		37	A^+	1000	0.023 ± 0.002	0.019 ± 0.002	12 ± 1.1	1.74 ± 0.12
TK.032	ybjE	AK		37	A^+	1000	0.020 ± 0.002	0.021 ± 0.002	15 ± 0.0	1.67 ± 0.15
TK.031	ybjE		DHDPS	37	A^+	10	0.021 ± 0.001	0.007 ± 0.000	5 ± 0.3	0.67 ± 0.05
TK.031	ybjE		DHDPS	37	A^+	100	0.022 ± 0.001	0.012 ± 0.001	8 ± 0.1	1.07 ± 0.16
TK.031	ybjE		DHDPS	37	A^+	1000	0.019 ± 0.001	0.011 ± 0.001	8 ± 0.7	1.15 ± 0.31
TK.033	ybjE	AK	DHDPS	37	A^+	10	0.019 ± 0.001	0.008 ± 0.001	6 ± 0.9	0.80 ± 0.20
TK.033	ybjE	AK	DHDPS	37	A^+	100	0.023 ± 0.001	0.010 ± 0.001	6 ± 0.3	0.80 ± 0.20
TK.033	ybjE	AK	DHDPS	37	A^+	1000	0.016 ± 0.002	0.014 ± 0.002	12 ± 0.1	1.02 ± 0.11
TK.032	ybjE	AK		37	A^+	1000	0.018 ± 0.002	0.019 ± 0.003	15 ± 0.1	1.33 ± 0.18
TK.036	ybjE		PEPC	37	A^+	10	0.022 ± 0.002	0.009 ± 0.002	6 ± 0.9	0.61 ± 0.12
TK.036	ybjE		PEPC	37	A^+	100	0.020 ± 0.002	0.009 ± 0.001	6 ± 0.4	0.58 ± 0.03
TK.036	ybjE		PEPC	37	A^+	1000	0.018 ± 0.001	0.008 ± 0.001	5 ± 0.9	0.55 ± 0.03
TK.032	ybjE	AK		37	A^+ w/ 24 mM NO_3	100	0.013 ± 0.001	0.006 ± 0.001	7 ± 0.4	1.14 ± 0.46
TK.032[a]	ybjE	AK		37	A^+ w/ 24 mM NH_4	100	0.017 ± 0.001	0.020 ± 0.002	18 ± 0.0	3.11 ± 0.22
TK.032[b]	ybjE	AK		27	GBF	1000	0.014 ± 0.002	0.003 ± 0.000	3 ± 0.3	0.28 ± 0.06
TK.032	ybjE	AK		27	A^+	1000	0	nd	nd	nd

Note: All experiments done with 1% (v/v) CO_2 and 200 µmol photons $m^{-2}s^{-1}$ and induction with 1 mM IPTG.

Blocked rows report data from experiments run at the same time. [a]pH was manually adjusted to ≈ 8 using NaOH daily. [b] Gravity Belt Filtrate (GBF) was diluted to 12.5% (v/v) using secondary effluent both obtained from the Nine Springs Wastewater Treatment Plant (Dane County, Wisconsin, USA)

Induction of the AK in strain TK.032 diminished the linear growth rate relative to the base strain, AM.319 (**Fig. 5-3A, Table 5-2**), but lysine production rates, titers, and the percentage of fixed carbon directed to lysine increased as the aTc dosage increased from 10 ng ml^{-1} to 1000 ng ml^{-1} (**Fig. 5-3B**). Volumetric productivities were much higher in the AK containing strain (TK.032 - 0.010-0.19 mM hr^{-1}) than the parent strain (AM.319 - 0.004 mM hr^{-1}) and increased with increasing aTc induction of AK. The increased productivity resulted in a 2-fold increase in lysine titer after 93 hrs (1.74 vs 0.78 mM) and a six-fold increase in the fraction of carbon directed to lysine (up to 12%). Given the decrease in growth rate relative to its parent, ALM.319, we were curious if production of lysine altered photosynthetic properties in TK.032. We extracted and measured the chlorophyll *a* content of ALM.319 and TK.032 46 hours post induction. Relative to ALM.319, chlorophyll *a* content was significantly reduced in TK.032 at all induction levels (**Fig. 5-3C**). We also tested the effect of Medium A^+ adjusted to a pH of 8.2 or 6.8 on TK.032's lysine production, given pH's effects on lysine transport (Kelle et al., 1996), however, no difference was found using carbon partitioning as a metric (**Data Not Shown**). These results indicate that AK activity is key node in lysine biosynthesis, full induction with aTc was the optimal level, and lysine productivity impacts cell growth.

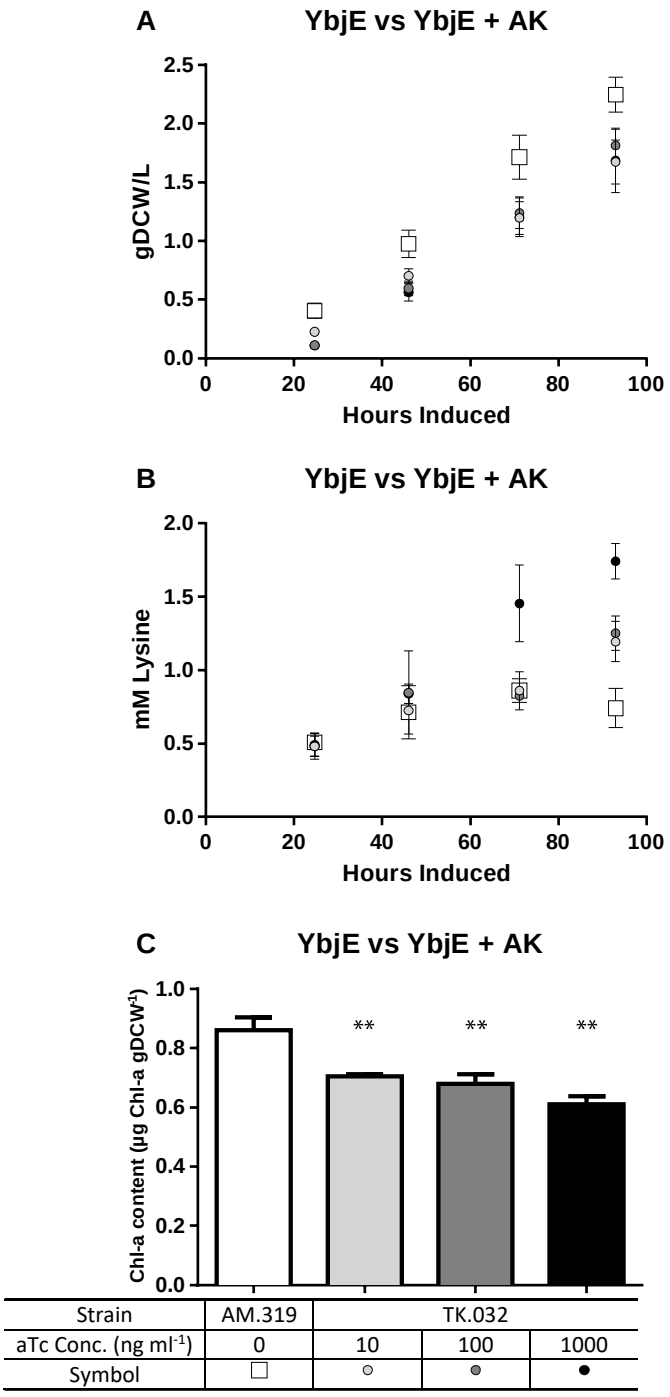

Figure 5-3. (A) Growth, (B) Lysine Production, and (C) Chlorophyll a Content of ALM.319 and TK.032.

The values represent the mean ± SD of biological triplicates. Experiments were performed with ALM.319 induced with 1 mM IPTG, and TK.032 induced with 10-1000 ng ml^{-1} aTc and 1 mM IPTG under continuous illumination (200 µmol photons m^{-2} s^{-1}) with 1 % CO_2 at 37°C. Chlorophyll a was extracted 46 hrs post induction. Chl a levels in TK.032 with 10, 100, and 1000 ng ml^{-1} aTc were greatly reduced relative to ALM.319 (** represent p-value<0.05).

Next, we compared overexpression of AK and *ybjE* (strain TK.032) to DHDPS and *ybjE* (strain TK.031) across three inducer concentrations. The linear growth rate of TK.031 was comparable to TK.032 in each culture (**Fig. 5-4A**), but lysine production in TK.031 plateaued at 100 ng ml^{-1} aTc at lower levels (productivity: 0.01 mM h^{-1}, titer: 1.2 mM, 8% carbon flux) (**Fig. 5-4B, Table 5-2**). These data indicated that AK has a stronger influence on lysine flux than DHDPS, but DHDPS also has influence on lysine flux. Therefore, we compared the AK expressing strain (TK.032) to a strain simultaneously expressing AK, and DHDPS (TK.033). In this experiment, there was a notable lag phase with increasing aTc dosage with TK.033 (**Fig. 5-5A**), decreasing the linear growth rate from 0.019 g DCW L^{-1} hr^{-1} with 10 ng ml^{-1} aTc to 0.016 g DCW L^{-1} hr^{-1} with 1000 ng ml^{-1}. This may be due to the extreme limitation of biosynthetic flux towards the other amino acids in the aspartate superfamily, resulting in a synthetic auxotrophy. In comparison, the linear growth rate for TK.032 with 1000 ng ml^{-1} aTc was 0.020 g DCW L^{-1} hr^{-1} consistent with past trials. Lysine production from strain TK.033 peaked at the maximum aTc concentration (productivity: 0.013 mM hr^{-1}; titer: 1 mM; 12% carbon to lysine) but remained inferior to strain TK.032 (**Fig. 5-5B**). From these data, we conclude that AK is more important to deregulating lysine flux than DHDPS in *Synechococcus* sp. strain PCC7002.

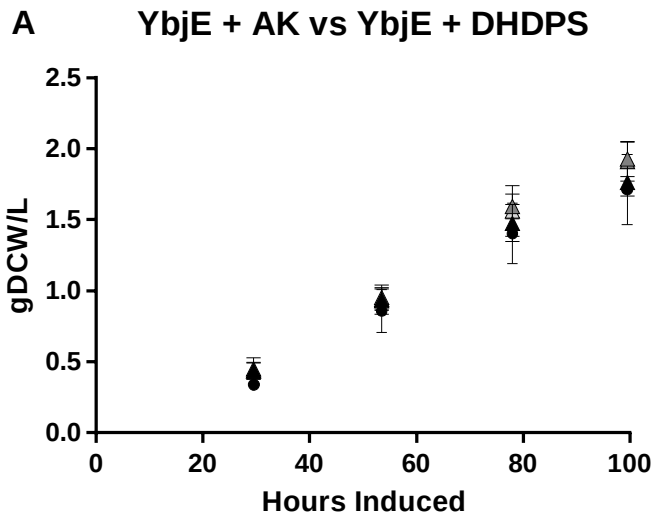

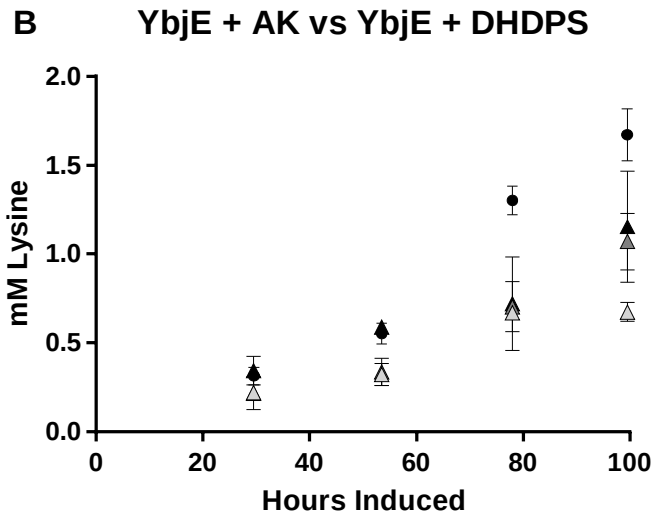

Strain	TK.032	TK.031		
aTc Conc. (ng ml^{-1})	1000	10	100	1000
Symbol	●	△	▲	▲

Figure 5-4. (A) Growth and (B) Lysine Production of TK.032 and TK.031.
The values represent the mean ± SD of biological triplicates. Experiments were performed with TK.031 induced with 10-1000 ng ml^{-1} aTc and 1 mM IPTG, and TK.032 induced with 1000 ng ml^{-1} aTc and 1 mM IPTG under continuous illumination (200 µmol photons m^{-2} s^{-1}) with 1 % CO_2 at 37°C

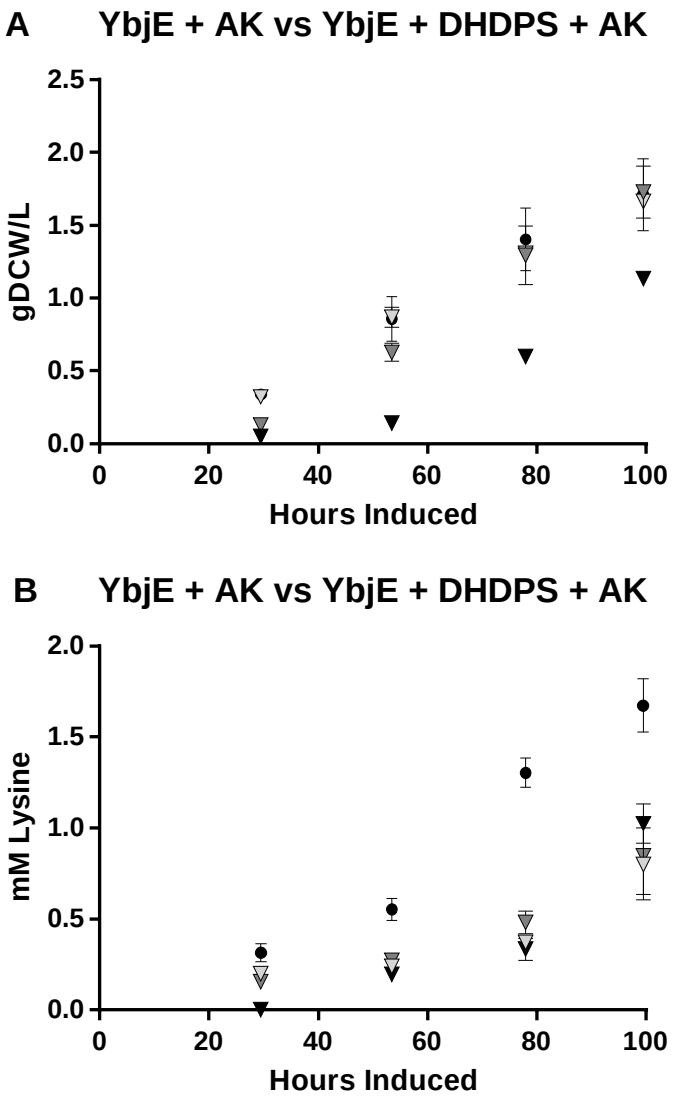

Strain	TK.032	TK.033		
aTc Conc. (ng ml^{-1})	1000	10	100	1000
Symbol	●	▽	▼	▼

Figure 5-5. (A) Growth and (B) Lysine Production of TK.032 and TK.033.
The values represent the mean ± SD of biological triplicates. Experiments were performed with TK.033 induced with 10-1000 ng ml^{-1} aTc and 1 mM IPTG, and TK.032 induced with 1000 ng ml^{-1} aTc and 1 mM IPTG under continuous illumination (200 µmol photons m^{-2} s^{-1}) with 1 % CO_2 at 37°C.

Last, we compared the effects of the feedback-insensitive PEPC (TK.036) to the deregulated AK (TK.032) on lysine productivity. Attempts to introduce this engineered PEPC in our AK overexpressing strain background were unsuccessful. In contrast, we were able to introduce a PEPC expression cassette in the *ybjE* background (TK.036), but its performance was greatly inferior to TK.032 at all aTc concentrations (**Fig. 5-6**). Maximum lysine volumetric productivity for TK.036 was 0.009 mM hr^{-1} which equates to 6% of carbon going to lysine. Despite the greater percentage of carbon fluxed to lysine, the final titer of this strain was less than the AM.319 base. This is mostly due to the significant reduction in growth rate. Given the superior performance of TK.032 over all other genetic backgrounds, we concluded that AK was the most important point of lysine regulation and TK.032 was used for all subsequent experiments.

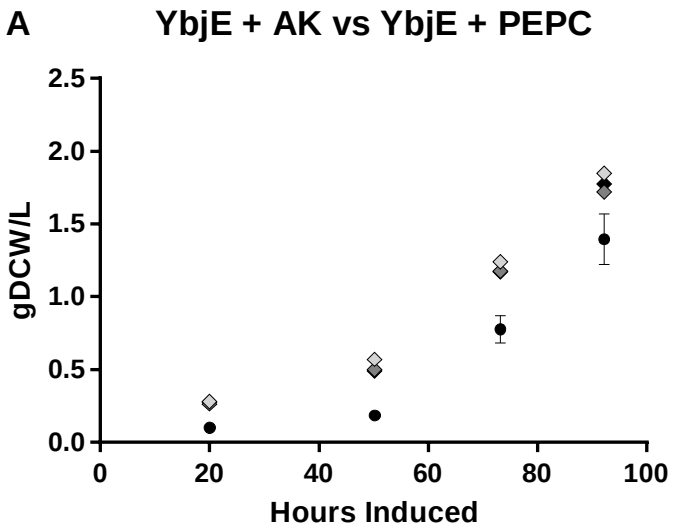

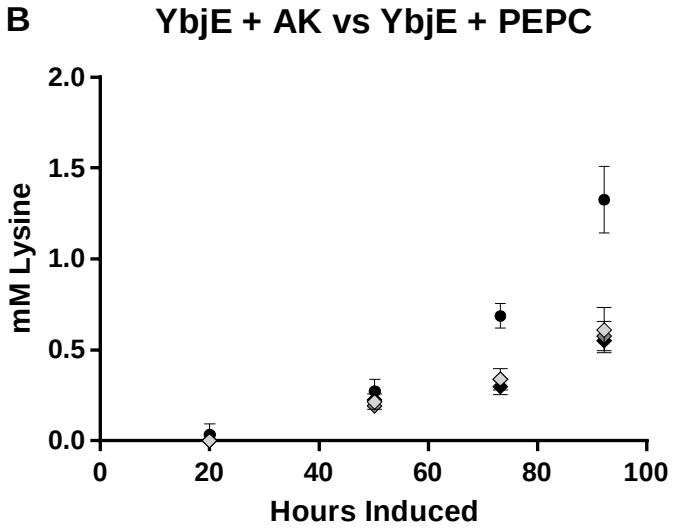

Strain	TK.032	TK.036		
aTc Conc. (ng ml^{-1})	1000	10	100	1000
Symbol	●	◇	◈	◆

Figure 5-6. (A) Growth and (B) Lysine Production of TK.032 and TK.036.
The values represent the mean ± SD of biological triplicates. Experiments were performed with TK.036 induced with 10-1000 ng ml^{-1} aTc and 1 mM IPTG, and TK.032 induced with 1000 ng ml^{-1} aTc and 1 mM IPTG under continuous illumination (200 µmol photons m^{-2} s^{-1}) with 1 % CO_2 at 37°C

5.4.3 Changing Nitrogen Sources

A key difference between producing amino acids and other organic acids is the presence of nitrogen (Wendisch et al., 2006). Balancing carbon and N-assimilation flux is complicated by their interconnected metabolic and regulatory pathways (Huergo and Dixon, 2015). Cyanobacteria growth media is commonly formulated with nitrate that must be reduced to ammonia (serving as a sink for excess electrons) prior to assimilation (McNeely et al., 2014). In contrast, when wild-type PCC 7002 is fed ammonia as a N-source, cells grow slower and display significant chlorosis (Korosh et al., 2017). This can be overcome by providing an alternative electron sink such as biomass (providing elevated P_{CO2}) or production of reduced compounds. For this reason, we hypothesized that a surplus of reducing power created by by-passing nitrate reduction could be used to enhance lysine biosynthesis. Therefore, we compared lysine production from TK.032 grown in media formulated with 24 mM NO_3 (2x prior studies) to 24 mM NH_4 (**Fig. 5-7**). Due in part to the NH_4 transporter-induced medium acidification (Britto and Kronzucker, 2005), culture pH was maintained around 8.0 by addition of NaOH. In these conditions, cells grew slower in both elevated N-media formulations, nitrate media (0.013 g DCW L^{-1} hr^{-1}) with growth on ammonium (0.013 g DCW L^{-1} hr^{-1}) slightly reduced from growth on Medium A^+. The lower growth rate and a reduced fraction of carbon going to lysine (7%) on nitrate media resulted in lower volumetric productivity 0.007 mM hr^{-1}. In contrast, cultures grown on ammonium media produced lysine at higher rates (0.020 mM hr^{-1}) and sent the largest percentage of carbon to lysine (18%). In addition, these cultures excreted other amino acids (**Data Not Shown**), which suggests that more lysine could be produced if the branch points could be more finely controlled. The difference in growth and productivity with ammonium

emphasizes the importance of reducing power in lysine biosynthesis, which had been demonstrated with *C. glutamicum* (Becker et al., 2011).

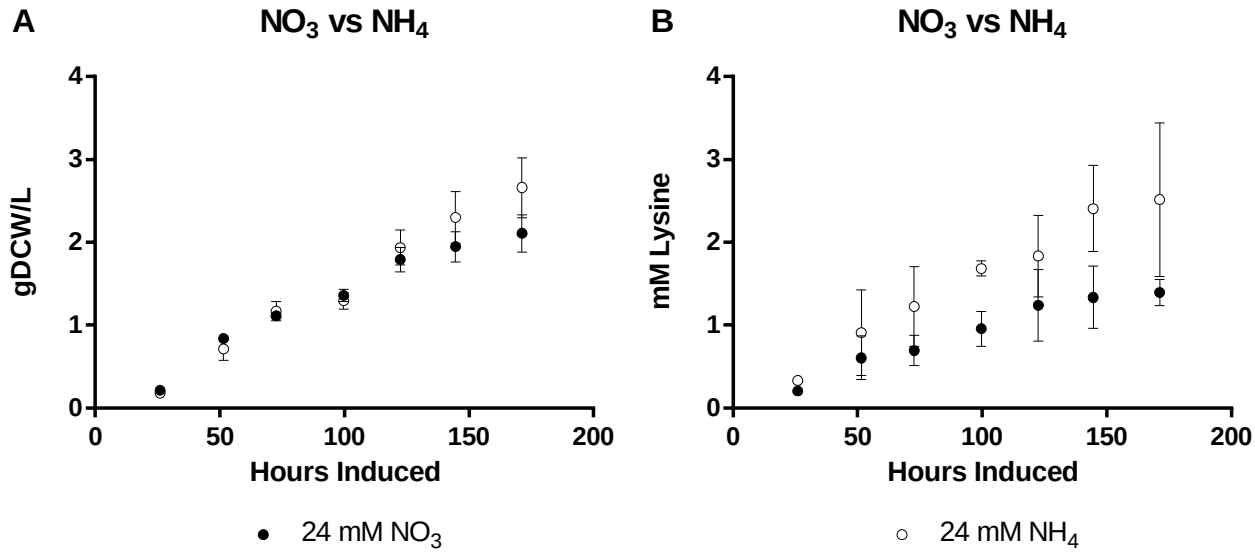

Figure 5-7. (A) Growth and (B) Lysine Production of TK.032 with NO_3 or NH_4.
The values represent the mean ± SD of biological triplicates. Experiments were performed with TK.032 cultivated induced with 100 ng ml^{-1} aTc and 1 mM IPTG under continuous illumination (200 µmol photons m^{-2} s^{-1}) with 1 % CO_2 at 37°C. pH control with 24 mM NH_4^+ was maintained at ≈ 8 by manually adjusting with NaOH.

5.4.4 Lysine Production in Dilute Anaerobic Digestate

Given the cost of fertilizers, it is attractive to consider alternative sources of low-cost nitrogen and phosphate such as anaerobic digester and/or municipal waste water streams. Anaerobic digestion effluent from municipal wastewater has previously been used as a nutrient source for cyanobacterial cultivation and lactate production (Hollinshead et al., 2014), but there are many potential toxicants that could limit its widespread adoption. We have previously demonstrated that a physiological adaptation at 27°C is necessary to allow growth of PCC 7002 in filtrate recycled from the gravity belt (GBF) of a local municipal water treatment plant (Korosh et al., 2017). The GBF provides a nitrogen- (predominantly NH_4^+) and phosphate-source. Therefore, we compared growth and lysine production in cultures of TK.032 using

diluted GBF or Medium A^+ at 27°C (**Fig. 5-8**). In GBF based media, TK.032 grew more slowly (0.014 g DCW L^{-1} hr^{-1}) and directed only 3% of carbon to lysine resulting in low titer (0.28 mM) and volumetric productivity 0.003 mM hr^{-1}. Interestingly, after induction in Medium A^+ at this temperature, cultures were notably chlorotic, growth ceased, and lysine was not detectable. This growth defect was only apparent upon induction (**Fig. 5-8C**) and is likely due to the transporter imposed nitrate limitation at low temperatures (Sakamoto and Bryant, 1998). We postulate that this perceived nitrate limitation at low temperatures is circumvented in wastewater based media, due to the high levels of ammonium naturally present.

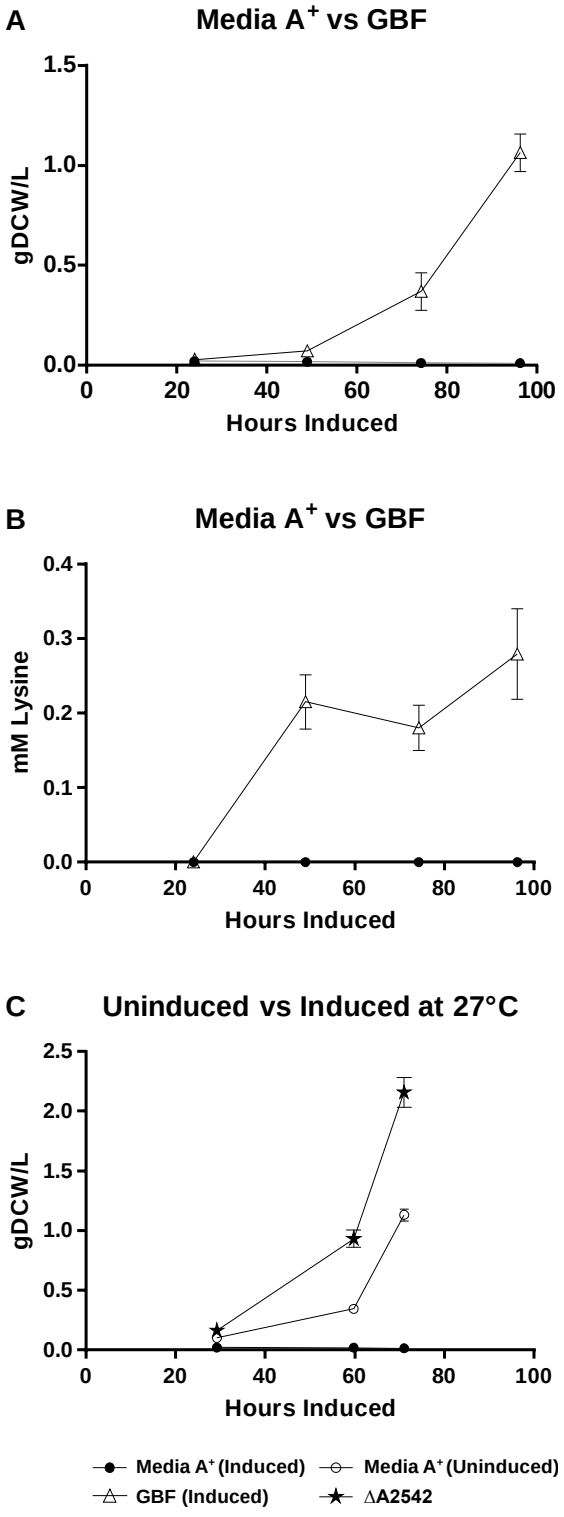

Figure 5-8. (A) Growth and (B) Lysine Production of TK.032 with Dilute Anaerobic Digestate (GBF) or Medium A^+ (C) Effect of Temperature on Growth of ΔA2542 and TK.032 +/- Induction in Medium A^+. The values represent the mean ± SD of biological triplicates. Experiments were performed with TK.032 induced with 1000 ng ml^{-1} aTc and 1 mM IPTG under continuous illumination (200 µmol photons m^{-2} s^{-1}) with 1 % CO_2 at 27°C.

5.4.5 Batch Growth and Lysine Production of TK.032 in Photobioreactors

Industrial implementation of cyanobacterial lysine production would likely occur in light-limited batch culture with lower surface to volume ratios than the flasks used in the work described above. To investigate the dynamics of lysine production in such a process, we cultivated TK.032 in homemade laboratory photobioreactors (Clark et al., 2017) in Medium A^+ supplemented with excess $NaNO_3$, KH_2PO_4, $FeCl_3$, and CO_2 (**Fig. 5-9**). The initial linear growth rate and linear rate of L-lysine production for each reactor was calculated from growth data from the first 76 hours of the linear growth phase. For three biological replicates, the mean linear growth rate of TK.032 was 10(±0.4) mg DCW L^{-1} hr^{-1} (S.E.) and the mean linear rate of L-lysine production was 13(±0.5) μM L-lysine hr^{-1}. This corresponds to directing 18% of carbon flux to lysine which was comparable to that of TK.032 grown in shake flasks at the same induction level. When the cultures entered stationary phase after 20 days, the biomass concentration was 2.4 (±0.1) g DCW L^{-1} and the L-lysine titer was 2.7 (±0.3) mM L-lysine.

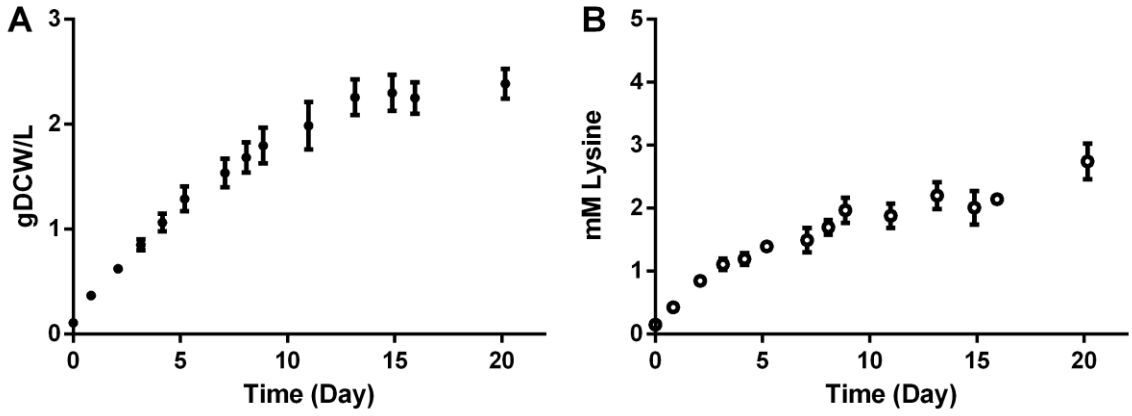

Figure 5-9. (A) Batch growth and (B) lysine production of TK.032 in a light-limited photobioreactor. Time zero was 48 hours after inoculation and induction (100 ng mL^{-1} aTc and 1 mM IPTG) where the cultures were at sufficient cell density to be in linear growth phase. Error bars represent the standard error of the mean of three biological replicates.

5.5 Discussion

In this project, we successfully engineered the cyanobacterium, *Synechococcus* sp. PCC 7002 to express feedback resistant versions of enzymes in the lysine biosynthetic pathway as a model for photosynthetic production of L-lysine. Simultaneous expression of an engineered aspartate kinase and lysine transporter was sufficient for high productivities, but also led to decreased chlorophyll content. Increasing the reductant supply by using NH_4^+, a more reduced nitrogen source relative to NO_3^-, gave a twofold increase in productivity. Our highest volumetric productivity for lysine was 0.003 g L^{-1} h^{-1}, which is comparable carbon partitioning for PCC 7002 engineered to produce ethanol (0.010 g L^{-1} h^{-1}) (Dühring et al., 2014). However, this pales in comparison to the heterotrophic lysine productivity of 4.0 g L^{-1} h^{-1} achieved with *C. glutamicum* (Becker et al., 2011).

Some of the limitations for producing amino acids in photoautotrophic hosts may be due to the relatively small flux of the TCA cycle, which has been demonstrated under numerous growth conditions in ^{13}C-MFA studies (Wan et al., 2017). The aspartate family of amino acids is intertwined in both catabolic and anabolic processes in the TCA cycle (Galili, 2011). During photoautotrophic growth, the TCA cycle has been shown to primarily operate as a bifurcated pathway to generate necessary precursor metabolites, oxaloacetate and α-ketoglutarate (Steinhauser et al., 2012), although several species of cyanobacteria have since been shown to have the enzymatic capacity to operate a closed TCA cycle through bypass reactions (Xiong et al., 2014; Zhang and Bryant, 2011). The exact reason for this discrepancy has been highly debated, but it has been proposed to be a result of niche specialization (Zhang et al., 2016). Researchers have recently modified photoautotrophic flux in the TCA cycle by the introduction

of a heterologous GABA shunt, which may be used to extend the plasticity of this metabolic node in future studies (Zhang et al., 2016).

Tools such as flux balance analysis may also reveal novel metabolic engineering approaches suitable for the constraints of photoautotrophic metabolism (Rügen et al., 2015). For example, introduction of a pyruvate carboxylase may also increase the metabolic flexibility of the PEP-pyruvate-oxaloacetate node, thereby leading to lead to an increase in precursor supply. While most organisms contain a subset of enzymes to ensure optimal carbon and energy flux at this anaplerotic node, *C. glutamicum* is a noted exception (Sauer and Eikmanns, 2005). In lysine producing strains of *C. glutamicum*, flux through the energy consuming C3 rather than the C4 carboxlylation reaction is the predominant anaplerotic route, suggesting a need for increased futile cycling in these conditions (Marx et al., 1999, 1996). The high pyruvate/PEP ratio in PCC 7002 (Dempo et al., 2014) may make this an attractive option for future work.

Lysine production in TK.032 was met with decreased chlorophyll content per cell (Fig. 3c). Decreased chlorophyll content has previously been seen in tobacco plants engineered to have elevated levels of free lysine (Azevedo et al., 1997). This implies a change in physiology during lysine production. This is contrary to cyanobacteria engineered to export sucrose (Ducat, 2016). This finding may represent the current ceiling in carbon-flux redistribution during photoautotrophic lysine production, due to the limited metabolic flux of the autotrophic TCA cycle, which has been put forth by experimental and computational approaches (Broddrick et al., 2016; Nogales et al., 2012; Song et al., 2015; Young et al., 2011).

Given our laboratory strain performance in wastewater medium, we can extrapolate to a conservative aerial lysine productivity of ~100 (Winter) - 250 (Summer) g of Lysine/m^2/year using estimates of aerial biomass productivities from 9.4 (Winter) - 23.5 (Summer)

gDCW/m^2/day in an open pond system with a marine cyanobacterium (Moreno et al., 2003), and the 3% of carbon flux to lysine in our wastewater production conditions. In comparison, current United States areal productivities are ~775 g of Lysine/m^2/Year. This figure is based on the mean annual yield of sugar crops in the United States (Michael McConnell, n.d.), assuming a glucose production rate of 6.5 mol/m2/Year and the maximum theoretical yield (0.82 mol L-lysine mol−1 glucose) for *C. glutamicum* (Wittmann and Becker, 2007). These figures highlight the areal productivity of cyanobacteria utilizing non-traditional nutrient sources, with the added benefit of wastewater polishing for discharge. That said, to take advantage of this trait, titers must be increased to keep the cost of purification low (Hermann, 2003) and productivities must be increased to reduce the capital costs needed to produce a target amount of amino acid. It is also important to note that these extrapolated productivities do not take into account operating costs associated with purification and extraction (Quiroz-Arita et al., 2017) or any spatial variation in the availability of wastewater (Roostaei and Zhang, 2017). The integration of the multitude of '-omics' data into genome scale metabolic models, in particular with isotopically nonstationary metabolic flux analysis in over producer strains (Adebiyi et al., 2015), will enable more accurate representations of the flux control of the branch points in non-model organisms, and further development of a photosynthetic chemical platform.

5.6 Acknowledgements

This work was funded by the US National Science Foundation (EFRI-1240268, GEO-1215871). TCK is the recipient of a National Institutes of Health (NIH) Biotechnology Training Fellowship (NIGMS-5 T32 GM08349) and a fellowship from the UW-Madison College of Engineering's Graduate Engineering Research Scholars (GERS) program. The authors are grateful to Austin

Comer for construction of pADC181, as well as Richard Mikel, Matthew Dysthe, and Derek Jacobs for help with routine sampling.

5.7 Literature Cited

Adebiyi, A.O., Jazmin, L.J., Young, J.D., 2015. 13C flux analysis of cyanobacterial metabolism. Photosynth. Res. 126, 19–32. doi:10.1007/s11120-014-0045-1

Azevedo, R.A., Arruda, P., Turner, W.L., Lea, P.J., 1997. The biosynthesis and metabolism of the aspartate derived amino acids in higher plants. Phytochemistry 46, 395–419. doi:10.1016/S0031-9422(97)00319-1

Baran, R., Bowen, B.P., Northen, T.R., 2011. Untargeted metabolic footprinting reveals a surprising breadth of metabolite uptake and release by Synechococcus sp. PCC 7002. Mol. Biosyst. 7, 3200–6. doi:10.1039/c1mb05196b

Becker, J., Zelder, O., Häfner, S., Schröder, H., Wittmann, C., 2011. From zero to hero-Design-based systems metabolic engineering of Corynebacterium glutamicum for l-lysine production. Metab. Eng. 13, 159–168. doi:10.1016/j.ymben.2011.01.003

Begemann, M.B., Zess, E.K., Walters, E.M., Schmitt, E.F., Markley, A.L., Pfleger, B.F., 2013. An organic acid based counter selection system for cyanobacteria. PLoS One 8, e76594. doi:10.1371/journal.pone.0076594

Brautaset, T., Ellingsen, T.E., 2011. Lysine: Industrial Uses and Production, in: Comprehensive Biotechnology. pp. 541–554. doi:10.1016/B978-0-08-088504-9.00220-8

Britto, D.T., Kronzucker, H.J., 2005. Nitrogen acquisition, PEP carboxylase, and cellular pH homeostasis: new views on old paradigms. Plant, Cell Environ. 28, 1396–1409. doi:10.1111/j.1365-3040.2005.01372.x

Broddrick, J.T., Rubin, B.E., Welkie, D.G., Du, N., Mih, N., Diamond, S., Lee, J.J., Golden, S.S., Palsson, B.O., 2016. Unique attributes of cyanobacterial metabolism revealed by improved genome-scale metabolic modeling and essential gene analysis. Proc. Natl. Acad. Sci. 113, E8344–E8353. doi:10.1073/pnas.1613446113

Chen, Z., Bommareddy, R.R., Frank, D., Rappert, S., Zeng, A.P., 2014. Deregulation of feedback inhibition of phosphoenolpyruvate carboxylase for improved lysine production in

Corynebacterium glutamicum. Appl. Environ. Microbiol. 80, 1388–1393. doi:10.1128/AEM.03535-13

Clark, R.L., McGinley, L.L., Quevedo, D.F., Root, T.W., Pfleger, B.F., 2017. Construction and Operation of an Affordable Laboratory Photobioreactor System for Simultaneous Cultivation of up to 12 Independent 1 L Cyanobacterial Cultures. bioRxiv.

Cremer, J., Eggeling, L., Sahm, H., 1991. Control of the lysine biosynthesis sequence in Corynebacterium glutamicum as analyzed by overexpression of the individual corresponding genes. Appl. Environ. Microbiol. 57, 1746–1752.

Davies, F.K., Work, V.H., Beliaev, A.S., Posewitz, M.C., 2014. Engineering Limonene and Bisabolene Production in Wild Type and a Glycogen-Deficient Mutant of Synechococcus sp. PCC 7002. Front. Bioeng. Biotechnol. 2, 1–11. doi:10.3389/fbioe.2014.00021

Dempo, Y., Ohta, E., Nakayama, Y., Bamba, T., Fukusaki, E., 2014. Molar-Based Targeted Metabolic Profiling of Cyanobacterial Strains with Potential for Biological Production. Metabolites 4, 499–516. doi:10.3390/metabo4020499

Ducat, D., 2016. Increased Photochemical Efficiency in Cyanobacteria via an Engineered Sucrose Sink. Plant Cell Physiol. 0, 1–10. doi:10.1093/pcp/pcw169

Dühring, U., Baier, K., Germer, F., Shi, T., 2014. Genetically enhanced cyanobacteria for the production of a first chemical compound harbouring zn2+, co2+ or ni2+ -inducible promoters.

Eggeling, L., Bott, M., 2015. A giant market and a powerful metabolism: l-lysine provided by Corynebacterium glutamicum. Appl. Microbiol. Biotechnol. 99, 3387–3394. doi:10.1007/s00253-015-6508-2

Falco, S.C., Guida, T., Locke, M., Mauvais, J., Sanders, C., Ward, R.T., Webber, P., 1995. Transgenic canola and soybean seeds with increased lysine. Biotechnology 13, 577–82. doi:10.1038/nbt0695-577

Galili, G., 2011. The aspartate-family pathway of plants. Plant Signal. Behav. 6, 192–195. doi:10.4161/psb.6.2.14425

Gibson, D.G., Young, L., Chuang, R.-Y., Venter, J.C., Hutchison, C.A., Smith, H.O., 2009. Enzymatic assembly of DNA molecules up to several hundred kilobases. Nat. Methods 6, 343–5. doi:10.1038/nmeth.1318

Hermann, T., 2003. Industrial production of amino acids by coryneform bacteria. J. Biotechnol. 104, 155–172. doi:10.1016/S0168-1656(03)00149-4

Hollinshead, W.D., Varman, A.M., You, L., Hembree, Z., Tang, Y.J., 2014. Boosting D-lactate production in engineered cyanobacteria using sterilized anaerobic digestion effluents. Bioresour. Technol. 169, 462–467. doi:10.1016/j.biortech.2014.07.003

Hudson, O., Singh, B.K., Leustek, T., Gilvarg, C., 2006. An LL -Diaminopimelate Aminotransferase Defines a Novel Variant of the Lysine Biosynthesis Pathway in Plants. Plant Physiol. 140, 292–301. doi:10.1104/pp.105.072629.have

Huergo, L.F., Dixon, R., 2015. The Emergence of 2-Oxoglutarate as a Master Regulator Metabolite. Microbiol. Mol. Biol. Rev. 79, 419–35. doi:10.1128/MMBR.00038-15

Jr, S.S., Patterson, C., Myers, J., 1973. The Production of Hydrogen Peroxide by Blue-Green Algae: A Survey. J. Phycol.

Kelle, R., Laufer, B., Brunzema, C., Weuster-Botz, D., Krämer, R., Wandrey, C., 1996. Reaction engineering analysis of L-lysine transport by Corynebacterium glutamicum. Biotechnol. Bioeng. 51, 40–50. doi:10.1002/(SICI)1097-0290(19960705)51:1<40::AID-BIT5>3.0.CO;2-0

Kirma, M., Araújo, W.L., Fernie, A.R., Galili, G., 2012. The multifaceted role of aspartate-family amino acids in plant metabolism. J. Exp. Bot. 63, 4995–5001. doi:10.1093/jxb/ers119

Korosh, T.C., Dutcher, A., Pfleger, B.F., McMahon, K., 2017. Cyanobacterial Growth on Municipal Wastewater Requires Low Temperatures. bioRxiv.

Malumbres, M., Martín, J.F., 1996. Molecular control mechanisms of lysine and threonine biosynthesis in amino acid-producing corynebacteria: Redirecting carbon flow. FEMS Microbiol. Lett. 143, 103 LP-114.

Markley, A.L., Begemann, M.B., Clarke, R.E., Gordon, G.C., Pfleger, B.F., 2015. A synthetic biology toolbox for controlling gene expression in the cyanobacterium Synechococcus sp. PCC 7002. ACS Synth. Biol. 4, 595–603. doi:10.1021/sb500260k

Marx, A., de Graaf, A.A., Wiechert, W., Eggeling, L., Sahm, H., 1996. Determination of the fluxes in the central metabolism of Corynebacterium glutamicum by nuclear magnetic resonance spectroscopy combined with metabolite balancing. Biotechnol. Bioeng. 49, 111–129. doi:10.1002/(SICI)1097-0290(19960120)49:2<111::AID-BIT1>3.0.CO;2-T

Marx, A., Eikmanns, B.J., Sahm, H., de Graaf, A.A., Eggeling, L., 1999. Response of the central metabolism in Corynebacterium glutamicum to the use of an NADH-dependent glutamate dehydrogenase. Metab. Eng. 1, 35–48. doi:10.1006/mben.1998.0106

McNeely, K., Kumaraswamy, G.K., Guerra, T., Bennette, N., Ananyev, G., Dismukes, G.C., 2014. Metabolic switching of central carbon metabolism in response to nitrate: Application to autofermentative hydrogen production in cyanobacteria. J. Biotechnol. 182–183, 83–91. doi:10.1016/j.jbiotec.2014.04.004

Michael McConnell, n.d. USDA ERS - Sugar and Sweeteners Yearbook Tables [WWW Document]. United States Dep. Agric. Res. Serv. URL http://www.ers.usda.gov/data-products/sugar-and-sweeteners-yearbook-tables.aspx#.U43Z6PldWJt (accessed 8.25.17).

Miyashita, H., Adachi, K., Kurano, N., Ikemot, H., Chihara, M., Miyach, S., 1997. Pigment composition of a novel oxygenic photosynthetic prokaryote containing chlorophyll d as the major chlorophyll. Plant cell Physiol. 38, 274–281.

Moreno, J., Vargas, M.Á., Rodríguez, H., Rivas, J., Guerrero, M.G., 2003. Outdoor cultivation of a nitrogen-fixing marine cyanobacterium, Anabaena sp. ATCC 33047. Biomol. Eng. 20, 191–197. doi:10.1016/S1389-0344(03)00051-0

Nogales, J., Gudmundsson, S., Knight, E.M., Palsson, B.O., Thiele, I., 2012. Detailing the optimality of photosynthesis in cyanobacteria through systems biology analysis. Proc. Natl. Acad. Sci. U. S. A. 109, 2678–83. doi:10.1073/pnas.1117907109

O'Regan, M., Thierbach, G., Bachmann, B., Villeval, D., Lepage, P., Viret, J.-F., Lemoine, Y., 1989. Cloning and nucleotide sequence of the phosphoenolpyruvate carboxylase-coding gene of Corynebacterium glutamicum ATCC13032. Gene 77, 237–251. doi:https://doi.org/10.1016/0378-1119(89)90072-3

Oliver, J.W.K., Atsumi, S., 2014. Metabolic design for cyanobacterial chemical synthesis. Photosynth. Res. 120, 249–61. doi:10.1007/s11120-014-9997-4

Pate, R., Klise, G., Wu, B., 2011. Resource demand implications for US algae biofuels production scale-up. Appl. Energy 88, 3377–3388. doi:http://dx.doi.org/10.1016/j.apenergy.2011.04.023

Porra, R.J., Thompson, W.A., Kriedemann, P.E., 1989. Determination of accurate extinction coefficients and simultaneous equations for assaying chlorophylls a and b extracted with four different solvents: verification of the concentration of chlorophyll standards by atomic absorption spectroscopy. Biochim. Biophys. Acta (BBA)-Bioenergetics 975, 384–394.

Qi, Q., Huang, J., Crowley, J., Ruschke, L., Goldman, B.S., Wen, L., Rapp, W.D., 2011. Metabolically engineered soybean seed with enhanced threonine levels: biochemical characterization and seed-specific expression of lysine-insensitive variants of aspartate kinases from the enteric bacterium Xenorhabdus bovienii. Plant Biotechnol. J. 9, 193–204. doi:10.1111/j.1467-7652.2010.00545.x

Quiroz-Arita, C., Sheehan, J.J., Bradley, T.H., 2017. Life cycle net energy and greenhouse gas emissions of photosynthetic cyanobacterial biorefineries: Challenges for industrial production of biofuels. Algal Res. 1–8. doi:10.1016/j.algal.2017.06.021

Roostaei, J., Zhang, Y., 2017. Spatially Explicit Life Cycle Assessment: Opportunities and challenges of wastewater-based algal biofuels in the United States. Algal Res. 24, 395–402. doi:10.1016/j.algal.2016.08.008

Rügen, M., Bockmayr, A., Steuer, R., 2015. Elucidating temporal resource allocation and diurnal dynamics in phototrophic metabolism using conditional FBA. Sci. Rep. 5, 15247. doi:10.1038/srep15247

Sakamoto, T., Bryant, D. a, 1998. Growth at low temperature causes nitrogen limitation in the cyanobacterium Synechococcus sp. PCC 7002. Arch. Microbiol. 169, 10–9.

Sauer, U., Eikmanns, B.J., 2005. The PEP-pyruvate-oxaloacetate node as the switch point for carbon flux distribution in bacteria. FEMS Microbiol. Rev. 29, 765–794. doi:10.1016/j.femsre.2004.11.002

Song, H.-S., McClure, R., Bernstein, H., Overall, C., Hill, E., Beliaev, A., 2015. Integrated in silico Analyses of Regulatory and Metabolic Networks of Synechococcus sp. PCC 7002 Reveal Relationships between Gene Centrality and Essentiality. Life 5, 1127–1140. doi:10.3390/life5021127

Steinhauser, D., Fernie, A.R., Araújo, W.L., 2012. Unusual cyanobacterial TCA cycles: not broken just different. Trends Plant Sci. 17, 503–9. doi:10.1016/j.tplants.2012.05.005

Thomas, E., 2015. Microbial growth and physiology: A call for better craftsmanship. Front. Microbiol. 6, 1–12. doi:10.3389/fmicb.2015.00287

Umbarger, H.E., 1978. Amino Acid Biosynthesis and its Regulation. Annu. Rev. Biochem. 47, 533–606. doi:10.1146/annurev.bi.47.070178.002533

Wan, N., DeLorenzo, D.M., He, L., You, L., Immethun, C.M., Wang, G., Baidoo, E.E.K., Hollinshead, W., Keasling, J.D., Moon, T.S., Tang, Y.J., 2017. Cyanobacterial carbon metabolism: Fluxome plasticity and oxygen dependence. Biotechnol. Bioeng. 1–32. doi:10.1002/bit.26287

Wendisch, V.F., Bott, M., Eikmanns, B.J., 2006. Metabolic engineering of Escherichia coli and Corynebacterium glutamicum for biotechnological production of organic acids and amino acids. Curr. Opin. Microbiol. 9, 268–74. doi:10.1016/j.mib.2006.03.001

Wittmann, C., Becker, J., 2007. The L-lysine story: from metabolic pathways to industrial production, in: Amino Acid Biosynthesis~ Pathways, Regulation and Metabolic Engineering. Springer, pp. 39–70.

Xiong, W., Brune, D., Vermaas, W.F.J., 2014. The γ-aminobutyric acid shunt contributes to closing the tricarboxylic acid cycle in Synechocystis sp. PCC 6803. Mol. Microbiol. 93, 786–796. doi:10.1111/mmi.12699

Young, J.D., Shastri, A. a, Stephanopoulos, G., Morgan, J. a, 2011. Mapping photoautotrophic metabolism with isotopically nonstationary (13)C flux analysis. Metab. Eng. 13, 656–65. doi:10.1016/j.ymben.2011.08.002

Zess, E.K., Begemann, M.B., Pfleger, B.F., 2016. Construction of new synthetic biology tools for the control of gene expression in the cyanobacterium Synechococcus sp. strain PCC 7002. Biotechnol. Bioeng. 113, 424–432. doi:10.1002/bit.25713

Zhang, S., Bryant, D.A., 2011. The tricarboxylic acid cycle in cyanobacteria. Science 334, 1551–3. doi:10.1126/science.1210858

Zhang, S., Qian, X., Chang, S., Dismukes, G.C., Bryant, D.A., 2016. Natural and Synthetic Variants of the Tricarboxylic Acid Cycle in Cyanobacteria: Introduction of the GABA Shunt into Synechococcus sp. PCC 7002. Front. Microbiol. 7, 1–13. doi:10.3389/fmicb.2016.01972

CHAPTER 6 CONCLUSIONS AND FUTURE DIRECTIONS

6.1 Conclusions

The work described in this document addressed important aspects for the realization of cyanobacterial biorefinery. First, we investigated the effect of utilizing a municipal wastewater stream as a source of nutrients under varying environmental conditions in **Chapter 3**, finding a means to circumvent toxicity by changing the cultivation temperature. Next, we then examined metabolic engineering design principles that enabled high productivities of L-lactate in **Chapter 4**, with an emphasis on leveraging the coordination between cofactor supply and demand, as well as carbon and nitrogen metabolism. Finally, we examined the importance of transporter expression and circumventing metabolic regulation to enable production of L-lysine in **Chapter 5**, utilizing a reduced nitrogen supply to boost productivities in defined medium and undefined, municipal wastewater-based medium.

We achieved similar carbon partitioning for both L-lactate and L-lysine, roughly 16% of fixed carbon going to product. These chemicals are derived from different metabolic nodes with varying degrees of flux as assessed via INST ^{13}C MFA under autotrophic conditions (Hendry et al., 2017; Young et al., 2011). Flux-balance analysis (Wan et al., 2017) and meta-analysis (Angermayr et al., 2015) have suggested that target molecules in a cyanobacterial biocatalyst should be derived from metabolites of the Calvin-Benson-Bassham cycle, pentose phosphate pathway, and lower glycolysis (L-lactate) due to their large pool size, rather than those made from substrates in the TCA cycle (L-lysine). Immediate work should examine the effect of a reduced nitrogen source (NH_4^+) towards L-lactate productivity in strain TK.029 (BsLDHV39R, Rre37) in an isogenic background to strain TK.032 (YbjE, AK). LDH expression should then be

titrated until maximum volumetric productivities are achieved. It will be of interest to discern the effects of the optimal production of these two products on photosynthetic parameters, such as chlorophyll content and rates of oxygen evolution.

6.2 Future Directions

There still exist several hurdles that must be addressed to increase the market share of microalgal biofuels into the larger renewables market. Studies have done several scenario-based analyses, taking into consideration the geographic constraints (solar availability and temperature) on microalgal biomass productivity (Pate et al., 2011; Quinn et al., 2012). These studies have concluded that the cost of CO_2 capture and delivery to the areas with sufficient photosynthetically active radiation is prohibitive with current technologies. Efforts should then be directed broadly towards increasing photosynthetic efficiency and improving carbon conversion. This may be achieved via two approaches: engineering of the environment or engineering of the host microbe. Design criteria for photobioreactors have been covered in depth elsewhere (Kunjapur and Eldridge, 2010; Posten, 2009; Suh and Lee, 2003), but biological approaches will be discussed below.

Several attempts improve to carbon partitioning and photosynthetic efficiency in cyanobacteria are already underway. Overexpression of several flux controlling enzymes in the Calvin-Benson-Bassham cycle resulted in higher rates of oxygen evolution and biomass accumulation in engineered strains of PCC 6803 (Liang and Lindblad, 2016). Carbon fixation pathways besides the Calvin-Benson-Bassham cycle exist in nature (Hügler and Sievert, 2010), and novel pathways have been constructed *in vitro* and demonstrate to have high carbon fixation efficiencies (Schwander et al., 2016). Metabolic engineering approaches could be used to

increase the amount of productive photosynthetically active radiation by reducing photoinhibition or shifting the absorption properties of the photopigments to non-natively used wavelengths (Ort et al., 2015). The effects of reducing photoinhibition in mass culture has been demonstrated in PCC 6803 through the truncation of light harvesting antennae by deletion of phycocyanin (Δcpc), thereby alleviating the excessive absorption of light by cells at the outermost layer (Kirst et al., 2014). This resulted in 57% greater biomass productivity at simulated peak sunlight illumination of 2000 µmol photons m^{-2} s^{-1}.

Despite the high productivities achieved for L-lactate and L-lysine with a cyanobacterium as described in this work, this is orders of magnitude lower than volumetric productivities reached with heterotrophic organisms fed low cost substrates (Wang et al., 2015; Wittmann and Becker, 2007). It has been proposed that resource allocation of the proteome (Burnap, 2015) and metabolome (Reimers et al., 2017) are some of the main factors accounting for the differences in maximal growth rates between autotrophic and heterotrophic organisms, due the intricacies of the photosynthetic lifestyle. This is reflected in the difference between adenylate energy charges for *E. coli* (0.90) and for PCC 7002 (0.35), which is already high relative to other cyanobacteria strains (Dempo et al., 2014). One way to improve this growth discrepancy is to design a minimal photoautotrophic cell (Delaye et al., 2011), with all non-essential genes removed (Rubin et al., 2015). However, the regulatory logic coordinating the dynamic aspects of photoautotrophic metabolism is not well understood even between "model" cyanobacterial strains (Jablonsky et al., 2016) and would be a significant undertaking.

The metabolic plasticity of studied strains of cyanobacteria likely arises from genetic drift and natural selection in various environmental and temporal niches. Studies have shown significant differences between metabolite distribution (Dempo et al., 2014), acclimation to

stress (Billis et al., 2014), and diversity of electron flow (Shimakawa et al., 2016) between various strains of cyanobacteria. Despite the close phylogenetic relationship between freshwater PCC 6803 and euryhaline PCC 7002 (Scanlan et al., 2009), PCC 7002 has been shown to be exceptionally tolerant to several stresses (Ruffing, 2014). This may be due to its high rates of electron transfer across a variety conditions (Bernstein et al., 2016; Shimakawa et al., 2016) and the ability to use CO_2 fixation (Ludwig and Bryant, 2012, 2011) and synthesis of sugar phosphates and organic acids as prominent electron sinks (Dempo et al., 2014). Upregulation of several AET processes which have been shown to enhance photoinhibitory tolerance in PCC 6803 and PCC7942 (Allahverdiyeva et al., 2013) in PCC 7002, had no effect on tolerance to 12.5% GBF at 37°C (Data not shown). This suggests that PCC 7002 naturally has a high capacity for electron transport processes in conducive environments and highlights the importance of strain selection in bioprocessing.

Given these conclusions, perhaps it will ultimately be more beneficial to approach microalgal production primarily as a method for wastewater treatment, rather than as a source of commodity or specialty chemicals in the near-term. Maintaining a monoculture in a biorefinery will likely be cost prohibitive if wastewater is used as a source of nutrients. However, exploiting the biodiversity of nature and utilizing ecological design principles will likely be an economically effective method of remediation (Fouilland, 2012; Kazamia et al., 2012). Close interactions between heterotrophs and autotrophs have been demonstrated in nature (Aylward et al., 2015; Leyn et al., 2017) and laboratory settings (Beliaev et al., 2014; Christie-Oleza et al., 2017; Oyserman et al., 2017). These communities exhibit high biomass productivities and functional stability over long periods, due to metabolite recycling and detoxification of oxidative stress (Beliaev et al., 2014; Li et al., 2017). However, this approach can also be used to generate

proteins and products of interest (Lindemann et al., 2016; Zengler and Palsson, 2012). Recent work examined the interactions between a cyanobacterial strain metabolically engineered to secrete sucrose with a variety of specialized heterotrophic partners and were able to produce alpha-amylase and polyhydroxybutyrate with CO_2 as the sole carbon source (Hays et al., 2017). We expect this approach to become more widespread as we increase our understanding of engineering synthetic microbial mutualisms.

6.3 Literature Cited

Allahverdiyeva, Y., Mustila, H., Ermakova, M., Bersanini, L., Richaud, P., Ajlani, G., Battchikova, N., Cournac, L., Aro, E.-M., 2013. Flavodiiron proteins Flv1 and Flv3 enable cyanobacterial growth and photosynthesis under fluctuating light. Proc. Natl. Acad. Sci. U. S. A. 110, 4111–6. doi:10.1073/pnas.1221194110

Angermayr, S.A., Gorchs Rovira, A., Hellingwerf, K.J., 2015. Metabolic engineering of cyanobacteria for the synthesis of commodity products. Trends Biotechnol. 33, 352–361. doi:10.1016/j.tibtech.2015.03.009

Aylward, F.O., Eppley, J.M., Smith, J.M., Chavez, F.P., Scholin, C.A., DeLong, E.F., 2015. Microbial community transcriptional networks are conserved in three domains at ocean basin scales. Proc. Natl. Acad. Sci. 112, 5443–5448. doi:10.1073/pnas.1502883112

Beliaev, A.S., Romine, M.F., Serres, M., Bernstein, H.C., Linggi, B.E., Markillie, L.M., Isern, N.G., Chrisler, W.B., Kucek, L.A., Hill, E.A., Pinchuk, G.E., Bryant, D.A., Steven Wiley, H., Fredrickson, J.K., Konopka, A., 2014. Inference of interactions in cyanobacterial-heterotrophic co-cultures via transcriptome sequencing. ISME J. doi:10.1038/ismej.2014.69

Bernstein, H.C., McClure, R.S., Hill, E.A., Markillie, L.M., Chrisler, W.B., Romine, M.F., McDermott, J.E., Posewitz, M.C., Bryant, D.A., Konopka, A.E., Fredrickson, J.K., Beliaev, A.S., 2016. Unlocking the Constraints of Cyanobacterial Productivity: Acclimations Enabling Ultrafast Growth. MBio 7, e00949-16. doi:10.1128/mBio.00949-16

Billis, K., Billini, M., Tripp, H.J., Kyrpides, N.C., Mavromatis, K., 2014. Comparative Transcriptomics between Synechococcus PCC 7942 and Synechocystis PCC 6803 Provide Insights into Mechanisms of Stress Acclimation. PLoS One 9, e109738. doi:10.1371/journal.pone.0109738

Burnap, R.L., 2015. Systems and photosystems: cellular limits of autotrophic productivity in cyanobacteria. Front. Bioeng. Biotechnol. 3, 1. doi:10.3389/fbioe.2015.00001

Christie-Oleza, J.A., Sousoni, D., Lloyd, M., Armengaud, J., Scanlan, D.J., 2017. Nutrient recycling facilitates long-term stability of marine microbial phototroph-heterotroph interactions. Nat. Microbiol. 2, 17100. doi:10.1038/nmicrobiol.2017.100

Delaye, L., González-Domenech, C.M., Garcillán-Barcia, M.P., Peretó, J., de la Cruz, F., Moya, A., 2011. Blueprint for a minimal photoautotrophic cell: conserved and variable genes in Synechococcus elongatus PCC 7942. BMC Genomics 12, 25. doi:10.1186/1471-2164-12-25

Dempo, Y., Ohta, E., Nakayama, Y., Bamba, T., Fukusaki, E., 2014. Molar-Based Targeted Metabolic Profiling of Cyanobacterial Strains with Potential for Biological Production. Metabolites 4, 499–516. doi:10.3390/metabo4020499

Fouilland, E., 2012. Biodiversity as a tool for waste phycoremediation and biomass production. Rev. Environ. Sci. Biotechnol. 11, 1–4. doi:10.1007/s11157-012-9270-2

Hays, S.G., Yan, L.L.W., Silver, P.A., Ducat, D.C., 2017. Synthetic photosynthetic consortia define interactions leading to robustness and photoproduction. J. Biol. Eng. 11, 4. doi:10.1186/s13036-017-0048-5

Hendry, J.I., Prasannan, C., Ma, F., Möllers, K.B., Jaiswal, D., Digmurti, M., Allen, D.K., Frigaard, N.-U., Dasgupta, S., Wangikar, P.P., 2017. Rerouting of carbon flux in a glycogen mutant of cyanobacteria assessed via isotopically non-stationary 13C metabolic flux analysis. Biotechnol. Bioeng. n/a-n/a. doi:10.1002/bit.26350

Hügler, M., Sievert, S.M., 2010. Beyond the Calvin Cycle: Autotrophic Carbon Fixation in the Ocean. Ann. Rev. Mar. Sci. 3, 261–289. doi:10.1146/annurev-marine-120709-142712

Jablonsky, J., Papacek, S., Hagemann, M., 2016. Different strategies of metabolic regulation in cyanobacteria: from transcriptional to biochemical control. Sci. Rep. 6, 33024. doi:10.1038/srep33024

Kazamia, E., Aldridge, D.C., Smith, A.G., 2012. Synthetic ecology – A way forward for sustainable algal biofuel production? J. Biotechnol. 162, 163–169. doi:10.1016/j.jbiotec.2012.03.022

Kirst, H., Formighieri, C., Melis, A., 2014. Maximizing photosynthetic efficiency and culture productivity in cyanobacteria upon minimizing the phycobilisome light-harvesting antenna size. Biochim. Biophys. Acta - Bioenerg. 1837, 1653–1664. doi:10.1016/j.bbabio.2014.07.009

Kunjapur, A.M., Eldridge, R.B., 2010. Photobioreactor Design for Commercial Biofuel Production from Microalgae. Ind. Eng. Chem. Res. 49, 3516–3526. doi:10.1021/ie901459u

Leyn, S.A., Maezato, Y., Romine, M.F., Rodionov, D.A., 2017. Genomic reconstruction of carbohydrate utilization capacities in microbial-mat derived consortia. Front. Microbiol. 8, 1–17. doi:10.3389/fmicb.2017.01304

Li, T., Li, C.-T., Butler, K., Hays, S.G., Guarnieri, M.T., Oyler, G.A., Betenbaugh, M.J., 2017. Mimicking lichens: incorporation of yeast strains together with sucrose-secreting cyanobacteria improves survival, growth, ROS removal, and lipid production in a stable mutualistic co-culture production platform. Biotechnol. Biofuels 10, 55. doi:10.1186/s13068-017-0736-x

Liang, F., Lindblad, P., 2016. Effects of overexpressing photosynthetic carbon flux control enzymes in the cyanobacterium Synechocystis PCC 6803. Metab. Eng. 38, 56–64. doi:10.1016/j.ymben.2016.06.005

Lindemann, S.R., Bernstein, H.C., Song, H.-S., Fredrickson, J.K., Fields, M.W., Shou, W., Johnson, D.R., Beliaev, A.S., 2016. Engineering microbial consortia for controllable outputs. ISME J. 10, 2077–2084. doi:10.1038/ismej.2016.26

Ludwig, M., Bryant, D.A., 2012. Acclimation of the Global Transcriptome of the Cyanobacterium Synechococcus sp. Strain PCC 7002 to Nutrient Limitations and Different Nitrogen Sources. Front. Microbiol. 3, 145. doi:10.3389/fmicb.2012.00145

Ludwig, M., Bryant, D.A., 2011. Transcription Profiling of the Model Cyanobacterium Synechococcus sp. Strain PCC 7002 by Next-Gen (SOLiDTM) Sequencing of cDNA. Front. Microbiol. 2, 41. doi:10.3389/fmicb.2011.00041

Ort, D.R., Merchant, S.S., Alric, J., Barkan, A., Blankenship, R.E., Bock, R., Croce, R., Hanson, M.R., Hibberd, J.M., Long, S.P., Moore, T.A., Moroney, J., Niyogi, K.K., Parry, M.A.J., Peralta-Yahya, P.P., Prince, R.C., Redding, K.E., Spalding, M.H., van Wijk, K.J., Vermaas, W.F.J., von Caemmerer, S., Weber, A.P.M., Yeates, T.O., Yuan, J.S., Zhu, X.G., 2015. Redesigning photosynthesis to sustainably meet global food and bioenergy demand. Proc. Natl. Acad. Sci. 112, 1–8. doi:10.1073/pnas.1424031112

Oyserman, B.O., Martirano, J.M., Wipperfurth, S., Owen, B.R., Noguera, D.R., McMahon, K.D., 2017. Community Assembly and Ecology of Activated Sludge under Photosynthetic Feast–Famine Conditions. Environ. Sci. Technol. 51, 3165–3175. doi:10.1021/acs.est.6b03976

Pate, R., Klise, G., Wu, B., 2011. Resource demand implications for US algae biofuels production scale-up. Appl. Energy 88, 3377–3388. doi:http://dx.doi.org/10.1016/j.apenergy.2011.04.023

Posten, C., 2009. Design principles of photo-bioreactors for cultivation of microalgae. Eng. Life Sci. 9, 165–177. doi:10.1002/elsc.200900003

Quinn, J.C., Catton, K.B., Johnson, S., Bradley, T.H., 2012. Geographical Assessment of Microalgae Biofuels Potential Incorporating Resource Availability. BioEnergy Res. doi:10.1007/s12155-012-9277-0

Reimers, A.-M., Knoop, H., Bockmayr, A., Steuer, R., 2017. Cellular trade-offs and optimal resource allocation during cyanobacterial diurnal growth. Proc. Natl. Acad. Sci. 201617508. doi:10.1073/pnas.1617508114

Rubin, B.E., Wetmore, K.M., Price, M.N., Diamond, S., Shultzaberger, R.K., Lowe, L.C., Curtin, G., Arkin, A.P., Deutschbauer, A., Golden, S.S., 2015. The essential gene set of a photosynthetic organism. Proc. Natl. Acad. Sci. U. S. A. 112, E6634-43. doi:10.1073/pnas.1519220112

Ruffing, A.M., 2014. Improved Free Fatty Acid Production in Cyanobacteria with Synechococcus sp. PCC 7002 as Host. Front. Bioeng. Biotechnol. 2, 17. doi:10.3389/fbioe.2014.00017

Scanlan, D.J., Ostrowski, M., Mazard, S., Dufresne, A., Garczarek, L., Hess, W.R., Post, A.F., Hagemann, M., Paulsen, I., Partensky, F., 2009. Ecological genomics of marine picocyanobacteria. Microbiol. Mol. Biol. Rev. 73, 249–99. doi:10.1128/MMBR.00035-08

Schwander, T., Schada von Borzyskowski, L., Burgener, S., Cortina, N.S., Erb, T.J., 2016. A synthetic pathway for the fixation of carbon dioxide in vitro. Science (80-.). 354, 900 LP-904.

Shimakawa, G., Akimoto, S., Ueno, Y., Wada, A., Shaku, K., Takahashi, Y., Miyake, C., 2016. Diversity in photosynthetic electron transport under [CO2]-limitation: the cyanobacterium Synechococcus sp. PCC 7002 and green alga Chlamydomonas reinhardtii drive an O2-dependent alternative electron flow and non-photochemical quenching of chlorophyll fl. Photosynth. Res. doi:10.1007/s11120-016-0253-y

Suh, I.S., Lee, C.-G., 2003. Photobioreactor engineering: Design and performance. Biotechnol. Bioprocess Eng. 8, 313–321. doi:10.1007/BF02949274

Wan, N., DeLorenzo, D.M., He, L., You, L., Immethun, C.M., Wang, G., Baidoo, E.E.K., Hollinshead, W., Keasling, J.D., Moon, T.S., Tang, Y.J., 2017. Cyanobacterial carbon metabolism: Fluxome plasticity and oxygen dependence. Biotechnol. Bioeng. 1–32. doi:10.1002/bit.26287

Wang, Y., Tashiro, Y., Sonomoto, K., 2015. Fermentative production of lactic acid from renewable materials: Recent achievements, prospects, and limits. J. Biosci. Bioeng. 119, 10–18. doi:10.1016/j.jbiosc.2014.06.003

Wittmann, C., Becker, J., 2007. The L-lysine story: from metabolic pathways to industrial production, in: Amino Acid Biosynthesis~ Pathways, Regulation and Metabolic Engineering. Springer, pp. 39–70.

Young, J.D., Shastri, A. a, Stephanopoulos, G., Morgan, J. a, 2011. Mapping photoautotrophic metabolism with isotopically nonstationary (13)C flux analysis. Metab. Eng. 13, 656–65. doi:10.1016/j.ymben.2011.08.002

Zengler, K., Palsson, B.O., 2012. A road map for the development of community systems (CoSy) biology. Nat. Rev. Microbiol. doi:10.1038/nrmicro2763